DISSERTATIONES ASTRONOMIAE UNIVERSITATIS TARTUENSIS

15

DISSERTATIONES ASTRONOMIAE UNIVERSITATIS TARTUENSIS
15

ELMO TEMPEL

Tracing galaxy evolution by their present-day luminosity function

TARTU UNIVERSITY PRESS

This study was carried out at the Tartu Observatory, Estonia.

The Dissertation was admitted on March 25, 2011, in partial fulfilment of the requirements for the degree of Doctor of Philosophy in physics (astrophysics), and allowed for defence by the Council of the Institute of Physics, University of Tartu.

Supervisors: Dr. Enn Saar,
Tartu Observatory,
Estonia

Dr. Peeter Tenjes,
Institute of Physics, University of Tartu,
Estonia

Opponents: Prof. Emeritus Mauri Valtonen,
Department of Physics and Astronomy, University of Turku,
Turku, Finland

Dr. Tõnu Viik
Tartu Observatory,
Estonia

Defence: June 3, 2011, University of Tartu, Estonia

ISSN 1406-0302
ISBN 978-9949-19-626-5 (trükis)
ISBN 978-9949-19-627-2 (PDF)

Tartu Ülikooli Kirjastus
www.tyk.ee
Tellimus nr. 200

CONTENTS

LIST OF ORIGINAL PUBLICATIONS

This thesis is based on the following publications:

I **Tempel, E.**, Einasto, J., Einasto, M., Saar, E., & Tago, E. 2009, *Anatomy of luminosity functions: the 2dFGRS example*, Astronomy & Astrophysics, 495, 37

II Tago, E., Saar, E., **Tempel, E.**, Einasto, J., Einasto, M., Nurmi, P., & Heinämäki, P. 2010, *Groups of galaxies in the SDSS data release 7. Flux- and volume-limited samples*, Astronomy & Astrophysics, 514, A102

III **Tempel, E.**, Tamm, A., & Tenjes, P. 2010, *Dust-corrected surface photometry of M 31 from Spitzer far-infrared observations*, Astronomy & Astrophysics, 509, A91

IV **Tempel, E.**, Tuvikene, T., Tamm, A., & Tenjes, P. 2011, *SDSS surface photometry of M 31 with absorption corrections*, Astronomy & Astrophysics, 526, A155

V **Tempel, E.**, Saar, E., Liivamägi, L. J., Einasto, M., Einasto, J., & Müller, V. 2011, *Galaxy morphology, luminosity, and environment in the SDSS DR7*, Astronomy & Astrophysics, 529, A53

Other related publications of the dissertant:

VI **Tempel, E.** & Tenjes, P. 2006, *Line-of-sight velocity dispersions and a mass-distribution model of the Sa galaxy NGC 4594*, Monthly Notices of the Royal Astronomical Society, 371, 1269

VII Tago, E., Einasto, J., Saar, E., **Tempel, E.**, Einasto, M., Vennik, J., & Müller, V. 2008, *Groups of galaxies in the SDSS Data Release 5. A group-finder and a catalogue*, Astronomy & Astrophysics, 479, 927

VIII Einasto, M., Tago, E., Saar, E., Nurmi, P., Enkvist, I., Einasto, P., Heinämäki, P., Liivamägi, L. J., **Tempel, E.**, Einasto, J., Martínez, V. J., Vennik, J., & Pihajoki, P. 2010, *The Sloan Great Wall. Rich clusters*, Astronomy & Astrophysics, 522, A92

Author's contribution to the publications

Author's research has given an essential contribution to all these publications. Here the author's contribution to the original publications is indicated. The Roman numerals correspond to those in the list of publications.

Publication I. The author performed the calculations of the luminosity functions. He designed the structure of the paper, prepared all the figures, and did most of the writing. He is responsible for the interpretation of the results, presented in this paper.

Publications II and VII. The author contributed to the preparation of the initial SDSS galaxy catalogue and is responsible for the calculation of the observed and total luminosities of galaxy groups. He contributed significantly to the development of the method to restore the total luminosities of galaxy groups.

Publications III and IV. The author contributed significantly to the development of the algorithm for the 3-dimensional galaxy modelling and to the dust-extinction calculations. He is entirely responsible for writing and developing the software package for galaxy modelling and did all the debugging and testing. For the SDSS data for M 31, he reduced most of the observational data. He did all the model calculations, and prepared most of the figures. He designed the structure of the papers and did most of the writing.

Publication V. The author is responsible for the morphological classification, derived in this paper. He carried out all the luminosity function calculations. He is responsible for most of the interpretations, based on the calculated luminosity functions. He designed the structure of the paper, prepared all the figures, and did most of the writing.

Publication VI. The author derived the formulae to calculate the observed rotational velocities and dispersions of the stellar components of a galaxy. He wrote the necessary software package for model calculations. He is responsible for the kinematical calculations, presented in this paper. He prepared all the figures and did about half of the writing.

Publication VIII. The author is responsible for data preparation that was essential for this study. Most, but not all, data preparation was done during the work on the Papers II and VII. He is responsible for many ideas, which make this paper more clear and readable.

INTRODUCTION

Galaxies, which are complex objects containing up to several tens of billions stars, as well as gas and dust, are remarkable objects. The Universe contains a very diverse "zoo" of galaxies: there are galaxies with a discy shape and spiral structure, galaxies, which almost look like a sphere of stars, or even galaxies, which show no sign of structure. This variety of galaxies leads to the basic question: how the galaxies form and evolve and which processes shape the structure of galaxies? Due to the complexity of galaxy formation and evolution, this question is still an unresolved puzzle and it is one of the biggest challenges in modern cosmology. This key question can also shed light to the formation and evolution of our own Galaxy, and consequently to the formation of our Sun and the Solar system.

The common understanding of galaxy formation is based on the notion that stars formed out of the gas that cooled and subsequently condensed to high densities in the cores of haloes, which are made of the mysterious dark matter. Despite the fact that we have the general picture how galaxies form, many aspects of the galaxy formation and evolution are still barely known. One of the reasons for this is the complexity of the physical processes governing the formation and evolution of galaxies. The complete picture demands a good understanding of star formation as well as of the influence of environment, where the galaxy is located. To study these aspects observationally, we need large samples of galaxies, which up to recent times were not available.

During the last decade, the situation has changed utterly and conclusively. In observational cosmology, large galaxy surveys are carried out, which cover up to a quarter of the entire sky. These extensive surveys allow to study galaxies in more detail than ever. Supported by the galaxy surveys, the general picture of the large-scale galaxy network in the Universe is now an undeniable fact. The large-scale network (the so called supercluster-void environment) is the place where all galaxies and stars form and evolve.

Using our knowledge about galaxies, powerful computational techniques of hydrodynamic simulations (e.g. Birnboim & Dekel 2003) and semi-analytic modelling (e.g. Baugh 2006, for a review) are capable of reproducing many of the complex processes, responsible for the galaxy formation and evolution in the Universe: e.g., star formation and supernovae feedback, galaxy mergers and close encounters, black holes, and the effect of active galactic nuclei. Despite knowing about many key physical processes, which influence the evolution of galaxies, it is not so well understood, how these processes depend on the large-scale environment: e.g., galaxy mergers and the effect of tidal fields, ram-pressure stripping of gas when galaxy moves through intra-cluster medium, etc. So, it still requires a considerable effort to model the intrinsic properties of galaxies and their dependence on the environment, where the galaxies are located.

The present thesis is based on large galaxy surveys and concentrates on the large-scale structure: how galaxy evolution is related with the surrounding large-scale environment of superclusters and voids. Galaxy luminosity functions are derived for different morphological types (spiral, elliptical) and various colours (red, blue) of galaxies, to trace the evolutionary effects of galaxies, which a priori should be different for void and supercluster galaxies. Additionally, since groups and clusters of galaxies are the most common environment of galaxies, we analyse, how the group content changes in the large-scale environment.

The thesis can be outlined as follows. In Chapter 1, the standard picture of galaxy formation is given, followed by a review of the previous studies of the luminosity function. Chapters 2 and 3 describes the galaxy surveys used, data reduction, and methods to analyse the data. Chapters 4 and 5 present the results, which are discussed and summarised in Chapters 6 and 7, respectively.

CHAPTER 1
RESEARCH BACKGROUND AND OBJECTIVES

1.1 Formation and evolution of galaxies and galaxy groups

The general paradigm for our Universe is that of a hot big bang universe. The final structure in such a universe is due to small fluctuations that were imprinted in the primordial density field, and which are amplified by gravity, eventually leading to nonlinear collapse and the formation of dark matter haloes. Global expansion and consequent cooling of the Universe causes the decoupling of matter and radiation, allowing gas to fall into the potential wells (provided by the hierarchically growing dark matter haloes), where it is shock-heated and thereafter cooled radiatively, enabling star and galaxy formation in the dark matter haloes.

According to the Cold Dark Matter (CDM) model, groups and clusters of galaxies (dark matter haloes) form by the gravitational collapse of dark matter around the peaks in the initial density field. Haloes assemble hierarchically, so that smaller haloes merge to form larger and more massive haloes in dense environments (Mo & White 1996; Sheth & Tormen 2002). According to the current paradigm of galaxy formation, galaxies form within haloes, due to the cooling of hot gas. Haloes and galaxies evolve simultaneously, and the evolution of a galaxy is affected largely by its host halo and its environment. If the halo is accreted by a larger halo, the galaxy will be affected by it as well: for example, the galaxy's diffuse hot gas reservoir may be stripped, removing the fuel for future star formation (e.g. Larson et al. 1980; Balogh et al. 2000; Weinmann et al. 2006b; van den Bosch et al. 2008a). Galaxies may also experience major mergers, which transform late-type (spiral) galaxies into early-type (elliptical) galaxies with an additional central bulge component (e.g. Driver et al. 2006; Drory & Fisher 2007). Mergers may drive gas towards the centre, where it can trigger a burst of star formation and fuel the central black hole, the feedback from which can heat the remaining gas and eventually quench star formation (e.g. Mihos & Hernquist 1996; Wild et al. 2007; Pasquali et al. 2008; Schawinski et al. 2009).

The haloes (galaxies) in the Universe are not distributed randomly. Most of the galaxies in the Universe are located in groups and clusters of galaxies. The presence of such galaxy groups is known long ago, and they have been studied continuously. For example, the dominating role of the brightest (first-ranked) cluster/group galaxies was known long ago, for early studies see Hubble & Humason (1931), Hubble (1936), and Sandage (1976). The nature of the physical processes, which influence the luminosity and morphology of galaxies in clusters (and groups) is also known: tidal-stripping of gas during close encounters and mergers (Spitzer & Baade 1951), ram-pressure sweeping of gas due to the motion of a galaxy through the intra-cluster medium (Gunn & Gott 1972; Chernin et al. 1976; van den Bosch et al. 2008b), galaxy mergers (Toomre & Toomre 1972).

Groups and clusters of galaxies are not the biggest structures in the Universe. In fact, groups and clusters of galaxies may reside in larger systems – in superclusters of galaxies or in filaments that cross under-dense regions between superclusters. As a consequence, the Universe contains filamentary superclusters and voids forming a web-like structure – the supercluster-void network (Einasto et al. 1980; Zeldovich et al. 1982; de Lapparent et al. 1986; Bond et al. 1996). All these previously mentioned physical processes are important for galaxy formation in groups and clusters, but the global environment determines, which processes dominate and how the forming galaxy will look like.

The timescale of the evolution of groups (and galaxies therein) also depends on their global environment (Tempel et al. 2009). N-body simulations show that haloes in high-density environments have a higher fraction of their mass assembled in major mergers (Gottlöber et al. 2001; Maulbetsch et al. 2007; Fakhouri & Ma 2009). In the high-density environments, the merger rate is higher at earlier times, contrary to the low-density environments, where the merger rate is higher at the present time. Thus the formation speed of haloes is different in various environments. It is not only the formation of dark matter haloes that is different, but several physical processes depend also on the environment. For example, the ram-pressure stripping of gas is greater in denser environments, likewise the timescale of gas accretion, and the effectivity of supernovae and stellar winds is different in high- and low-density environments. As a result, the properties of galaxies in groups depend on the environment where they are embedded; richer and more luminous groups tend to be located in higher-density environments than poor, less luminous groups (Einasto et al. 2003b,c, 2005a; Berlind et al. 2006). Consequently, understanding the properties and evolutionary state of groups and clusters of galaxies in different environments, and the properties of galaxies in them, is important for the study of groups and clusters, as well as for the study of the properties and evolution of galaxies and larger structures – superclusters of galaxies.

In addition, it should be noted that from the observational point of view, it is hard to determine the important physical processes related to a particular environment. To do it correctly, it would be necessary to compare the evolution of the same galaxy in different environments; from the observational viewpoint this is certainly an impossible task. Finally, to understand the evolution of galaxies, we should take into account the hierarchical evolution of cosmic structures; dark matter haloes form in a bottom-up fashion, with small systems forming first and subsequently merging to form more massive structures. In this framework, galaxies might experience different environments during their lifetimes. So, for example, galaxies residing in a cluster today might have suffered some degree of pre-processing in lower-mass systems as galaxy groups. In observations, it is impossible to follow this evolution directly. Luckily, we have large statistical samples of galaxies and groups, which can be used to study the importance of the key physical processes in different environments in an indirect way.

1.2 Galaxy morphology, environment, and evolution

It is well known that galaxies show a wide range of morphologies, correlated by other properties of galaxies, as the colour, luminosity, size, star-formation rate, etc. The galaxies in the "local Universe" can be classified into two broad types: the late-type (spiral) galaxies, with spiral arms, disc-dominated morphologies, ongoing star-formation, and blue optical colours; and the early-type (elliptical) galaxies, with elliptical or bulge-dominated morphologies, old stellar populations, and red colours. Somewhere between these two types are the lenticular galaxies. They are disc galaxies (like spiral galaxies), which have used up or lost most of their interstellar matter and therefore have very little ongoing star formation; most of them have also a dominant central bulge.

In past, many studies have found a strong correlation between the morphology and environment: i.e., the morphology-density relation. One of the first studies was by Hubble & Humason (1931), when it was realised that galaxy clusters were dominated by ellipticals and lenticulars, and that environmental factors played an important role in determining the morphology of galaxies. Later, Oemler (1974) and Einasto et al. (1974) found the morphology-radius relation; red (early-type) galaxies are located in the central areas of clusters while late-type, blue galaxies can preferentially be found outside of rich clusters, or in the outskirts of clusters. This relation was confirmed by Dressler (1980), who argued that the fraction of morphological types is a function of the local galaxy density.

So, the origin of the morphology of galaxies is one of the oldest mysteries of galaxy formation. Many studies have been devoted to the morphology-density relation and there has been a great deal of effort to understand the origin of morphology by inspecting the dependence of galaxy properties on the environment (e.g. Butcher & Oemler 1978; Einasto & Einasto 1987; Norberg et al. 2002a; Goto et al. 2003; Blanton et al. 2005a; Wolf et al. 2007; Ball et al. 2008). All these studies show that spiral (blue) galaxies tend to be located in low-density environments (in the outskirts of galaxy clusters) and elliptical (red) galaxies in more dense environments (in the centres of galaxy clusters). Additionally, some other bimodal galaxy properties have also been found to be correlated with the environment: blue galaxies with significant star-formation activity tend to reside in under-dense environments, while galaxies with red colours and low star-formation rates tend to reside in over-dense environments (e.g. Lewis et al. 2002; Gómez et al. 2003; Kauffmann et al. 2004; Sheth et al. 2006; Weinmann et al. 2006a; Bamford et al. 2008). But we do not know yet if the properties of galaxies depend on the cluster-centric radius or on the local density of galaxies in clusters, or on both (Whitmore & Gilmore 1991; Huertas-Company et al. 2009; Park & Choi 2009; Park & Hwang 2009).

The morphology of a galaxy is not determined at the time when the galaxy formed. In fact, the galaxy morphology can change significantly during the lifetime of the galaxy. The hierarchical formation of dark matter haloes and simultaneous mergings of galaxies may transform one morphological type to another. The prominent trend in merging is the formation of elliptical galaxies by merging of spirals or irregulars. Additionally, Delgado-Serrano et al. (2010) have showed that spiral galaxies may also form through merging. According to Delgado-Serrano et al. (2010), approximately half of the spirals were already in place 6 Gyr ago and another half formed in mergers of irregular galaxies. In general, for the transformation of one morphological type to another, various physical mechanisms may be responsible: galaxy-galaxy mergers (Barnes & Hernquist 1991), harassment (Moore et al. 1996), ram-pressure stripping (Gunn & Gott 1972), and tidal distortion by the cluster potential (Byrd & Valtonen 1990). Both mergers and harassment are likely to contribute significantly to the morphology-density relation found in the environments of low and intermediate density (e.g. Goto et al. 2003). Contrary, in a high-density environment as galaxy clusters, the latter two mechanisms are more efficient. In recent times, the transformation of late-type galaxies to lenticulars has been frequent, as evidenced, for instance, by the actual dominance of lenticulars in galaxy clusters in the "local Universe" (Fasano et al. 2000, and references therein).

In previous studies, the local, group environment was mainly considered. However, recent studies have demonstrated clearly that the large-scale (supercluster) environment, the so-called global environment, has also an important role in galaxy evolution (see, e.g. Costa-Duarte et al. 2010; Gavazzi et al. 2010). Firstly, the morphology of supercluster cores differs from the morphology of supercluster outskirts (Einasto et al. 2008): the cores of rich superclusters are specific regions that contain clusters and groups of galaxies, and may contain X-ray clusters of galaxies. Thus supercluster cores are not just a high-density environment that contains groups of galaxies, rather the cores of superclusters are specific regions, where the galaxy evolution is different from that in low-density regions. Secondly, Einasto et al. (2007) showed that all galaxies in superclusters are redder than those in voids and most luminous groups are preferentially located in superclusters than in voids (Einasto et al. 2003b,c). Semi-analytic models also predict that void galaxies should be fainter than galaxies in dense regions (Benson et al. 2003b; Tinker & Conroy 2009). Thus superclusters in general differ from the lower-density environments and detailed study of the global environment can provide new insight into the evolution of galaxies in high-density regions.

1.3 Previous studies of luminosity functions

One of the principal description functions for galaxies is the luminosity function $n(L)$ that describes the average number of galaxies per unit volume as a function of galaxy luminosity. The first determinations of the galaxy luminosity function (LF) were made several decades ago (Kiang 1961; Christensen 1975; Schechter 1976; Abell 1977; Kirshner et al. 1979); in the following studies, the number of galaxies used to calculate the luminosity function has increased continuously (Tully 1988; Efstathiou et al. 1988; Loveday et al. 1992). The Las Campanas Redshift Survey measured the general luminosity function of galaxies with a good accuracy (Lin et al. 1996; Bromley et al. 1998; Christlein 2000).

Our current understanding of the galaxy luminosity function owes much to the 2dFGRS (Norberg et al. 2002b) and SDSS surveys (Blanton et al. 2003b; Montero-Dorta & Prada 2009). These new samples of galaxies make it possible to study the dependence of the luminosity function on a large number of different galaxy properties, as galaxy morphology, colours, star formation rate, local and global density environment, etc. In this respect, the luminosity function plays an important role in our understanding how galaxies form and evolve (see, e.g. Yang et al. 2003; Cooray & Cen 2005; van den Bosch et al. 2008a).

Already early studies of the distribution of galaxies of different luminosity showed that clustering of galaxies is tightly related with their luminosity (Hamilton 1988; Einasto 1991), and the luminosity function of galaxies depends on the environment where the galaxy is located (see, e.g. De Propris et al. 2003; Cuesta-Bolao & Serna 2003; Xia et al. 2006; Hansen et al. 2009).

So, to understand how galaxies form, we need to understand where galaxies are located; it is essential to study the dependence of the luminosity function on the environment. It is well known from the halo occupation distribution (HOD) models that the local environment largely determines the properties of galaxies (e.g. Zandivarez et al. 2006; Park et al. 2007): luminous galaxies tend to occupy high mass haloes and low luminosity galaxies reside mainly in low mass haloes. Halo occupation distribution models have been also used to link the observed luminosity function with the distribution of dark matter halo masses (see, e.g. Yang et al. 2004; Zehavi et al. 2005; Cooray 2006; Lin et al. 2006; van den Bosch et al. 2007; Vale & Ostriker 2008; Wang et al. 2010). Using the HOD model and the fact that early-type galaxies are more strongly clustered than late-type galaxies (the morphology-density relation), van den Bosch et al. (2003) found that the fraction of late-type galaxies must be a strongly declining function of halo mass.

The fact that the local/group environment is a dominant factor in galaxy evolution, motivates the study of the luminosity function in galaxy groups (e.g. Colless 2004; González et al. 2005; Xia et al. 2006; Zandivarez et al. 2006; Adami et al. 2007). As a recent study, we emphasise the work by Hansen et al. (2009) and Yang et al. (2009). Hansen et al. (2009) analysed the luminosity functions for central and satellite galaxies of groups separately, taking into account also the colours of the galaxies. Hansen et al. (2009) found that the luminosity functions of both red and blue satellites are only weakly dependent on the cluster richness. However, the ratio of the numbers of faint red and blue galaxies depends strongly on the cluster-centric distance. For brightest cluster galaxies, Hansen et al. (2009) found that the luminosity of the central galaxy of a cluster is tightly correlated with the cluster richness. A complementary study by Yang et al. (2009) found that among the satellite population, there are in general more red galaxies than blue ones. For the central population, the luminosity function is dominated by red galaxies at the massive end, and by blue galaxies at the low-mass end. At the very low-mass end, however, there is a marked increase in the number of red centrals.

A likewise important, but not so well understood factor is the global environment where the galaxy is located – its place in the supercluster-void environment. In Tempel et al. (2009) we have found that the global environment has an important role in determining galaxy properties. Some studies have been dedicated only to special regions: e.g., Mercurio et al. (2006) investigate the Shapley supercluster and Hoyle et al. (2005) concentrates on the void galaxies. The dependence on the environment has been also studied numerically (Mo et al. 2004) and using semi-analytical models (Benson et al. 2003b; Khochfar et al. 2007). These semi-analytical models allow us to study the influence of different physical processes on the morphological evolution, how the morphology of a galaxy changes in time. For example Khochfar et al. (2007) found that the main driver for the evolution of the faint-end slope of the luminosity function is the evolution of the underlying dark matter halo mass function and the supernova feedback, where both cause a relative flattening of the faint-end slope. Mo et al. (2004) used the halo-occupation model and studied how tightly the large-scale environment determines the properties of the halo population.

The influence of the global environment on the luminosity function has been investigated by Hoyle et al. (2005), using the SDSS data, and by Croton et al. (2005), using the 2dFGRS data. These results show strong environmental trends: galaxies in higher density regions tend to be redder, of earlier type, have a lower star formation rate, and are more strongly clustered. Some of these trends can be explained by the well known morphology-density relation (Einasto et al. 1974; Dressler 1980; Postman & Geller 1984) and by the luminosity-density relation (Hamilton 1988). It is less well known how far these trends extend when moving toward extreme environments, into deep voids or superclusters.

The luminosity function have been determined also for different morphological types of galaxies. The morphology of a given galaxy is a reflection of its initial conditions and merger history. In studies of the luminosity function, galaxy morphology has been determined either by its colours (Yang et al. 2009), spectra (Folkes et al. 1999; Madgwick et al. 2002; de Lapparent et al. 2003) or the photometric profile (Bell et al. 2003; Driver et al. 2007a). The most accurate, but by far the most time consuming approach is to use visual classification (Marzke et al. 1994, 1998; Kochanek et al. 2001; Cuesta-Bolao & Serna 2003; Nakamura et al. 2003). For the SDSS survey, visual classification has become possible thanks to the Galaxy Zoo project (Lintott et al. 2008) that will help us to study the morphology and the luminosity function in detail in the future. In all these studies, the classification of early-type and late-type galaxies is based on slightly different methods and/or parameters, but all studies agree that later-type galaxies have a fainter characteristic magnitude and a steeper faint-end slope of the luminosity function. The biggest differences in previous studies are found at the faint-end of the luminosity function, where classification is less certain than for brighter galaxies.

Additionally, recent studies have shown that dust plays an important role in galaxy evolution and it may significantly influence the luminosities and colours of galaxies (Pierini et al. 2004; Tuffs et al. 2004; Driver et al. 2007b; Rocha et al. 2008; Tempel et al. 2010), especially for late-type galaxies. Thus, in order to study intrinsic properties of galaxies, it is necessary to take dust extinction into account. Using the SDSS data, Shao et al. (2007) have studied the influence of dust on the luminosity function. In general, dust is important for late-type spiral galaxies; nearly edge-on galaxies are most affected.

1.4 Motivation of present work

Understanding the formation and evolution of galaxies is one of the biggest challenges of observational cosmology. The luminosity function is in this respect one of the most fundamental of all cosmological observables, helping us to describe the global properties of galaxy populations and to study the evolution of galaxies. The dependence of the luminosity function on cosmic time, galaxy type, and environmental properties gives insight into the physical processes that govern the assembly of the stellar content of galaxies.

In the general picture of galaxy formation and evolution, it is expected that the morphologies of galaxies and various galaxy properties (e.g. colours) are differently correlated with the environment. Besides, the group content in different environments is expected to be different: high-density environments tend to harbour larger groups. Today's picture of galaxy formation and evolution relies largely on semi-analytical models, which allow to study the galaxy evolution: how the properties of a galaxy change in time. To compare these models with the real Universe, we need to know the observed luminosity function in detail.

Additionally to the luminosity function, the global galaxy luminosity densities reflect the processes of galaxy formation and evolution. So, the environmental densities must be also taken into account in the galaxy evolution studies.

Precise determination of galaxy luminosity functions in different environments is needed to constrain current theories of galaxy formation and evolution. Consequently, new advances in galaxy statistics with respect to various parameters (morphology, colour, group content, etc.) could make a strong impact on our understanding of the physical processes that drive the birth and life of galaxies in the Universe.

To shed the light on the evolution of galaxies in the Universe, in this study we investigate how the large-scale environment influences the evolution of galaxies and groups. We have chosen specifically the large-scale environment, since the local/group environment have been studied exhaustively. We hope that the large-scale environment can provide a new viewing angle to understand better the evolution of galaxies. To do that, we study the luminosity functions of galaxies for different morphological types of galaxies, and for different types of group galaxies (group brightest galaxies, satellite galaxies). In this study, we take advantage of the large spectroscopic galaxy surveys (2dFGRS and SDSS), which enable us to study the details of galaxy properties in different environments.

In general, the present analysis has three goals: to determine the luminosity functions of the group brightest (first-ranked), second-ranked, and satellite galaxies; to investigate the nature of the satellite and isolated galaxies; and, as most important, to analyse the global (large-scale) environmental dependency of galaxy luminosities for galaxies of different types and colours.

CHAPTER 2
DATA AND METHOD OF ANALYSIS

This chapter gives the overview of the data used in the present thesis and describes the methods used to analyse the data.

2.1 2dFGRS – Two-degree Field Galaxy Redshift Survey

The Two-degree Field Galaxy Redshift Survey (2dFGRS) is one of the two largest spectroscopic galaxy surveys available. The 2dFGRS uses the 2dF multi-fibre spectrograph on the Anglo-Australian Telescope. The survey contains redshifts for 221414 galaxies brighter than the extinction-corrected magnitude limit $b_{\rm J} = 19.45$[1]. The survey consists of two main areas in the Northern (75×10 square degrees) and Southern (80×15 square degrees) hemispheres, with a total area about 1500 square degrees, and of 100 randomly located individual fields in the Southern hemisphere. Survey releases and observational details are described in Colless et al. (2001, 2003).

In the present thesis the group catalogue for the 2dFGRS sample by Tago et al. (2006) is used. The author of the present thesis did not participate in the construction of this catalogue. However, since the present thesis is based on this catalogue, a brief description of the 2dFGRS data is given.

The Tago et al. (2006) catalogue covers the 2dFGRS contiguous Northern and Southern Galactic patches (NGP and SGP, respectively). In this catalogue, we exclude distant galaxies with redshifts $z > 0.2$ ($574\,h^{-1}$Mpc), since being a flux-limited survey, the 2dFGRS becomes very diluted at large distances. We also apply a lower redshift limit $z > 0.008$ ($25\,h^{-1}$Mpc), as at smaller redshifts the catalogue contains mostly unclassified objects of the Local Supercluster. Figure 2.1 shows the galaxy distribution in the sky for the NGP and SGP samples.

For luminosity function estimation, we excluded the galaxies brighter than $b_{\rm J} = 14.0$. Those galaxies are located nearby, in a small volume of space, and their magnitudes are difficult to determine precisely. The 2dFGRS team has used the same limit in their luminosity function study (Cross et al. 2001). Although the 2dFGRS sample was originally planned to have a uniform lower magnitude limit $b_{\rm J} = 19.45$, in fact the faint magnitude limit fluctuates from field to field. In the present study, these fluctuations are taken into account using the lower magnitude limit maps given by the 2dF survey team (Colless et al. 2003).

[1] $b_{\rm J}$ is equal to the Johnson *B* magnitude for an object with a zero colour in the Johnson-Cousins system.

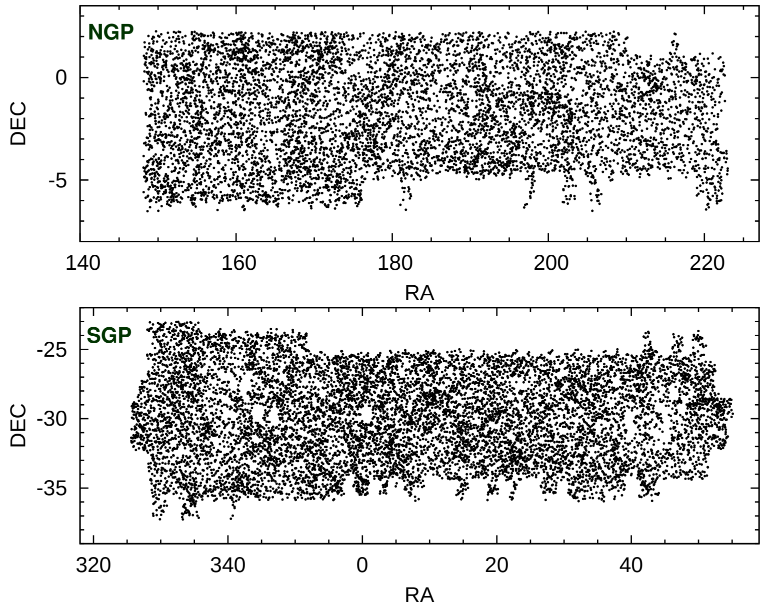

Figure 2.1: Galaxies in the Northern (*upper panel*) and Southern (*lower panel*) Galactic patches of the 2dFGRS survey.

The magnitude limits define the photometric properties of the sample. Secondly, for statistical analysis, the incompleteness of the redshift catalogue has to be taken into account. We use the redshift completeness mask, defined by the 2dF survey team (Colless et al. 2003), for that. This is essential for calculating the luminosity density field. In our final sample of galaxies we use only such fields where at least half of the galaxies have measured redshifts.

With all these restrictions, the Tago et al. (2006) final sample contains 75953 galaxies in the Northern sky and 102610 galaxies in the Southern sky. We corrected the redshifts for the motion relative to the cosmic microwave background (CMB). For linear dimensions we use the co-moving distances (see, e.g. Martínez & Saar 2002). For the present thesis, the distances were computed using the matter and dark energy density parameters derived from the seven-year Wilkinson Microwave Anisotropy Probe (WMAP) observations, $\Omega_\mathrm{m} = 0.27$ and $\Omega_\Lambda = 0.73$ (Komatsu et al. 2011).

To transfer the apparent magnitude m into the absolute magnitude M, we use the usual formula

$$M = m - 25 - 5\log_{10}(d_L) - K, \tag{2.1}$$

where the luminosity distance $d_L = d(1+z)$, d is the co-moving distance in the units of h^{-1}Mpc, and z is the redshift. The term $K \equiv k+e$ is the sum of the

k-correction and the evolution correction, necessary for deep cosmological redshift surveys. We adopted the $k+e$-correction for the 2dFGRS sample according to Norberg et al. (2002b), using morphological classes, based on the spectral classification parameter ν (given in the 2dFGRS dataset), as described in Madgwick et al. (2002). The value of the classification parameter ν correlates with the strength of the absorption/emission features. Galaxies with an old stellar population and strong absorption features have negative values of ν, while galaxies with a young stellar population and strong emission lines have positive values of ν. For some galaxies with poor spectra, the spectral type parameter ν was not determined. In these cases we adopted the mean relation: $k+e = (z + 6.0z^2)/(1 + 20.0z^3)$.

To transfer the absolute magnitude M to the luminosity in solar units L, we use the usual formula $L = L_\odot 10^{0.4(M_\odot - M)}$, where $M_\odot$ is the absolute magnitude of the Sun. Following Eke et al. (2004) we accepted $M_\odot = 5.33$ in the b_J photometric system.

2.2 SDSS – Sloan Digital Sky Survey

The Sloan Digital Sky Survey (SDSS) is one of the largest and most complex surveys in the history of astronomy. The SDSS used a dedicated 2.5-meter telescope at Apache Point Observatory, New Mexico. Over eight years of operation, it obtained a huge number of multi-colour images and spectra for galaxies in a region covering more than a quarter of the sky. The SDSS final data release (DR7), described in Abazajian et al. (2009), contains more than 930 000 galaxies with measured spectra.

In the present thesis we use the groups of galaxies found in the SDSS as described in Tago et al. (2008) and Tago et al. (2010). The main difference between these group catalogues is the release number of the SDSS dataset. Tago et al. (2010) uses the final SDSS data release (DR7) and in the present thesis we use that catalogue for our analysis. For our group catalogue based on the final SDSS data release, we used only the main contiguous area of the survey, roughly 7500 square degrees. This sample was selected from the standard main galaxy sample described by Adelman-McCarthy et al. (2008) and downloaded from the SDSS web page. In our catalogue, we used only galaxies brighter than the spectroscopic survey limiting Petrosian (1976) magnitude $m_r = 17.77$ (Strauss et al. 2002). We used also an upper limiting magnitude $m_r = 12.5$, since bright objects are over-saturated in the SDSS photometric survey. We put a lower redshift limit $z = 0.009$ (27 h^{-1}Mpc) to our sample to exclude the galaxies of the Local Supercluster. As the SDSS sample becomes very diluted at large distances, we restricted our sample by an upper redshift limit $z = 0.2$ (574 h^{-1}Mpc).

The total number of galaxies in the catalogue of groups and single galaxies by Tago et al. (2010) is 583362. The distribution of galaxies in the sky is

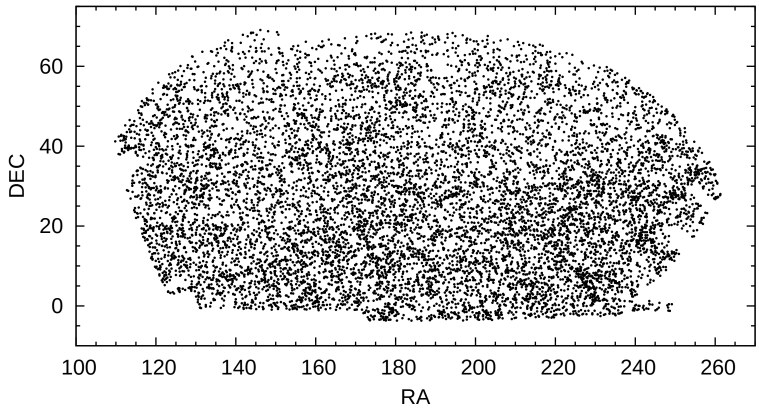

Figure 2.2: Galaxies in the SDSS survey main sample.

shown in Fig. 2.2. The redshifts were corrected for the motion relative to the CMB. As for the 2dFGRS sample, we use for linear dimensions co-moving distances (see, e.g. Martínez & Saar 2002) with standard cosmological parameters: $H_0 = 100\,h\,\mathrm{km\,s^{-1}Mpc^{-1}}$, the matter density $\Omega_\mathrm{m} = 0.27$, and the dark energy density $\Omega_\Lambda = 0.73$ (Komatsu et al. 2011).

The catalogue of Tago et al. (2010) lists the Petrosian r magnitudes. In the present thesis we use the composite model magnitudes, as suggested and described in the SDSS web page[2]

$$m_\mathrm{cmodel} = -2.5\log_{10}\left[frac_\mathrm{deV}F_\mathrm{deV} + (1 - frac_\mathrm{deV})F_\mathrm{exp}\right], \tag{2.2}$$

where F_deV and F_exp are the de Vaucouleurs and exponential fluxes of the object in question and $frac_\mathrm{deV}$ is the coefficient of the de Vaucouleurs term (varying from zero to one). The surface luminosity distribution of each galaxy in the SDSS has been fitted by the pure exponential and the de Vaucouleurs profiles. The best linear combination of these is used to represent the profile of the galaxy, and $frac_\mathrm{deV}$ indicates the fraction of luminosity contributed by the de Vaucouleurs profile. According to the SDSS web page[3], composite model magnitudes are in excellent agreement with Petrosian magnitudes and are the preferred magnitudes for photometry of galaxies.

For luminosity function calculation, we shall use a rather stringent bright luminosity limit $m_r = 14.5$, as suggested by the SDSS team; this limit is better for statistical analysis of the data. Additionally, since the conversion from Petrosian to composite model magnitudes introduces incompleteness near the faint luminosity

[2] http://www.sdss.org/dr7/algorithms/photometry.html#cmodel

[3] http://www.sdss.org/dr7/algorithms/photometry.html#which_mags

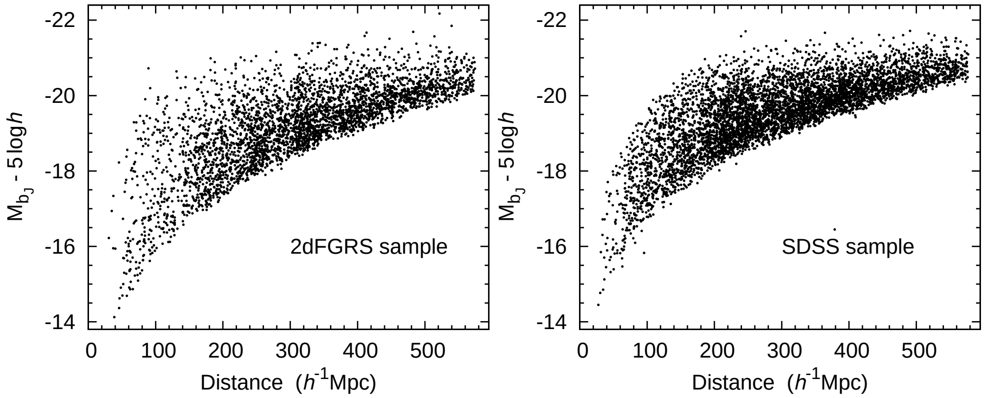

Figure 2.3: Absolute magnitudes of galaxies in the 2dFGRS sample (*left panel*) and in the SDSS sample (*right panel*) at various distances from the observer. To have a better comparison between these two samples, the magnitudes of the SDSS sample were converted to the b_{J} system, using the calibration of Norberg et al. (2002b).

limit, we shall use the limit $m_r = 17.6$ for composite model magnitudes; this leads to a uniform distribution of galaxies in the sample.

To transfer the apparent magnitude into the absolute magnitude, we use the formula (2.1), where the k-corrections for the SDSS galaxies are calculated using the KCORRECT algorithm v4_2 (Blanton et al. 2003a; Blanton & Roweis 2007). The evolution correction e has been calculated according to Blanton et al. (2003b). To transfer the absolute magnitudes into solar luminosities, we use the solar luminosities as given in Blanton & Roweis (2007). In the r-band, used in the present thesis for luminosity function calculations, $M_{\odot} = 4.64$.

In Fig. 2.3 the absolute magnitudes of the 2dFGRS and the SDSS samples are shown. The flux-limited selection effects are well seen: at lower distances, the brightest galaxies are absent due to the upper limiting magnitude; at further distances, only the bright galaxies are seen. While the SDSS sample includes more than three times more galaxies than the 2dFGRS sample, the 2dFGRS sample is slightly deeper than the SDSS sample (see Fig. 2.3). The latter is the reason why we use also the 2dFGRS sample, since it gives more information for the faint end of the luminosity function. Additionally, for our study of the luminosity functions in groups (Tempel et al. 2009), we have used the2dFGRS sample and for the study of the luminosity functions for different morphological types of galaxies (Tempel et al. 2011a), we have used the SDSS sample.

2.3 Homogeneous galaxy group catalogues for the 2dFGRS and SDSS surveys

Clusters and groups of galaxies are the basic building blocks of the Universe, they are natural environments for galaxies. Observations of the local Universe have shown that basically all galaxies are located in groups. Therefore, it is essential to extract groups of galaxies from the galaxy surveys, and their study can provide new understanding of the evolution of galaxies, of the large-scale structure, and of the underlying cosmological model. To achieve this goal, we extract groups and clusters of galaxies from the 2dFGRS and SDSS surveys.

One of the most conventional method to search for groups of galaxies is cluster analysis that was introduced in cosmology by Turner & Gott (1976). This method was named the "friends-of-friends" (FoF) by Press & Davis (1982) and promoted by Zeldovich et al. (1982) and Huchra & Geller (1982). In the FoF method, galaxies are linked into systems, using a certain linking length (or neighbourhood radius). Choosing the right linking length is rather complicated. In most cases, the linking length is not constant, but varies with distance and/or other parameters.

Our experience and analysis show that the choice of the linking length depends on the goals of the specific study. For example, while Weinmann et al. (2006a) searched for compact groups in the SDSS DR2 sample, applying strict criteria in the FoF method, then Berlind et al. (2006) applied the FoF method to the volume-limited samples of the SDSS with the goal to measure the group multiplicity function and to constrain dark matter haloes. In our group catalogue, our goal is to obtain the groups for the determination of the luminosity density field and for studying the properties of the galaxy network. Hence, our goal is to find as many groups as possible, whereas the group properties must not change in distance. In our group definition, we tried to avoid the inclusion of large sections of surrounding filaments or parts of superclusters into groups.

The group finding algorithm, presented shortly in this section, was developed in Tago et al. (2006) and Tago et al. (2008). The details of the group finding algorithm is described for the 2dFGRS sample in Tago et al. (2006) and for the SDSS sample in Tago et al. (2008, 2010). The author of the present thesis is responsible for the data preparation for the SDSS group catalogue and for the luminosity (observed and total) calculation for galaxies and groups of galaxies.

For the 2dFGRS sample a constant linking length was used to extract groups of galaxies. For the SDSS sample, the linking length is increasing moderately with distance. To find the proper scaling for the linking length with distance in the SDSS sample, we created a test group catalogue with a constant linking length. Then we selected in the nearby volume ($d < 200\,h^{-1}$Mpc) all groups with more than 20 group members. Assuming that the group members are all at the mean distance of the

Table 2.1: Data on the 2dFGRS and SDSS galaxies and groups.

Sample	N_{gal}	N_{gr}	D1	D2	D3	D4
2dFGRS (all)	178563	25215	24491	64987	70210	15996
2dFGRS (groups)	–	25215	2337	8674	10809	2357
2dFGRS (isolated)	101398	–	18818	40728	34518	5555
SDSS (all)	516368	74511	54942	173320	208210	66884
SDSS (groups)	–	74511	5500	24388	33552	9668
SDSS (isolated)	275109	–	42422	108535	97050	19311

Notes: N_{gal} – the number of galaxies in a sample; N_{gr} – the number of groups (and first-ranked galaxies) in a sample; D1 to D4 – the number of galaxies in a given density environment (D1 is the least dense and D4 is the most dense environment). The sum of D1 to D4 is less than $N_{\mathrm{gal/gr}}$, due to the edges of the survey, where the densities are undetermined.

group, we determined their absolute magnitudes and peculiar radial velocities. Then we shifted these nearby groups, calculating the parameters of the groups (new $k+e$-corrections and apparent magnitudes for the group members), as if the groups were located at larger distances. As with the increasing distance more and more fainter members of groups fall outside the observational window of apparent magnitudes, the group membership changes. We then determined new properties of the groups – their multiplicities, characteristic sizes, rms velocities, and number densities. We also calculated the minimum FoF linking length necessary to keep the group together at this distance. To determine that, we built the minimal spanning tree (MST) for each group (see, e.g. Martínez & Saar 2002) and found the maximum length of the MST links. Determining the mean values of the group linking lengths, we found that the linking length in our group finding algorithm changes moderately with distance. A good parameterisation of the scaling law for the linking length (d_{LL}) is the arctan function

$$d_{LL}(z) = d_{LL,0}\left[1 + a\arctan(z/z_\star)\right], \tag{2.3}$$

where $d_{LL,0}$ is the value of linking length at the initial redshift; a and $z_\star$ are the parameters. For the SDSS groups, the parameters have the values $a = 1.00$ and $z_\star = 0.050$.

Our final group catalogues are rather homogeneous. The group richness, mean sizes and velocity dispersion do not practically change over distance, excluding the effect of a flux-limited sample. The homogeneity of our catalogues have been tested also by others. For example, Tovmassian & Plionis (2009) select poor groups from our SDSS catalogues and conclude that the main parameters of our groups are distance independent and well suited for statistical analysis.

As a final result, the group catalogue for the 2dFGRS includes 25215 groups and for the SDSS, 78800 groups with two or more members. The number of galaxies and groups in the 2dFGRS and SDSS samples as used in the present thesis are given in Table 2.1. The total number of groups and galaxies, used in the present thesis, for the SDSS sample is less than in the group catalogue by Tago et al. (2010), since the luminosity limits are tighter. The Table 2.1 gives also the numbers of galaxies and groups in the four density regions; the calculation of the environmental densities is described in Sect. 2.5.

2.4 Selection effects and luminosity function estimation

To calculate the luminosity function (LF) of galaxies, we need to know the number of galaxies of a given luminosity bin per unit volume. The principal selection effect that influences the determination of the luminosity functions in flux-limited surveys is the absence of galaxies fainter or brighter than the survey limiting magnitudes. This effect is well seen in Fig. 2.3, showing the absolute luminosities of galaxies plotted against their distance; at large distances only the brightest galaxies are seen.

To take this effect into account in the determination of the luminosity function, the standard V_{max}^{-1} weighting procedure can be used. The differential luminosity function $n(L)\mathrm{d}L$ (the expectation of the number density of galaxies of the luminosity L to $L+\mathrm{d}L$) can be found as usual

$$n(L)\mathrm{d}L = \sum_i \frac{\mathbf{I}_{(L,L+\mathrm{d}L)}(L_i)}{V_{\mathrm{max}}(L_i)}, \tag{2.4}$$

where $\mathrm{d}L$ is the luminosity bin width, $\mathbf{I}_A(x)$ is the indicator function that selects the galaxies that belong to a particular luminosity bin, $V_{\mathrm{max}}(L)$ is the maximum volume where a galaxy of a luminosity L can be observed in the present survey, and the sum is over all galaxies of the survey. This procedure is non-parametric, and gives both the form and true normalisation of the luminosity function. The choice of the luminosity bin width $\mathrm{d}L$ determines the smoothness of the luminosity function.

The Eq. (2.4) gives us the binned density histogram that depends both on the bin widths and the locations of the bin edges; a better way is to use kernel smoothing (see, e.g. Wand & Jones 1995), where the number density of galaxies is represented by a sum of kernels centred at the data points:

$$n(L) = \frac{1}{a}\sum_i \frac{1}{V_{\mathrm{max}}(L_i)} K\left(\frac{L-L_i}{a}\right). \tag{2.5}$$

The kernels $K(x)$ are distributions ($K(x) > 0$, $\int K(x)\,\mathrm{d}x = 1$) of zero mean and of a typical width a. The width a is an analogue of the bin width, but there are no bin edges to worry about.

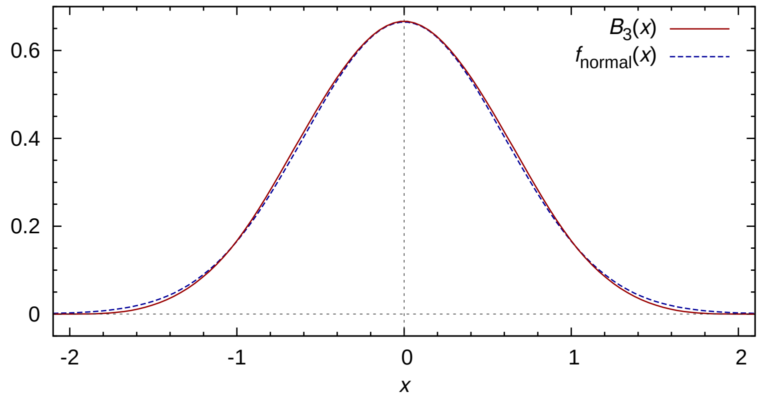

Figure 2.4: The shape of the kernel $B_3(x)$ (red solid line). For comparison, a normal distribution with $\sigma = 0.6$ is given (blue dashed line).

As the luminosity function is rapidly changing with luminosity, especially at the bright end of the luminosity function, the bin widths should vary. This is most easy to implement by adaptive kernel estimation of the luminosity function – instead of Eq. (2.5) we write

$$n(L) = \sum_i \frac{1}{V_{\rm max}(L_i)} \frac{1}{a_i} K\left(\frac{L-L_i}{a_i}\right), \tag{2.6}$$

where the kernel widths depend on the data, $a_i = a(L_i)$.

The choice of the kernel widths is a matter of ongoing study, but recommendations are available (see, e.g. Silverman 1997). The kernel widths are known to depend on the density $f(x)$ itself, with $a \sim f(x)^{-1/5}$ for densities similar to normal distribution. This choice requests a pilot estimate for the density that can be found using a constant width kernel.

We used the magnitude scale for our luminosity function (all luminosities and kernel widths are in magnitudes), and the B_3 box spline kernel:

$$K(x) = B_3(x) = \frac{1}{12}\left(|x-2|^3 - 4|x-1|^3 + 6|x|^3 - 4|x+1|^3 + |x+2|^3\right). \tag{2.7}$$

This kernel is well suited for estimating densities – it is compact, differing from zero only in the interval $x \in [-2, 2]$, and it conserves mass: $\sum_i B_3(x-i) = 1$ for any x (see Fig. 2.4 for illustration of the B_3 box spline kernel).

For the pilot estimate, we used a wide kernel with the scale $a = 0.5$ mag. For the adaptive kernel widths, we adopted $a = 0.05$ mag (the typical SDSS rms magnitude error) as the minimum width (for the maximum density) and rescaled it by the $a \sim f_{\mathrm{pilot}}(x)^{-1/5}$ law. The luminosity function drops sharply at the bright end, leading to very wide kernels; we restricted the kernel width by $a = 0.2\,\mathrm{mag}$.

The maximum volume $V_{\max}(L)$, where a galaxy of a luminosity L can be observed in a present survey, is determined by the minimum and maximum distances where a particular galaxy can be observed. The distance limits are calculated, using the limiting magnitudes of the survey and Eq. (2.1), where the $k+e$-corrections for each galaxies are calculated taking into account the dependence of the correction on distance that is slightly different for each galaxy. Firstly, we find the average $k+e$-corrections that are calculated using the galaxies near the limiting magnitudes of the survey and then calculate the moving average for every distance. Next, to get the $k+e$-corrections for a single galaxy at a given distance, we find the ratio of the calculated average $k+e$-correction to the true $k+e$-correction for this galaxy at its distance (when the galaxy belongs to a group, we use the distance of the group) and divide the calculated average $k+e$-corrections by this value. The use of the average $k+e$-corrections is justified, since the k-correction is colour and distance-dependent.

We are also interested in the "error bars", pointwise confidence intervals for the number density of galaxies ($n(L)$). These can be obtained by smoothed bootstrap (Silverman & Young 1987; Davison & Hinkley 1997; Fiorio 2004). Here the data points for the bootstrap realisations are chosen, as usual, randomly from the observed data with replacement, but they have an additional smoothing component:

$$L_i^\star = L_j + h\varepsilon_j, \tag{2.8}$$

where ε is a random variable of the density $K(x)$ and $h \in (0, 1)$; we used $h = 0.5$.

We generated 10000 bootstrap realisations, using the adaptive kernel widths as for the true luminosity function estimate. We show the centred 95% confidence regions in our figures in this thesis.

The method described above gives the estimated observational luminosity function. To facilitate comparison with different luminosity functions and with different studies, we fit the luminosity functions with analytical functions. For the analytical function, we shall use the popular Schechter (1976) function

$$n(L)\mathrm{d}L \propto (L/L^*)^\alpha \exp\left(-L/L^*\right)\mathrm{d}(L/L^*), \tag{2.9}$$

where α and L^* (or the respective absolute magnitude M^*) are parameters. The parameter α is the exponent at low luminosities and L^* is the characteristic luminosity of the turning point of the function.

Additionally, we shall use a double-power-law form of the luminosity function. A double-power-law form of the group luminosity function was used already by Christensen (1975), Kiang (1976), Abell (1977), and Mottmann & Abell (1977). In these papers a sharp transition between two power indices at a characteristic luminosity L^* was applied. We shall use a smooth transition:

$$n(L)\mathrm{d}L \propto (L/L^*)^\alpha \left[1 + (L/L^*)^\gamma\right]^{\frac{\delta-\alpha}{\gamma}} \mathrm{d}(L/L^*), \tag{2.10}$$

where α is the exponent at low luminosities $(L/L^*) \ll 1$, δ is the exponent at high luminosities $(L/L^*) \gg 1$, γ is a parameter that determines the speed of transition between the two power laws, and L^* is the characteristic luminosity of the transition, similar to the characteristic luminosity of the Schechter function.

The Schechter function is simpler and the interpretation of the Schechter parameters (α and L^*) are more straightforward. However, as shown in several papers, the Schechter function is not always a best fit for the luminosity function (Blanton et al. 2005b; Mercurio et al. 2006; Yang et al. 2008; Tempel et al. 2009), especially at the bright end, where the Schechter function underestimates the amount of bright galaxies. Therefore, we shall use both, the Schechter function and the double-power law, for analytical fits.

The parameters for the two analytical functions, derived from the SDSS data, are shown in Table 3 in Tempel et al. (2011a), and for the luminosity functions, derived from the 2dFGRS data in Table 4 in Tempel et al. (2009).

2.5 Determining the environmental densities

Many galaxy properties, including luminosities, depend on the environment, where the galaxy is located. Since one of our goals is to examine the variations of the luminosity function with the environment, we have to compute the global environmental densities. While we are mainly focusing on the global environment, the so called supercluster-void network, we also determine the local environment, to compare the effects of both environments and to emphasise the importance of the global environment.

We calculate the environmental densities in a similar way as done by Lauri Juhan Liivamägi (see, e.g. Liivamägi et al. 2010) for supercluster search. The method to estimate the total luminosities of groups has been used earlier by Einasto et al. (2003a) and is further specified, developed, and applied to the 2dFGRS and SDSS samples by the author of the present thesis.

To calculate the luminosity density field, we need to know the expected total luminosities of groups and isolated galaxies. The primary factor that determines the calculation of group luminosities is the selection effect, present in a flux-limited survey: further away, only the brightest galaxies are seen and in nearby regions, the brightest galaxies are left out of the sample. To take this into account, we calculated for each galaxy a distance-dependent weight factor W_d

$$W_d = \frac{\int_0^\infty L\, n(L) \mathrm{d}L}{\int_{L_1}^{L_2} L\, n(L) \mathrm{d}L}, \tag{2.11}$$

where $L_{1,2} = L_\odot 10^{0.4(M_\odot - M_{1,2})}$ are the luminosity limits of the observational window at distance d, corresponding to the absolute magnitude limits of the window M_1 and M_2, and $n(L)$ is the luminosity function for all galaxies. To calculate the magnitudes M_1 and M_2 we use the average $k+e$-corrections at a given distance. We used the double-power-law approximation for the luminosity function, with the parameters $\alpha = -1.30$, $\gamma = 1.73$, $\delta = -7.78$, and $M^* = -21.98\,$mag.

To calculate the expected total luminosities of groups, we regard every galaxy as a visible member of a group. For isolated/single galaxies we made an assumption that only the brightest galaxy of the group is visible and therefore the isolated galaxy is also part of some group. This assumption is based on observations of nearby galaxies, which indicate that practically all galaxies are located in systems of galaxies of various size and richness.

Assuming that every galaxy also represents a related group of galaxies, which may lie outside the observational window of the survey, the estimated total luminosity per one visible galaxy is

$$L_{\mathrm{tot}} = L_{\mathrm{obs}} \cdot W_d, \tag{2.12}$$

where L_{obs} is the observed luminosity of the galaxy. The luminosity L_{tot} takes into account the luminosities of unobserved galaxies and therefore it can be used to calculate the full luminosity density field.

To determine the luminosity density field, we must convert the spatial positions of galaxies $\mathbf{r}_i$ and their luminosities $L_{\mathrm{tot},i}$ into spatial densities. The standard approach is to use the kernel densities (Silverman 1997):

$$D(\mathbf{r}) = \sum_i K^{(3)}(\mathbf{r} - \mathbf{r}_i; a)\, L_{\mathrm{tot},i}, \tag{2.13}$$

where $K^{(3)}(\mathbf{x}; a)$ is a suitable kernel of a width a with a unit volume integral, and $L_{\mathrm{tot},i}$ is the weighted luminosity of the i-th galaxy that also takes into account the luminosities of unobserved galaxies. The sum extends formally over all galaxies, but the kernel is usually chosen to differ from zero only in a limited range of the argument; this limits the number of galaxies in the sum. Good kernels for calculating densities on a spatial grid are generated by the B_3 spline kernel (see Eq. (2.7)). This kernel is close to Gaussian with $\sigma = 0.6a$ (see Fig. 2.4). The three-dimensional kernel $K^{(3)}(\mathbf{x}; a)$ is given by a direct product of three one-dimensional kernels. Although this is a direct product, it is isotropic to a good degree (Saar 2009).

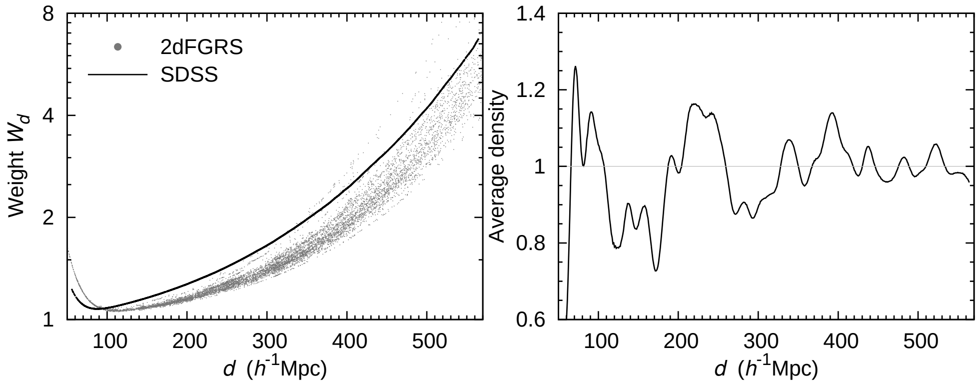

Figure 2.5: *Left panel*: the weight factor W_d at different distances for the 2dFGRS (grey dots) and SDSS (black line) samples. The scatter for the 2dFGRS sample is caused by the varying minimum magnitude limit of the sample. *Right panel*: the average global density in thin concentric shells, in units of the global mean density ($0.01526 \times 10^{10}\, hL_{\odot}\mathrm{Mpc}^{-3}$) for the SDSS sample.

Using the rms sizes of galaxy groups and their radial velocity dispersions from the Tago et al. (2010) catalogue we suppress the cluster finger redshift distortions, spherising the clusters. This removes the smudging effect the fingers have on the density field. After calculation of the density field, the densities are converted into units of mean density, where the mean density is defined as the average over all pixel values inside the survey mask. The survey mask is designed to follow the edges of the survey and the galaxy distribution inside the mask is assumed to be homogeneous in the average.

We use the kernel width $8\,h^{-1}$Mpc for the global environmental densities and $1\,h^{-1}$Mpc to determine the local environmental densities. The main difference between these two densities is the environment that they determine: the local densities refer to the group/cluster environment, while the global densities refer to the large-scale (supercluster-void) environment. In essence, these two densities refer to completely different structures in the Universe.

The left panel of Fig. 2.5 shows the weight factor W_d for the 2dFGRS and SDSS samples. The weight factor for the 2dFGRS is varying, since the lower magnitude limit is varying in the 2dF survey. The weight factor for the SDSS is slightly larger than that for the 2dFGRS sample because the 2dF survey extends to fainter magnitudes (see Fig. 2.3). The right panel of Fig. 2.5 shows the average global densities in thin concentric shells as a function of distance for the SDSS sample. The global density is nearly constant over the distance, when the weight factor is applied. Variations in average density are due to the large-scale structure. This shows that statistically,

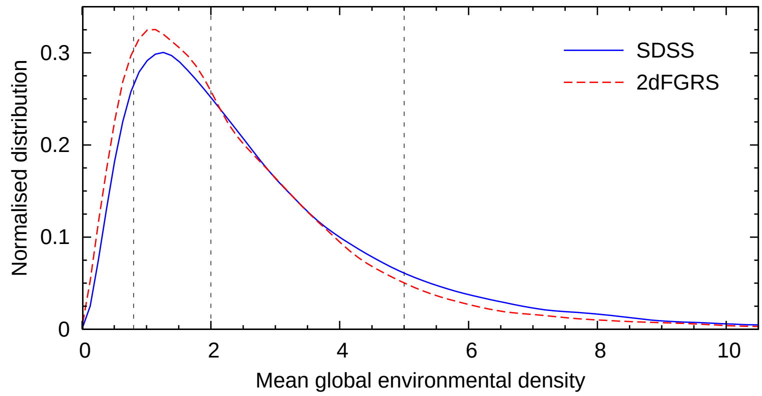

Figure 2.6: The density distribution of galaxies for the SDSS and 2dFGRS samples. The vertical lines show the limits for the four density environments.

the global environmental density is independent of distance and it is a good estimator for the full galaxy sample.

In the present thesis we shall divide all galaxies into four classes, according to the value of the global environmental density D at their location. The highest density class represents the supercluster region, the lowest class is the void region, and the two intermediate classes are between these two classes. Both the void and the supercluster region contain approximately 10% of all galaxies. The rest of the galaxies are divided nearly equally between the two other regions. We designate these four regions as D1, D2, D3, and D4, where D1 is the void region and D4 is the supercluster region. The number of galaxies in each class for the 2dFGRS and SDSS samples are given in Table 2.1. Figure 2.6 shows the distribution of densities at galaxy locations in the SDSS and 2dFGRS sample; the vertical dashed lines show the boundaries (0.8, 2.0, and 5.0) for these four density regions.

CHAPTER 3
ACCOUNTING FOR DUST ATTENUATION IN SPIRAL GALAXIES

In this chapter we delineate the necessary steps to correct the galaxy luminosities for internal attenuation. Since dust affects mostly late-type, spiral galaxies, we start this chapter with classifying galaxies into spirals and ellipticals. Since dust attenuation also depends on the galaxy inclination angle and galaxy colour (or galaxy type), we build the necessary tools to take that into account. We will end this chapter by showing how our attenuation correction works.

Since we study the dust attenuation only in the SDSS sample, we derive the attenuation corrections only for SDSS galaxies.

3.1 Automated galaxy classification in surveys

Spiral galaxies have more dust than ellipticals and therefore the observed luminosities of spiral galaxies are more affected by dust. If we want to correct for dust attenuation, we have to know the morphology of a galaxy.

As one source, we will use the morphological classification by the Galaxy Zoo project (Lintott et al. 2008). The Galaxy Zoo project has led to morphological classification of nearly one million objects from the SDSS data set through visual inspection. Banerji et al. (2010) used the Galaxy Zoo data to develop a machine learning algorithm (an artificial neural network) for galaxy classification; they have also published distribution histograms for different parameters of various types of objects: stars, spirals, ellipticals, and mergers. In the present thesis we use these histograms as the basis for selecting dominantly spiral or elliptical galaxies. Additionally, we will use the galaxy colour distributions from Lintott et al. (2008).

We will compare the distributions from the Galaxy Zoo project with our own visual classifications. We have classified a small sample (of nearly one thousand) galaxies in the Sloan Great Wall region (Einasto et al. 2010). In this study we use only galaxies with a clear classification to test the distributions taken from the Galaxy Zoo project. Additionally, we found another criterion ($frac_{\rm deV}$) to classify galaxies into spirals and ellipticals; this criterion, together with the visual ellipticity of the galaxy, gives a good base for morphological classification.

In the SDSS one of the main parameters that determines the type of a galaxy is the photometric parameter $frac_{\rm deV}$ – the point-spread function corrected indicator of galaxy morphology. The surface luminosity distribution of each galaxy in the SDSS has been fitted by the exponential and the de Vaucouleurs profiles. The best linear combination of these is used to represent the profile of the galaxy, and $frac_{\rm deV}$ indicates the fraction of luminosity contributed by the de Vaucouleurs profile. Bernardi et al. (2005) used $frac_{\rm deV} > 0.8$ to select early-type galaxies. Shao et al. (2007) used $frac_{\rm deV} < 0.5$ to select galaxies that are dominated by the exponential component (i.e. spiral galaxies).

We combine the value $frac_{\rm deV}$ with the exponential profile axis ratio $q_{\rm exp}$ to make the primary classification. In Fig. 3.1 we show the $frac_{\rm deV}$ versus $q_{\rm exp}$ plot; crosses are spiral galaxies and circles are elliptical galaxies as classified by Einasto et al. (2010). As seen in this Figure, all galaxies, which have $q_{\rm exp} < 0.4$, are spirals; the corresponding distribution in Banerji et al. (2010) confirms that. Also van den Bosch & van de Ven (2009) showed that for elliptical galaxies, the axial ratio is mostly greater than 0.5. We see also that when moving toward lower values of $frac_{\rm deV}$, the spiral dominated region becomes larger: the value of $q_{\rm exp}$ can be larger. This is expected, since low values of $frac_{\rm deV}$ point to disc-dominated objects. In our classification we will take this behaviour into account and it agrees well with the colour distribution of galaxies. The dashed line in Fig. 3.1 shows the limit for spiral galaxies. We will also leave unclassified those galaxies where $frac_{\rm deV} > 0.95$ or $frac_{\rm deV} < 0.05$, since classification at these extreme values may be rather uncertain.

For all other galaxies that can not be classified directly in the $frac_{\rm deV}$ versus $q_{\rm exp}$ plot, we use the galaxy colours as additional parametres. The distributions of galaxy colours for different types of galaxies have taken from Banerji et al. (2010) and Lintott et al. (2008); additionally, we have checked these distributions, using our own small sample of visually classified galaxies. The details of classification are given in Tempel et al. (2011a).

Figure 3.1 shows our classification in the $frac_{\rm deV}$ versus $q_{\rm exp}$ plot: all galaxies that are marked by red points, are classified as spirals; all galaxies that are marked with blue points, are classified as ellipticals; grey points are non-classified galaxies. Figure 3.2 shows the classical colour magnitude diagram for our galaxies; spirals are statistically bluer and fainter and ellipticals are brighter and redder. Since we use also other parameters than colours for galaxy classification, some of the spirals are located in the region, where mostly ellipticals reside; however, the number of these spirals is relatively small (20% of all spirals). Most of these red spirals are those where $frac_{\rm deV}$ is large: e.g., their luminosity profile is bulge-dominated, but the visible axial ratio ($q_{\rm exp}$) is small and therefore we have classified these galaxies as spirals. Practically all the disc-dominated spirals are located below elliptical galaxies in this colour-magnitude diagram.

Recently, Huertas-Company et al. (2011) have published automated morphological classification of galaxies from the SDSS sample. They associate with each galaxy

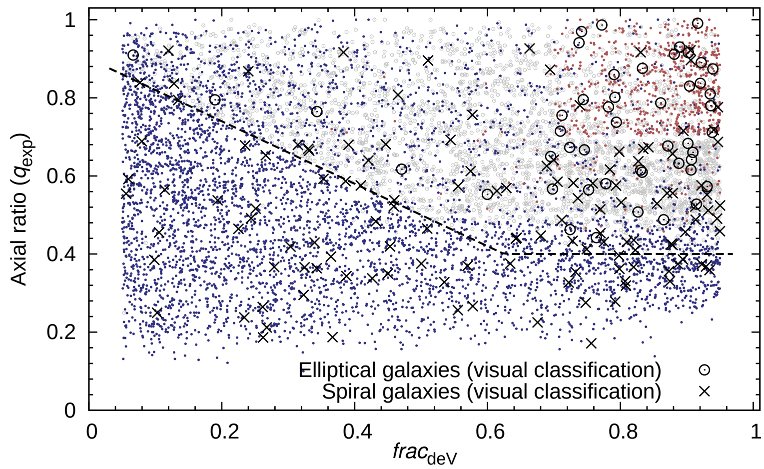

Figure 3.1: Classification of galaxies into spirals and ellipticals. Red points (mostly in the upper right corner) are ellipticals and blue points (mostly below the dashed line) are spirals. Empty circles are elliptical galaxies classified by visual inspection; crosses are visually classified spiral galaxies. Grey points are galaxies where classification is unclear. The dashed line shows our spiral galaxy selection criterion (see text).

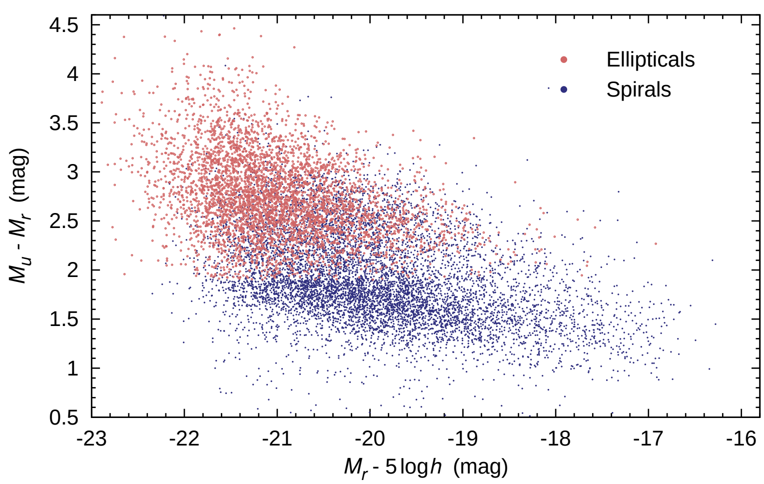

Figure 3.2: The colour-magnitude diagram for spiral and elliptical galaxies. The spirals are marked by blue dots (the lower cloud) and the ellipticals by red dots (the upper cloud).

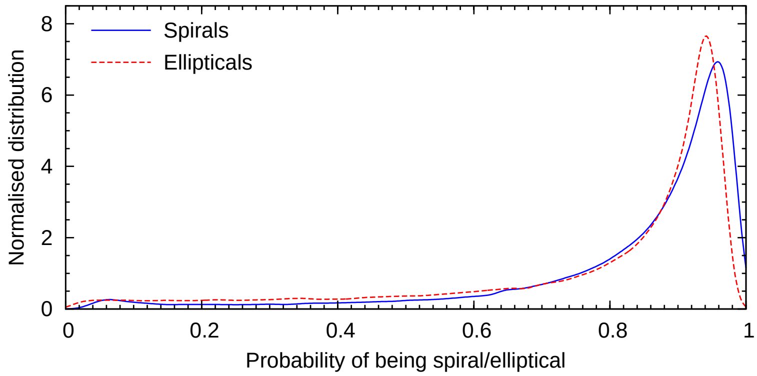

Figure 3.3: The distribution of the Huertas-Company et al. (2011) probabilities of being early- or late-type galaxies for our classified spirals (blue solid line) and ellipticals (red dashed line).

a probability of being in the four morphological classes: two early-type classes (E and S0) and two late-type classes (Sab and Scd). We assign the Huertas-Company et al. (2011) probability of being early- or late-type to our galaxies. In Fig. 3.3 the distributions of these probabilities are shown. It is well seen that our classification agrees well with the Huertas-Company et al. (2011) classification.

In our classification for the SDSS sample about half of the galaxies (45%) are spirals, about one quarter (25%) are ellipticals and for 30% of galaxies, the classification is unclear.

3.2 Restoring the intrinsic inclination angle

The intrinsic absorption is closely related to the morphology of a galaxy. Additionally, the attenuation depends on the inclination angle (Tuffs et al. 2004; Driver et al. 2007b; Tempel et al. 2010). To take this effect into account, we need to know the intrinsic inclination for every galaxy. Since the intrinsic inclination angle depends both on the visible and the intrinsic axial ratios, we can restore the intrinsic inclination angle only statistically. When studying dust attenuation, the inclination angle is needed only for spiral galaxies.

Assuming that we know the axial ratios and the intrinsic inclination angle of a galaxy, we can calculate the apparent axial ratio $q \equiv b/a$ using the formula given by Binney (1985)

$$\left(\frac{b}{a}\right)^2 = \frac{A + C - \sqrt{(A-C)^2 + B^2}}{A + C + \sqrt{(A-C)^2 + B^2}}, \tag{3.1}$$

where

$$A \equiv \frac{\cos^2\theta}{\xi^2}\left(\sin^2\phi + \frac{\cos^2\phi}{\zeta^2}\right) + \frac{\sin^2\theta}{\zeta^2}, \tag{3.2}$$

$$B \equiv \left(1 - \frac{1}{\zeta^2}\right)\frac{1}{\xi^2}\cos\theta\sin 2\phi, \tag{3.3}$$

$$C \equiv \left(\frac{\sin^2\phi}{\zeta^2} + \cos^2\phi\right)\frac{1}{\xi^2}. \tag{3.4}$$

In the last equation, $1 \geq \zeta \geq \xi$, ξ is the ratio of the shortest semi-axis to the longest semi-axis and ζ is the axial ratio of the two longest semi-axes. θ is the inclination of a galaxy – the angle between the plane of the galaxy and the plane of the sky; ϕ is the angle between the the longest semi-axis and the line of sight.

The SDSS gives the apparent axial ratio q of the galaxy image. For spiral galaxies we use the r-band axial ratio $q_{\rm exp}$, taken from the best fit of the image with an exponential profile convolved with the point spread function (Stoughton et al. 2002).

To calculate the inclination angle θ from Eq. (3.1), we use a statistical approach. We assume that the longest semi-axes are randomly oriented in space and the ratios ξ and ζ are random, with given probability distributions. We use the Monte Carlo method to select random values for the inclination angle and axial ratios.

To find the intrinsic ratio of the shortest semi-axis to the longest semi-axis, we use galaxies with a small value of $q_{\rm exp}$ and assume that this value is the ratio ξ. As demonstrated by Shao et al. (2007), the apparent axial ratio depends on the apparent size and therefore, the value of ξ depends also on it. More details are given in Tempel et al. (2011a).

Since the discs of spiral galaxies are not round, the ratio ζ is less than one. Ryden (2004) showed that the intrinsic axial ratio of discs is $0.85^{+0.1}_{-0.2}$, that is slightly smaller than derived by Andersen & Bershady (2002) ($0.9^{+0.06}_{-0.18}$). Both values are close to that derived for elliptical galaxies by van den Bosch & van de Ven (2009). In this study we adopt the ζ distribution with the maximum at 0.9; toward larger values, the 2-σ deviation is 0.05, and toward smaller values this deviation is 0.1. Additionally we demand that the value of ζ has to be larger than the shortest-to-longest axis ratio.

3.3 Model for dust attenuation calculation in galaxies

To study the dust attenuation in galaxies, and how the attenuation depends on the viewing angle of a galaxy, we use the model of the nearby galaxy M 31. In this section we construct the model of M 31, change the viewing angle of the galaxy and study how the attenuation changes. The details of model construction and application to M 31 are described in Tempel et al. (2010) and Tempel et al. (2011b).

The physical properties of dust and the extinction of the stellar light in a galaxy are determined by an interplay between the spatial radiation field and the dust grains at each location within the galaxy. The calculations of the intrinsic extinction in a galaxy should thus be based on the spatial luminosity distribution of the galaxy and the spatial density distribution of the dust grains.

3.3.1 The density distribution model for the stellar components

In this subsection, we develop a sufficiently flexible model for describing the spatial distribution of the luminosity of a galaxy. A two-dimensional projection of the model can be compared to the observed surface brightness distribution and the model parameters can be adjusted.

The model galaxy is given as a superposition of its individual stellar components. Each visible component is approximated by an ellipsoid of rotational symmetry with a constant axial ratio q; its spatial density distribution follows Einasto's law

$$l(a) = l(0)\exp\left[-\left(\frac{a}{ka_0}\right)^{1/N}\right], \tag{3.5}$$

where $l(0) = hL/(4\pi q a_0^3)$ is the central density and L is the luminosity of the component; $a = \sqrt{r^2 + z^2/q^2}$, where r and z are two cylindrical coordinates; a_0 is the harmonic mean radius that characterises the real extent of the component. The coefficients h and k are normalising parameters, dependent on the structure parameter N. The definition of the normalising parameters h and k and their calculation is described in appendix B of Tenjes et al. (1994). The luminosity density distribution (Eq. (3.5)) proposed by Einasto (1965) is similar to the Sérsic (1968) law for surface densities. The differences between the Sérsic law and the two-dimensional projection of Eq. (3.5) are listed in Tamm & Tenjes (2005).

In the case of a young disc the spatial density distribution is assumed to have a toroidal form, approximated as a superposition of positive and a negative density components, both following Eq. (3.5).

The density distributions of all visible components are projected along the line of sight and their sum yields the surface brightness distribution of the model

$$L(A) = 2\sum_j \frac{q_j}{Q_j}\int_A^\infty \frac{l_j(a)a\,\mathrm{d}a}{(a^2 - A^2)^{1/2}}, \tag{3.6}$$

where A is the major semi-axis of the equidensity ellipse of the projected light distribution and Q_j are their apparent axial ratios $Q^2 = \cos^2 i + q^2 \sin^2 i$. The inclination angle between the plane of the galaxy and the plane of the sky is denoted by i. The summation index j designates each visible component.

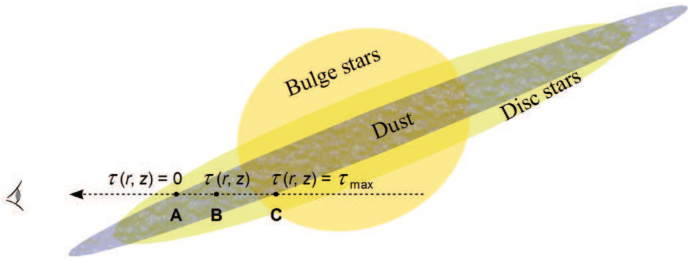

Figure 3.4: Geometry of the dust disc model. The line-of-sight optical depth for three positions A, B, and C is indicated. The figure is illustrative only.

3.3.2 The dust disc component

Let us now implant a dust disc component into our galaxy model, allowing us to calculate absorption along each line of sight through the galaxy.

Equation (3.6) will give the luminosity density along a line-of-sight, if no dust extinction exists. The intrinsic luminosity density for each component can be calculated by the equation

$$L(X,Y) = \int_X^\infty \frac{\sum_{j=1}^{2} \left[l(r,z_j)\,\mathrm{e}^{-\tau(r,z_j)} \right]}{\sin i \sqrt{r^2 - X^2}} r\,\mathrm{d}r, \tag{3.7}$$

$$z_{1,2} = \frac{Y}{\sin i} \pm \frac{\sqrt{r^2 - X^2}}{\tan i}, \tag{3.8}$$

where $l(r,z)$ denotes the spatial luminosity density (Eq. (3.5)) of the component, $L(X,Y)$ is the corresponding surface brightness distribution, X and Y are the coordinates in the plane of the sky, and $\tau(r,z)$ is the optical depth along the line-of-sight (see Fig. 3.4).

The optical depth $\tau(r,z)$ is zero between the observer and the dust disc and $\tau(r,z) = \tau_{\max}$ behind the dust disc. $\tau_{\max}$ is the total optical depth along a given line of sight and is thus a function of (X,Y). Inside the dust disc, $\tau(r,z)$ varies between 0 and $\tau_{\max}$.

The optical depth between the observer and a point inside the dust disc can be written as

$$\tau(r,z) = \tau_{\max}(X,Y) \frac{\int_{\mathrm{A}}^{\mathrm{B}} n_{\mathrm{dust}}(s)\,\mathrm{d}s}{\int_{\mathrm{A}}^{\mathrm{C}} n_{\mathrm{dust}}(s)\,\mathrm{d}s}, \tag{3.9}$$

where integration is done along the line of sight s and $n_{\rm dust}(s)$ is the density of the dust disc.

To gain a simple but nevertheless flexible model for the dust disc, we adopt the following form for $n_{\rm dust}$:

$$n_{\rm dust}(r,z) = f_{\rm dust}(r) \cdot n(a), \tag{3.10}$$

where $n(a)$ is the exponential law (Eq. (3.5)) and $f_{\rm dust}(r)$ describes deviations from the exponential law. The density of dust decreases exponentially in the z-direction according to Eq. (3.5). Multiplication by $f_{\rm dust}(r)$ allows the density behaviour to be more flexible along the r-direction.

Assuming that the column density of dust is proportional to the far-infrared flux, the map of $\tau_{\rm max}(X,Y)$ can be derived from far-infrared imaging:

$$\tau_{{\rm max},f}(X,Y) = c_{f,\lambda',T'} F_{\lambda'}(X,Y) \frac{\lambda^{\beta} B(\lambda',T')}{(\lambda')^{\beta} B(\lambda, T(X,Y))}, \tag{3.11}$$

where $F_{\lambda'}(X,Y)$ is the far-infrared flux map at a reference wavelength λ', T' is a reference temperature, $T(X,Y)$ is a map of the dust temperature, $B(\lambda,T)$ is the black-body function, β is the dust emissivity index, and c is an empirical calibration constant, corresponding to the reference wavelength and temperature, and to the filter f of the optical observations ($c \propto A_\lambda/E(B-V) = R_V A_\lambda/A_V$).

Equation (3.11) gives the total extinction map in the plane of the sky. To calculate the actual intrinsic extinction, we also need the density distribution of the dust disc $n_{\rm dust}(r,z)$ for Eq. (3.9). We can compare the projection of the model density distribution (given by Eq. (3.6)) with the observed column density distribution for dust (i.e. the far-infrared maps) to determine the function $f_{\rm dust}(r)$ and the parameters for $n(a)$. The observed column density of the dust disc is thereby converted into its spatial density. More precisely, we can only determine the shape of the density distribution of the dust disc; its absolute calibration $n(0)$ remains unknown. In the present case, the calibration constant cancels out in Eq. (3.9) and is not required for our model.

In the final step, the derived optical depth map $\tau_{{\rm max},\lambda}(X,Y)$ and the function $n_{\rm dust}(r,z)$ are inserted into Eq. (3.9) and the extinction-corrected surface brightness along each line of sight can be calculated from Eq. (3.7).

3.3.3 The photometrical model and the dependence of attenuation on inclination

The model described above was applied to M 31 in Tempel et al. (2010) and Tempel et al. (2011b). In the context of the present thesis, we are interested only in the dependence of attenuation on the viewing angle for a galaxy.

With the help of the model, we can study the dependence of dust extinction on the inclination angle, on the total optical depth and on the thickness of the dust disc. In Fig. 3.5 we show the results for three relative thicknesses (the axial ratios q) of the dust disc: 0.005, 0.014, and 0.042, designated as 'thin', 'medium', and 'thick', respectively, and for three values of the optical depth τ: $0.5\tau_{\max}$, $1.0\tau_{\max}$, and $2.0\tau_{\max}$, where $\tau_{\max}$ is the optical depth as derived for M 31. The other parameters have been set according to the model derived for M 31. In the upper panel, the extinction is calculated for the whole galaxy, in the middle panel, for a pure bulge component, and in the lower panel, for a pure disc component.

In the case of the above-described model of M 31, the total extinction would be maximum if the inclination angle of the galaxy were approximately 88°. At lower inclination angles (a more face-on orientation) the total extinction decreases as a result of the decreasing line-of-sight optical depth. For an edge-on galaxy ($1 - \cos(i) = 1$), the visible area of the dust disc becomes negligible, and the total extinction is low. It is seen from Fig. 3.5 that extinction is lower for the disc component than for the bulge and increases more rapidly while moving to higher inclination values. The extinction maximum occurs at higher inclinations for a disc than for a bulge. A similar dependence of dust attenuation on inclination was predicted by Tuffs et al. (2004) and was confirmed observationally by Driver et al. (2007b), using different models and data.

Figure 3.5 also shows that the extinction maximum shifts slightly towards lower inclination angles as the optical depth increases; of course, the total extinction increases as well. On the other hand, the total extinction is almost insensitive to the thickness of the dust disc at low and intermediate inclination angles. This is expected, since the extinction of light emitted outside the dust disc only depends on the optical depth of the dust disc and the geometry of the dust disc affects only the extinction of light emitted inside the dust disc. In most cases, the line-of-sight thickness of the dust disc is smaller than that of the stellar components and therefore the total extinction does not change when changing the geometry of the disc.

For very high inclination angles, the thickness of the dust disc becomes much more important, especially if the optical depth is high as well. However, already for M 31 and for galaxies at lower inclination angles, the line-of-sight optical depth is the dominant factor.

3.4 Accounting for dust attenuation in spiral galaxies

In this section we describe the necessary steps to take dust attenuation into account when estimating the luminosity function (LF) of galaxies. We will use the morphological classification, derived in Sect. 3.1; dust attenuation will be considered for spiral galaxies only. Late-type spiral galaxies have generally more dust than early-type

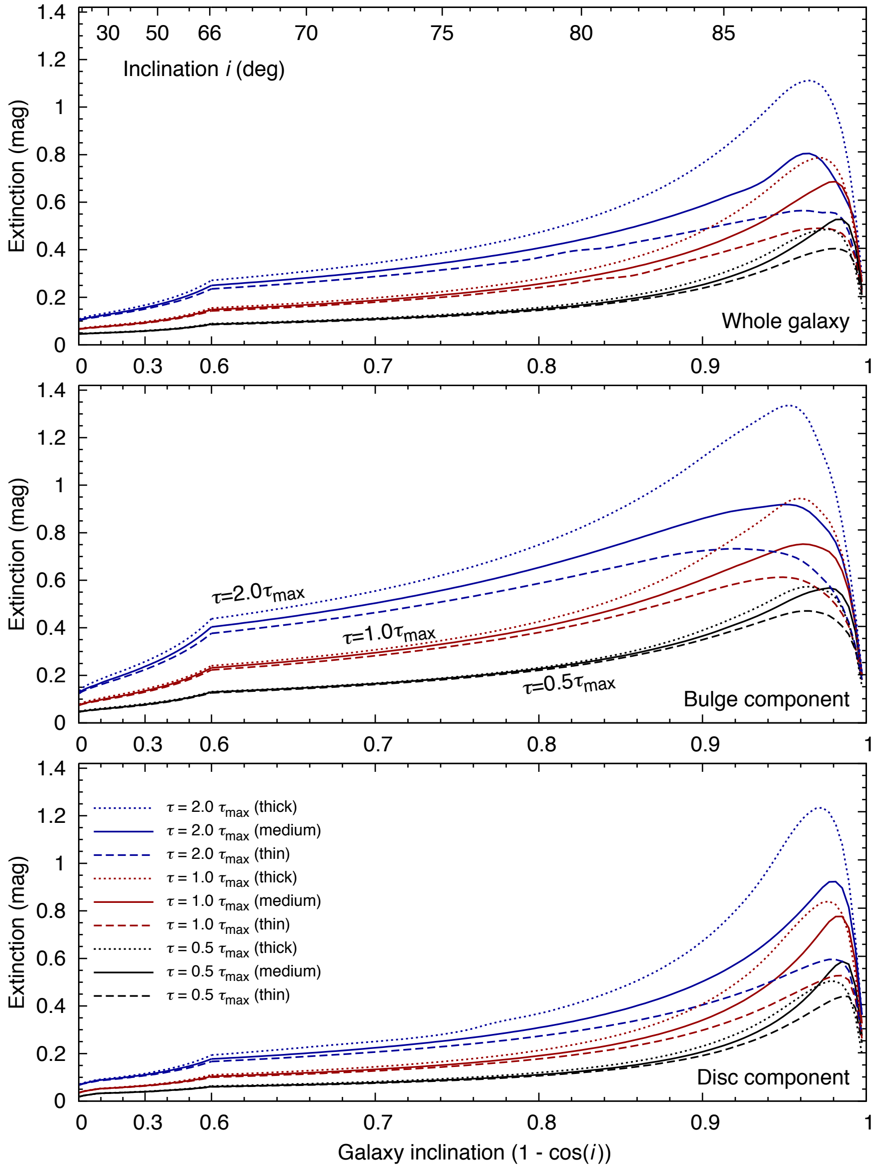

Figure 3.5: Integrated dust extinction inside M 31 in the V-band as a function of the inclination of the galaxy for several optical depths and dust disc thicknesses. The parameter $\tau_{\max}$ is the optical depth used in our model. *Upper panel* shows the extinction for the whole galaxy, *middle panel* – for a bulge component, and *lower panel* – for a disc-like component.

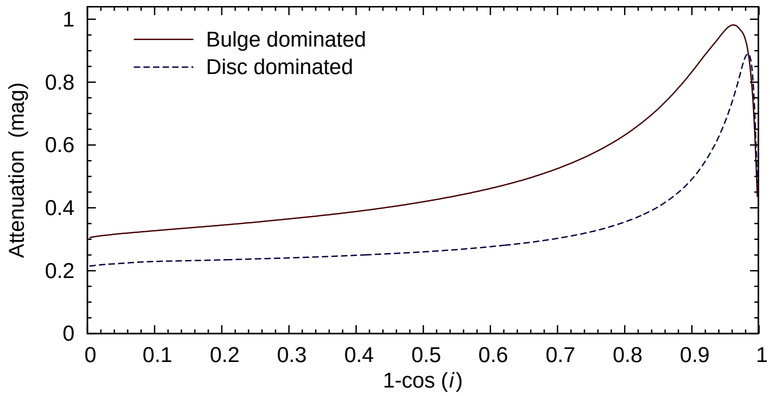

Figure 3.6: The dependence of attenuation on galaxy inclination for disc-dominated and bulge-dominated spiral galaxies.

spirals, thus dust attenuation is higher there; we will take that into account. It is known that blue galaxies have more dust and therefore dust attenuation is larger; for redder galaxies dust attenuation is less important. The colour of a galaxy is also an indicator of the galaxy type. Muñoz-Mateos et al. (2009) have shown that dust attenuation for spiral galaxies has a large scatter and is nearly constant for mid- and late-type spirals. For early-type spirals, the attenuation decreases.

Additionally, dust attenuation also depends on the inclination angle, as shown in Sect. 3.3.3. The inclination-dependent attenuation curves used in this study are shown in Fig. 3.6. To classify galaxies into bulge-dominated or disc-dominated spirals, we use the parameter $frac_{\mathrm{deV}}$: for lower values, the galaxy is disc-dominated and for larger values, the galaxy is bulge-dominated. We use linear interpolation for $frac_{\mathrm{deV}}$ when moving from disc-dominated galaxies to bulge-dominated galaxies. Since we do not know how the attenuation depends exactly on the inclination angle and galaxy colour, we have used only the general trends to statistically correct the LF. We calibrated the corrections by comparing the LFs for galaxies at different inclination angles. For each galaxy subtype (colour) we modify the attenuation curves given in Fig. 3.6, to minimise the differences between the shapes of the LFs for different inclination angles. For that, we multiply the attenuation curve by a factor x that depends on the galaxy rest-frame u-r colour. For red spiral galaxies (with u-$r > 2.2$), $x = 0.5$ provided the best fit. This is expected, because red galaxies tend to contain less dust. For galaxies with u-$r < 1.8$, $x = 1.0$. For the intermediate galaxies, the factor x changes linearly with the u-r colour.

Figure 3.7 shows the LFs for the observed and attenuation-corrected luminosities for the edge-on and the face-on samples of galaxies. For the edge-on sample

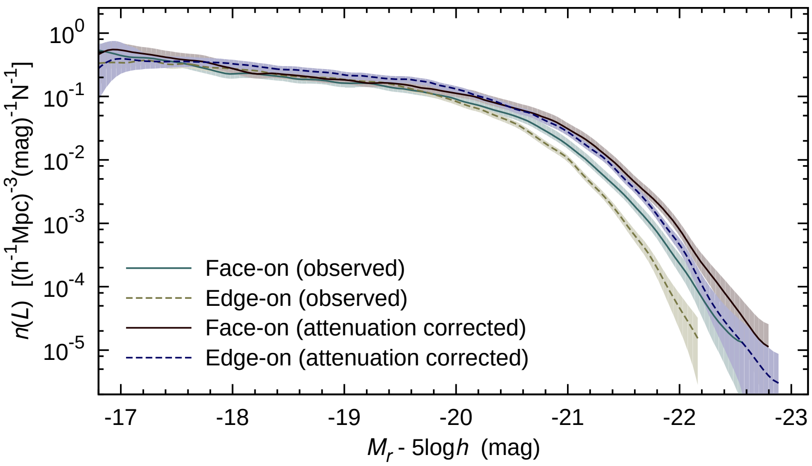

Figure 3.7: Luminosity functions for the edge-on and face-on samples of spiral galaxies. Dark lines show the attenuation-corrected luminosity functions, dim lines show the luminosity functions for observed luminosities. The filled areas show the 95% confidence regions.

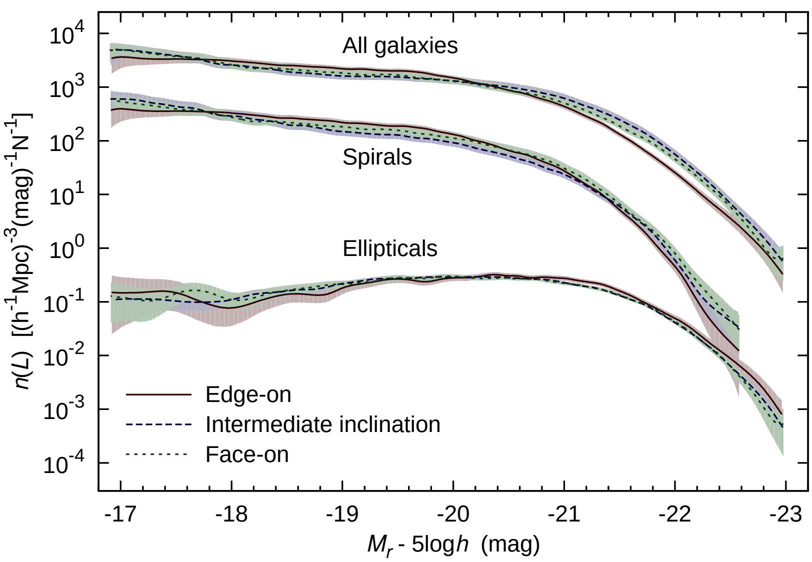

Figure 3.8: Luminosity functions for edge-on, face-on, and intermediate inclination angle galaxies. We show the luminosity functions for spirals, ellipticals, and all galaxies. The luminosity functions of spirals and all galaxies are shifted up by three and four units in logarithmic scale, respectively, to better separate the three types of galaxies.

$\cos\theta < 0.2$, for the face-on sample $\cos\theta > 0.8$. It is well seen that the observed LFs are quite different for the face-on and edge-on galaxies, while the attenuation-corrected LFs are quite similar. Figure 3.8 shows the attenuation-corrected luminosity functions for the spirals and the ellipticals and for all galaxies together at different inclination angles: edge-on, face-on, and intermediate inclination angles. The intermediate inclination angle sample is defined by $0.5 < \cos\theta < 0.6$. We see that the LF is nearly inclination independent. For the edge-on spirals and for all edge-on galaxies together, small differences are still noticeable.

From Figs. 3.7 and 3.8 we can conclude, that the inclination angles and the attenuation for spiral galaxies have been restored correctly for subsequent statistical analysis and for luminosity function calculations.

CHAPTER 4
LUMINOSITY FUNCTION FOR THE 2DFGRS SAMPLE

This chapter covers the main results of Tempel et al. (2009). Since we modified slightly our method to calculate the luminosity function after the paper was published, we have recalculated all the luminosity functions presented in this chapter, using the method described in Sect. 2.4. Additionally, we use a slightly different environmental density calculation algorithm and thereof the density limits for various environments have been changed. The method to calculate environmental densities used in this thesis is described in Sect. 2.5. Consequently, the luminosity functions presented in this thesis are slightly different from those given in Tempel et al. (2009). However, the general picture remains the same. The 2dFGRS catalogue used is described in Sect. 2.1, and the corresponding group catalogue is described in Tago et al. (2006).

4.1 The luminosity function in different environments

Calculation of environmental densities around each galaxy is described in Sect. 2.5. We have divided all galaxies into four classes, according to the value of the global environmental density D. The limiting densities for this four classes are 0.8, 2.0, and 5.0 in units of the mean density. The limits are chosen so that the lowest (D1) and highest (D4) density regions include roughly 10% of all galaxies, and two intermediate regions (D2 and D3) include a roughly equal number of galaxies (see Sect. 2.5 for more details). The numbers of galaxies in each sample are given in Table 2.1. To study in detail the luminosity function of galaxies in groups, we shall derive the luminosity functions for the group brightest (first-ranked), second-ranked, and satellite galaxies separately. Additionally, we derive the luminosity functions for isolated galaxies.

The study of galaxies in groups is tightly related with the halo occupation distribution models (see e.g. Yang et al. 2004; Zehavi et al. 2005; van den Bosch et al. 2007). In these studies, the properties of central and satellite galaxies and their surrounding haloes are analysed. In this chapter, we use the luminosity function to study the galaxies in groups. A short comparison between our results and the halo occupation distribution models are given in Chapter 6.

4.1.1 The brightest group galaxies

We use our galaxy samples and the catalogue of groups of galaxies to calculate the LF for the first-ranked (brightest group) galaxies. The galaxy catalogue by

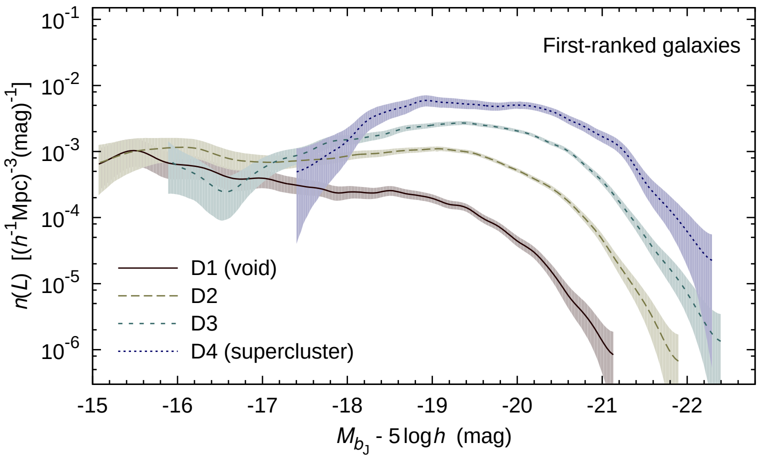

Figure 4.1: Differential luminosity functions of first-ranked galaxies. The functions have been calculated for four classes of global environmental density: D1, D2, D3, D4 (from voids to superclusters). The filled areas show the 95% confidence regions.

Tago et al. (2006) includes 25215 groups with two or more members. The catalogue gives for each group the luminosity of the first-ranked galaxy (the most luminous galaxy in the b_J-filter). In the present study we shall not use other galaxy properties, such as spectral type, colour index or possible activity, to identify the first-ranked galaxies. These morphological aspects deserve a more detailed study that is outside the scope of the present investigation.

We calculated the differential LFs of first-ranked galaxies in various environments. The numbers of first-ranked galaxies used are given in Table 2.1 (see the 2dFGRS groups row, since the number of groups equals the number of first-ranked galaxies).

The differential LFs of first-ranked galaxies are shown in Fig. 4.1 for different environmental densities. We note that the normalisation of the LF in the present thesis is different from that in Tempel et al. (2009). In the present thesis, the LFs are normalised to the volume of each environmental density, while in Tempel et al. (2009) the LFs are normalised to the volume of the full sample. The same is valid for other LFs presented in this section.

Figure 4.1 shows that there exist large differences between LFs in different environments. The brightest first-ranked galaxies in voids have a factor of 3 to 4 lower luminosity than the brightest first-ranked galaxies in regions of higher environmental densities. For this reason the whole LF of void first-ranked galaxies is shifted toward lower luminosities. While moving toward higher environmental densities, there are more brighter galaxies per unit volume. Meanwhile, the numbers of faint galaxies

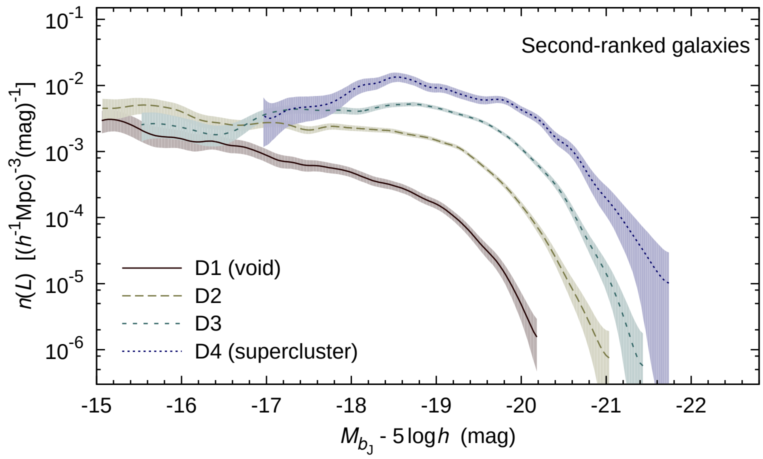

Figure 4.2: Differential luminosity functions of the second-ranked galaxies of groups in different global environments. The filled areas show the 95% confidence regions.

are almost the same in all environments.

The second large difference between the first-ranked galaxy luminosities in various environments is the clear decrease of the numbers of faint galaxies in the most dense (supercluster) environment. Contrary, in the least dense (void) environment, the numbers of faint galaxies increase toward smaller luminosities. The LFs for the two intermediate density regions (D2 and D3) show that the changeover from one region to the other is smooth. Additionally, the supercluster environment forces the decrease of the faint end of the LF also for other galaxies (satellites and isolated galaxies), but in this case, the decrease is shallower, as we shall see below.

4.1.2 The second-ranked galaxies of groups

We define the group second-ranked galaxy as the most luminous satellite galaxy in the group: it is the second luminous galaxy in the group.

In Fig. 4.2 we plot the differential LFs of the second-ranked galaxies of groups in different environments. The overall picture is similar to the LFs of the first-ranked galaxies. The primary difference is that the bright end of the LF (number densities of bright galaxies) for the second-ranked sample is shifted toward lower luminosities.

In Tempel et al. (2009) we proposed that the second-ranked galaxies in high density environments had been first-ranked galaxies before they were drawn into a larger cluster via merging of groups into larger systems. As a simple test of this, we plot in Fig. 4.3 the differential LFs of two populations: the first population consists of the second-ranked galaxies in the supercluster environment; the second population

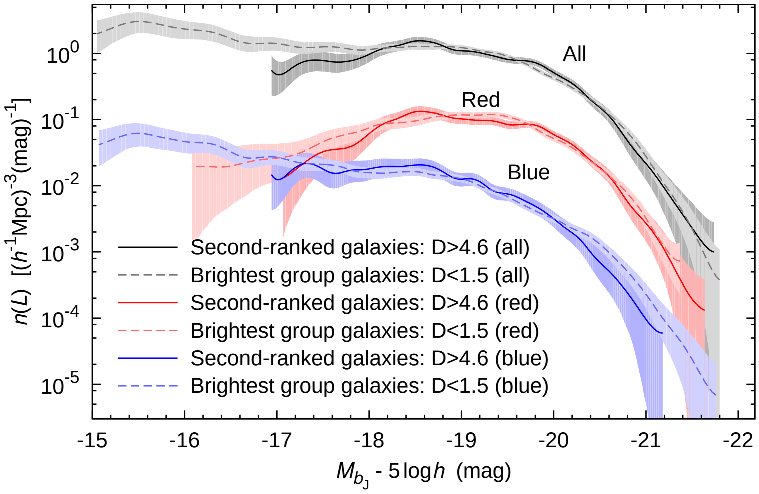

Figure 4.3: The differential luminosity functions of two populations: solid lines – the second-ranked galaxies in the supercluster environment ($D > 4.6$); dashed lines – the first-ranked galaxies in the void environment ($D < 1.5$). The upper (black) lines are for all galaxies; the middle (red) lines are for the red population (shifted down by one unit in the $\log(n(L))$ scale); the bottom (blue) lines are for the blue population (shifted down by two units in the $\log(n(L))$ scale). The filled areas show the 95% confidence regions.

consists of the first-ranked galaxies in the void region. The density limits (1.5 and 4.6) in Fig. 4.3 are chosen to compare better the high and low density regions. We see that these two distributions are pretty similar. There are differences at the faint end of the LFs, but these are caused by the environment; there are only a few faint first- and second-ranked galaxies in high-density regions. Thus we see that the second-ranked galaxy LF in high-density regions is similar to the first-ranked galaxy LF in the low-density environment. In this test we assume that there is no significant evolution of galaxy luminosity during the merger in high density environments for these galaxies, which are the brightest galaxies of groups before the merger. This assumption is plausible, since in high-density regions rapid evolution of the first-ranked galaxies occurs mainly in the early stages of evolution and before the last merger event, the evolution of the first-ranked galaxies should be finished.

To show that this similarity is not accidental, we divided these galaxies into two samples (red and blue galaxies), using information about the colours of galaxies (the rest-frame colour index, $col = (B - R)_0$, Cole et al. (2005)). We used the limit $col = 1.07$ to separate the populations of red (passive) and blue (actively star-forming) galaxies. For these two samples the LFs are still similar (see Fig. 4.3), only

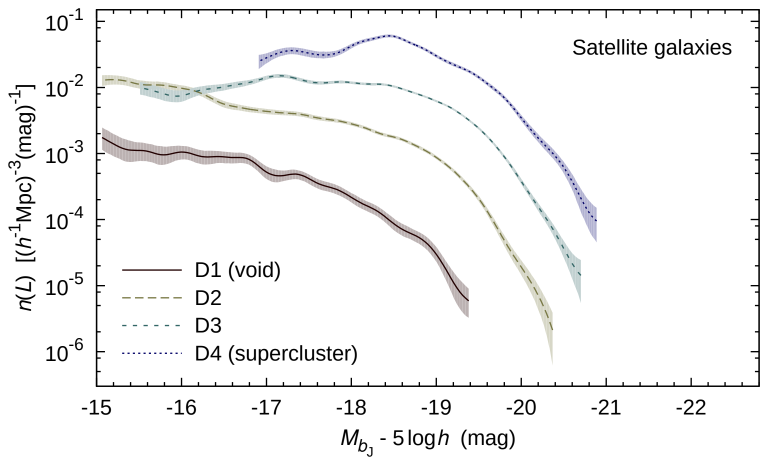

Figure 4.4: The differential luminosity functions of satellite galaxies in different global environments. The filled areas show the 95% confidence regions.

the supercluster galaxies are in average 0.15 mag redder than the void galaxies. This shift was also seen in Einasto et al. (2007) where it was shown that not only the brightest galaxies, but all galaxies in superclusters are redder than those in voids.

As a conclusion, the first-ranked galaxy population is different from that of the satellite (second-ranked) galaxy population, but the changeover from one population to the other is smooth, depending also on the global environment, where the galaxies/groups are located.

4.1.3 Other satellite galaxies

We define the group satellite galaxies as all galaxies in groups, excluding the first- and second-ranked galaxies.

In Fig. 4.4 we show the differential LFs of the satellite galaxies in groups. These LFs are similar to the LFs of the second-ranked galaxies, except at the bright end, where the satellite galaxy LFs have slightly smaller luminosities, as expected by definition. The primary difference is that when moving toward higher density environments, there are more satellite galaxies per unit volume than of the second-ranked galaxies. For the second-ranked galaxies, at the faint end of the LF, all environments have a roughly equal number of galaxies per unit volume, while for the satellite galaxies, there are differences between various environments: the most noticeable difference is for the void environment. This suggests that the groups are rather small in voids. We arrive at the same conclusion, when looking at the numbers of groups and galaxies in Table 2.1: the mean number of galaxies per group in the void environment

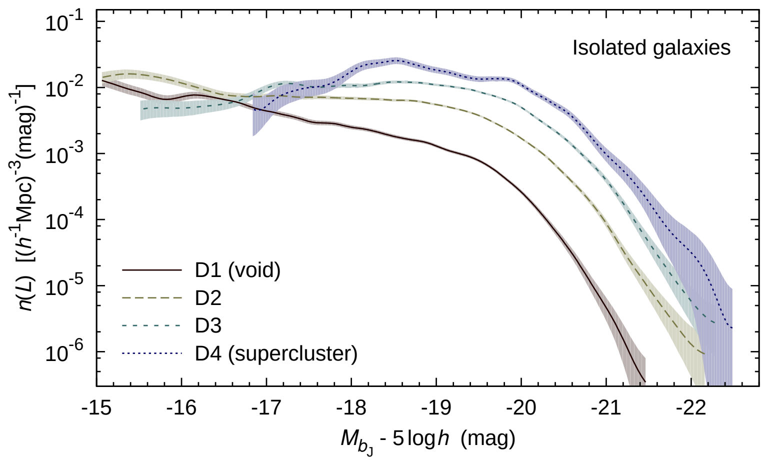

Figure 4.5: Differential luminosity functions of isolated galaxies in different global environments. The filled areas show the 95% confidence regions.

is rather small. Later, in Fig. 4.6 we will see that in the void environment, the LFs of the second-ranked and satellite galaxies are rather similar. The last similarity also suggests that the evolution/formation of void satellite galaxies is similar: i.e., there are no big differences between the second-ranked and other satellite galaxies in the groups in voids. This is reasonable, since in the void environment mergers are rare, and the mechanism that formed the second-ranked galaxies in high-density environments, does not work here; the second-ranked galaxies form and evolve as other satellite galaxies in the void environment.

Similarly for the first-ranked galaxies, satellites and the second-ranked galaxies in the highest density environment have a decreasing faint end of the LF.

4.1.4 Isolated galaxies

We define all galaxies that do not belong to groups/clusters in the Tago et al. (2006) group catalogue, as isolated galaxies. In this section we present the LFs of isolated galaxies; we shall discuss the nature of isolated galaxies later, in a separate section.

In Fig. 4.5 we show the differential LFs of isolated galaxies in different environments. The LF of isolated galaxies in the supercluster environment is decreasing at the faint end (similar to other populations). The differences in the LFs of bright isolated galaxies between various environments are slightly smaller than for other populations.

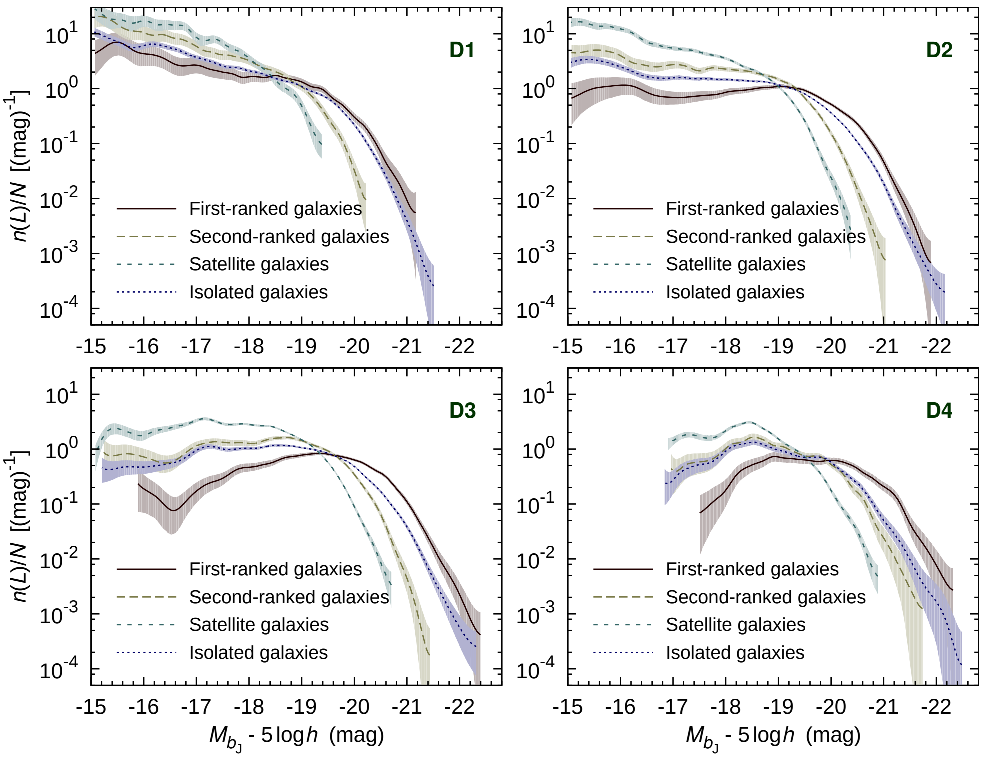

Figure 4.6: Differential luminosity functions in different environments and for different galaxy populations. Solid lines show the first-ranked galaxies; dashed lines – the second-ranked galaxies; short-dashed lines – satellite galaxies; dotted lines – isolated galaxies. The filled areas show the 95% confidence regions.

4.1.5 Comparison of LFs in different environments

To see more clearly the trends between different populations in various environments, we show in Fig. 4.6 differential LFs of galaxy populations in various environments. In Fig. 4.6, the LFs have been normalised to the mean number density. Each panel represents a different environment, and in each panel we show the LFs of different populations (the first-ranked, second-ranked, satellite, and isolated galaxies).

Figure 4.6 (upper-left panel) shows that in voids, the bright end of the LFs of all galaxy populations is shifted toward lower luminosities. Interestingly, the bright end of the LF for isolated galaxies in voids is comparable to that of the first-ranked galaxies. We discuss the possible reasons for that in the next section. The LFs of the second-ranked galaxies and of other satellites are comparable.

In the D2 environment (Fig. 4.6, upper-right panel) the bright ends of the LFs for the first-ranked galaxies and for isolated galaxies are similar, while the brightest second-ranked galaxies and satellite galaxies are fainter. The LFs of the second-ranked galaxies and of other satellites are comparable, although there is a slight increase of the LF of satellite galaxies at the lowest luminosities. The LF of the first-ranked galaxies, in contrary, has a plateau at the faint end, without signs of distinct increase.

The LFs for the D3 environment are shown in the lower-left panel of Fig. 4.6. For a wide range of luminosities, the LF for the first-ranked galaxies is slowly decreasing toward fainter luminosities, while the LFs for other galaxy populations have a plateau (or a slight decrease at the faintest end).

The LFs for the supercluster (D4) environment are shown in Fig. 4.6, lower-right panel. We notice the striking difference between the LFs in superclusters and the LFs in other environments: here all LFs have a well-seen decrease at the faint end of the LF, which for the first-ranked galaxies was seen already in the D3 environment.

When comparing the first-ranked and isolated galaxies, the LFs in the void (D1) environment are quite similar. In the void environment, the differences between the first-ranked and isolated galaxies are the smallest: i.e., in the void environment the first-ranked galaxies of groups are fainter than those in higher density environments, which was also noticed by Einasto et al. (2007). When moving toward higher densities, the differences between these two populations increase: the bright end of the LF of the first-ranked galaxies becomes more luminous and at the faint end, isolated galaxies start to dominate.

Another comparison can be made between the second-ranked and other satellite galaxies. In the void (D1) environment, the LFs of these populations are similar, except at the bright end, where small differences are noticeable. These differences at the bright end are noticeable also in other environments, which is excepted, since by definition the satellite galaxies are fainter than the second-ranked galaxies.

Furthermore, at the faint end of the LF, in the void environment, the differences between these four populations are quite small. When moving toward higher global environments, the differences at the faint end of the LF are increasing. This suggests that in the void environment, the formation of faint galaxies is similar for all populations. In the void environment, mergers are not the dominant factor in galaxy evolution and quiescent evolution can form galaxies of all types in a quite similar way.

In summary, the most dense environment (superclusters) is different from other environments: the numbers of faint galaxies decrease while moving toward yet fainter galaxies, and the brightest first-ranked galaxies are brighter than the first-ranked galaxies in lower density environments (compared with other populations).

4.2 Nature of isolated galaxies

We propose that a fraction of isolated galaxies are the first-ranked galaxies of groups/clusters, which have all its fainter members outside the visibility window of the survey. A direct way to verify this assumption is actual observation of fainter galaxies around isolated galaxies; this would need a dedicated observational programme. However, we can check if the presence of fainter companions is compatible with other data on the distribution of magnitudes of galaxies in groups. First, we analyse the luminosity function of isolated galaxies and examine how many isolated galaxies could actually be the first-ranked galaxies and how this ratio depends on the environment.

4.2.1 The luminosity function of isolated galaxies

Figure 4.7 shows the LFs for different types of galaxies in all environments together. The overall shape of the LFs in Fig. 4.7 suggests that isolated galaxies may be a superposition of two populations: the bright end of their LF is close to that of the first-ranked galaxy LF, and the faint end of the LF is similar to the LF of satellite (or the second-ranked) galaxies. Actually, in Fig. 4.7, the bright end of the LF of isolated galaxies is between the LFs for the first- and second-ranked galaxies, but in Fig. 4.6 we see that for the D1 to D3 environments, the bright end of the LF of isolated galaxies is closer to the bright end of the LF of the first-ranked galaxies, and in the D4 environment, the bright end of the LF of isolated galaxies is close to the bright end of the LF of the second-ranked galaxies. Previously, we showed that the second-ranked galaxies in high-density environments have been the first-ranked galaxies, hence we can count them as the first-ranked galaxies. Consequently, Fig. 4.7 is compatible with the assumption that the brightest isolated galaxies in our sample are actually the brightest galaxies of invisible groups.

In the supercluster environment the brightest isolated galaxies are fainter than the brightest first-ranked galaxies (see Fig. 4.6), but they are brighter than the second-ranked galaxies in this environment. Earlier we showed that the second-ranked galaxies in high-density regions are similar to the first-ranked galaxies in lower-density regions. In other words, the second-ranked galaxies in the supercluster environment can be considered as the first-ranked galaxies of groups/clusters before the last merger event.

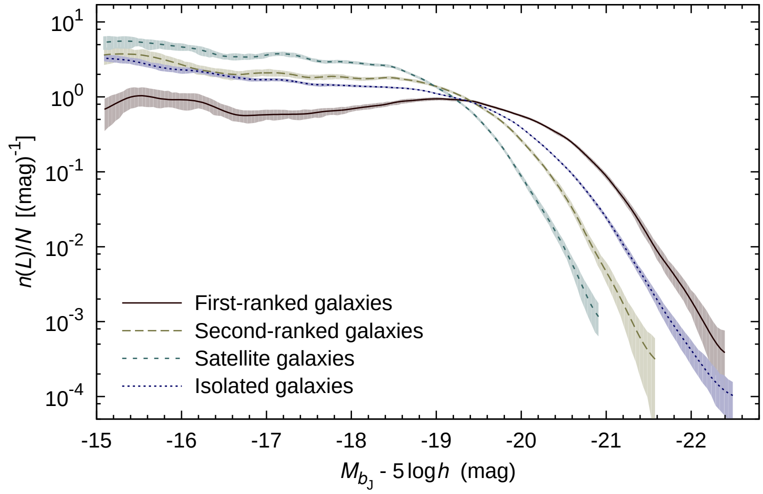

Figure 4.7: Luminosity functions of different types of galaxies for the full sample volume. The solid line shows the first-ranked galaxies; the dashed line – the second-ranked galaxies; the short-dashed line – satellite galaxies; the dotted line – isolated galaxies. The filled areas show the 95% confidence regions.

4.2.2 Magnitude differences between the first-ranked and second-ranked galaxies in groups

A simple test to examine the assumption that isolated galaxies can be the first-ranked galaxies, is the following. A group has only one galaxy in the visibility window, if its second-ranked galaxy (and all fainter group galaxies) are fainter than the faint limit of the luminosity window at the distance of the galaxy. Thus we calculated for each isolated galaxy the magnitude difference $M_{\rm diff,iso} = M_l - M_{b_{\rm J}}$, where M_l is the absolute magnitude corresponding to the faint limit of the apparent magnitude window (on average $m_l = 19.45$, but it fluctuates from field to field), and $M_{b_{\rm J}}$ is the absolute magnitude of the galaxy in the $b_{\rm J}$-filter. These magnitudes should also be corrected for the $k+e$-effect, but as the correction is the same for both, it does not influence their difference.

The distribution of the magnitude differences should be compared with the distribution of the actual magnitude differences between the first-ranked and second-ranked group galaxies, $M_{\rm diff,12} = M_2 - M_1$. The differential distributions of the magnitude differences between the first-ranked and second-ranked group galaxies $M_{\rm diff,12}$, and of the difference $M_{\rm diff,iso} = M_l - M_{b_{\rm J}}$ of isolated galaxies, are shown in Fig. 4.8. The distributions look rather similar. The difference can be barely noticed for very small magnitude differences, where the probability density for isolated

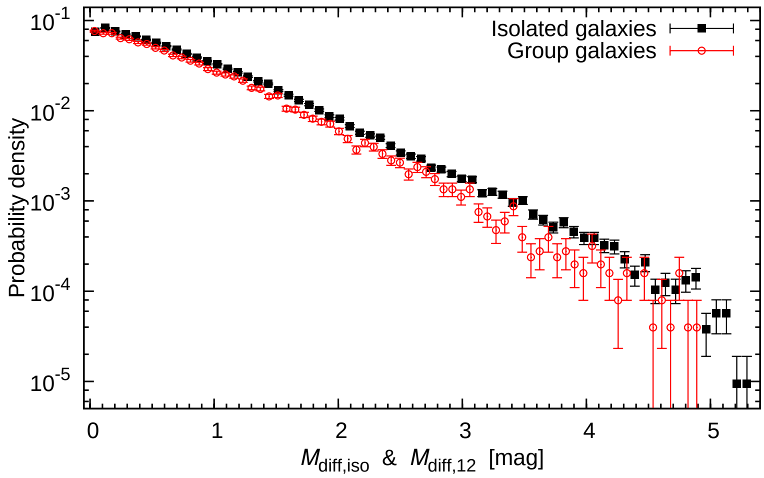

Figure 4.8: Differential distributions of magnitude differences $M_{\mathrm{diff},12}$ for the first-ranked and second-ranked galaxies of groups (open circles) and of the differences $M_{\mathrm{diff,iso}}$ between the magnitudes of isolated galaxies and of the faint limit of the visibility window (filled squares).

galaxies drops sharply (notice that the plot is in logarithmic scale). In the case of very small magnitude differences between the first-ranked and second-ranked galaxies the second-ranked galaxy is also observed, and the galaxies are not isolated. In general, the distribution for the isolated galaxy sample lies slightly above that for the group galaxy sample, that indicates that there are probably some isolated galaxies that do not belong to any group.

The overall similarity of both distributions suggests that our assumption (that isolated galaxies are actually the first-ranked galaxies with fainter companions located outside the observational window) passes the magnitude difference test. Of course, this test does not exclude the possibility of existence of truly isolated galaxies as mentioned earlier.

4.2.3 Luminosity functions of the brightest + isolated galaxies

To test the assumption that isolated galaxies are the first-ranked galaxies, we can also examine how distance-dependent selection effects influence the LFs of the first-ranked galaxies and isolated galaxies.

Figure 4.9 shows the LFs of the first-ranked and first-ranked + isolated galaxies for different distance intervals. The numbers of the first-ranked and isolated galaxies in each distance interval are given in Table 4.1. The LFs of the first-ranked galaxies

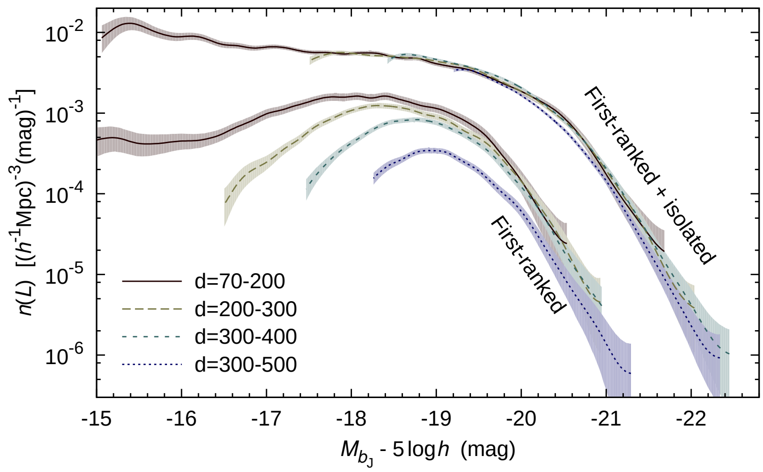

Figure 4.9: The luminosity functions of the first-ranked and the first-ranked + isolated galaxies for different distance intervals (the distances are in units of h^{-1}Mpc). The luminosity functions of the first-ranked galaxies are shifted to the left by 1 mag.

Table 4.1: The numbers of the first-ranked and isolated galaxies in samples at different distances.

Distance interval[a]	First-ranked gal.	Isolated gal.	Fraction[b]
70–200	4905	15602	0.24
200–300	6621	21634	0.23
300–400	7144	27288	0.21
400–500	3818	21453	0.15

[a] Distances are in units of h^{-1}Mpc.
[b] The fraction of the first-ranked galaxies in the first-ranked + isolated sample.

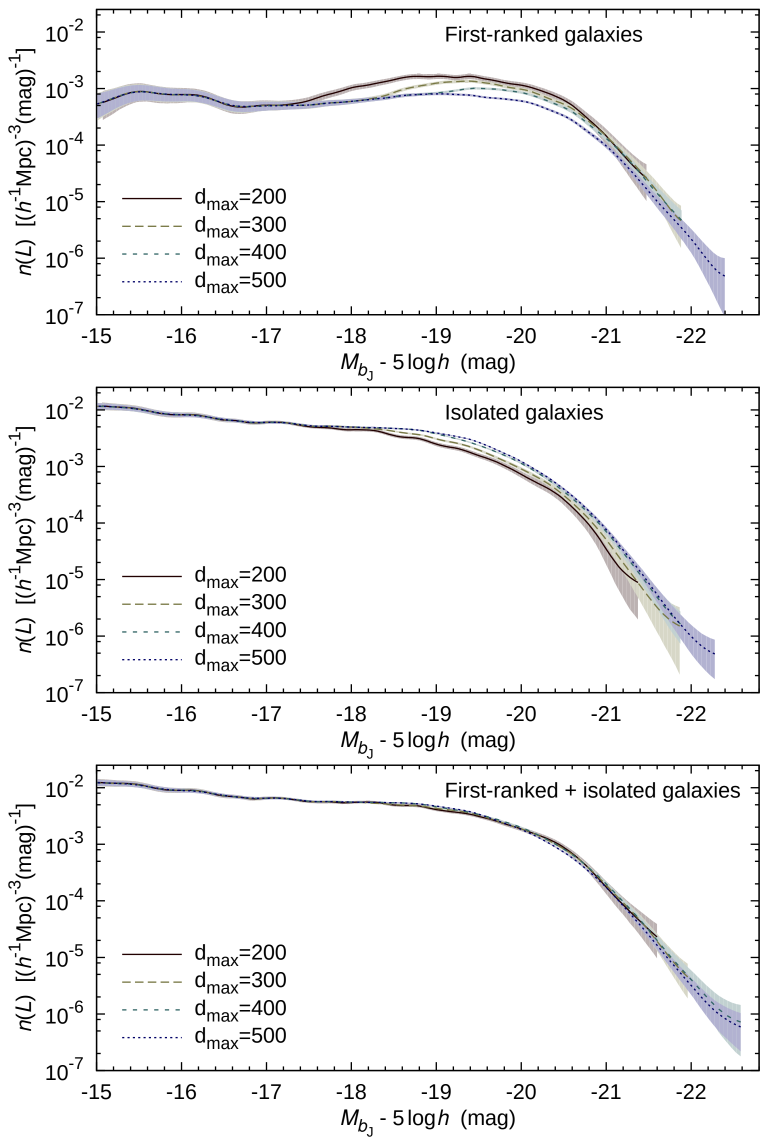

Figure 4.10: Differential luminosity functions of the first-ranked (*upper panel*), isolated (*middle panel*) and the first-ranked + isolated (*lower panel*) galaxies for samples of different maximum distance ($d_{\max} = 200, 300, 400, \text{and } 500\,h^{-1}$Mpc).

are distance-dependent: with increasing distance the number of faint galaxies decreases. If we add the isolated galaxy sample (we assume that isolated galaxies are the first-ranked galaxies) to the first-ranked sample, then the combined LFs are almost independent of distance. The remaining differences are only in the lowest luminosity ranges where the data are incomplete; the differences are much smaller than for the first-ranked samples.

In the second test, we calculated the LFs of the first-ranked galaxies, isolated galaxies, and the first-ranked + isolated galaxies for a number of limiting distances from the observer: $d_{\rm max} = 200$, 300, 400, and 500 h^{-1}Mpc. The minimum distance is the same for all samples (70 h^{-1}Mpc). The total number of the first-ranked galaxies in these subsamples is 5184, 12115, 19565, and 23453, respectively.

The calculated LFs are shown in Fig. 4.10. If we look only at the first-ranked or the isolated galaxy samples, then the LFs depend on distance. If we combine these two samples, then the combined LFs are independent of distance. This supports our assumption that most of isolated galaxies are actually the first-ranked galaxies with satellite galaxies outside the visibility window. With increasing distance, the fraction of (visible) brightest galaxies decreases (see Table 4.1). With increasing environmental density, the fraction of the first-ranked galaxies increases (see Table 2.1).

Our tests show that all (or almost all) bright isolated galaxies are actually the first-ranked galaxies. We cannot say that for fainter galaxies: there might be some fainter galaxies that are truly isolated.

CHAPTER 5
THE LUMINOSITY FUNCTION FOR THE SDSS SAMPLE

In this section we derive the luminosity function of galaxies of the Sloan Digital Sky Survey (SDSS) sample. The SDSS sample is described in Sect. 2.2. While in the previous chapter we concentrated our attention on the luminosity functions of galaxies in groups (the group brightest, satellite, and isolated galaxies), in this chapter we focus on the comparison of the luminosity functions of different morphological types of galaxies (spirals and ellipticals). The morphological classification of galaxies into spirals and ellipticals is described in Sect. 3.1. The results on the luminosity functions of spiral and elliptical galaxies in this chapter are based on Tempel et al. (2011a). Since one purpose of this chapter is to analyse how the luminosity function depends on attenuation, we will firstly derive the luminosity functions for the observed and attenuation-corrected cases. Later we shall use only the attenuation-corrected luminosity functions. Additionally, at the end of this chapter, we will derive the luminosity functions for the galaxies in groups and will briefly compare the results with the luminosity functions derived for the 2dFGRS sample.

5.1 Attenuation-corrected luminosity functions

We have classified the SDSS galaxies into spirals and ellipticals, and we have applied the attenuation corrections to spiral galaxies, as described in Sect. 3.4.

Figure 5.1 shows the LFs for all galaxies, for spirals, and for ellipticals in the attenuation-corrected (lower panel) and uncorrected (upper panel) case. At the bright end of the LF, most of the galaxies are ellipticals, and at the faint end, most of the galaxies are spirals, as found in many previous studies. Correction for dust attenuation increases the brightness of spiral galaxies; the shift is especially noticeable at the bright end of the LF. However, even with the attenuation correction applied, the brightest spiral galaxies are still less luminous than the brightest elliptical galaxies by about 0.5 mag. Table 3 in Tempel et al. (2011a) gives the analytical fits to the LFs; these are shown in Fig. 5.1 as solid lines. The parameters are given for the double-power law as well as for the Schechter function. In general, the double-power law gives a better fit. The Schechter function underestimates the amount of bright galaxies, which can be clearly seen in the inset panels of Fig. 5.1.

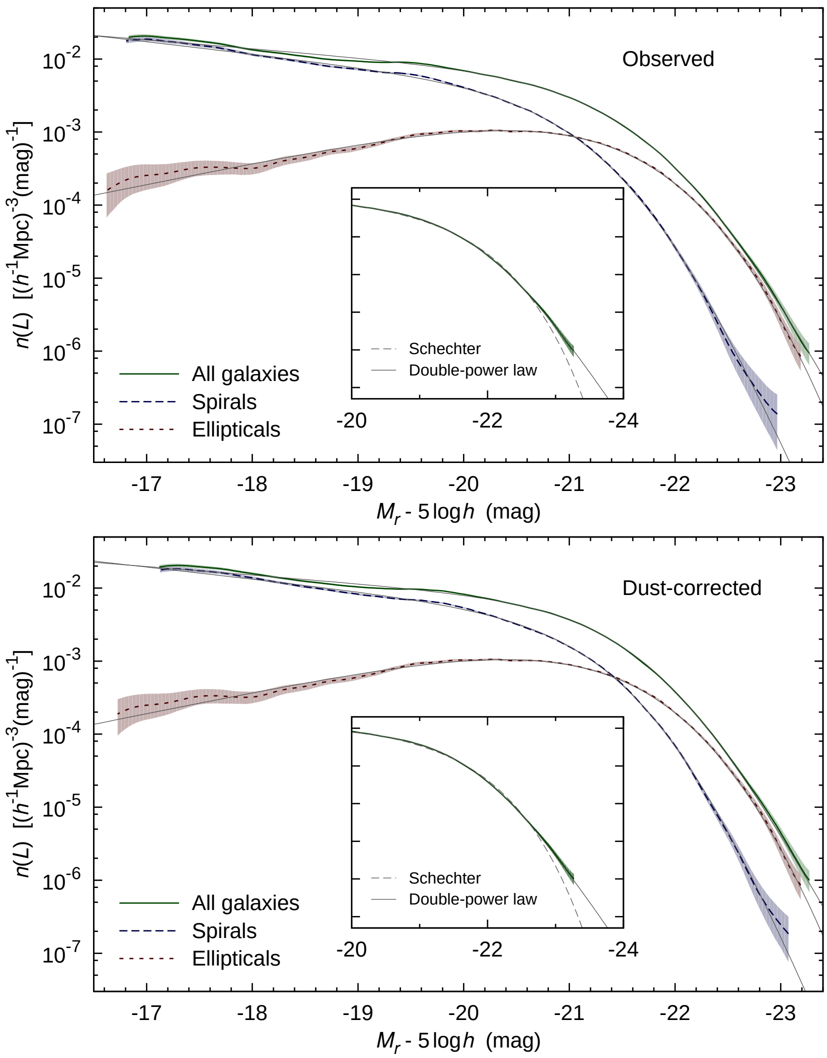

Figure 5.1: The luminosity functions for all, spiral, and elliptical galaxies. *Upper panel*: the observed luminosity functions. *Lower panel*: the attenuation-corrected luminosity functions. The filled areas show the 95% confidence regions. The light grey lines show the analytical double-power-law fits. *The inset panels* show the Schechter and double-power-law fits to the luminosity functions for all galaxies.

Table 5.1: The numbers of galaxies in the SDSS sample in different global environments.

Sample	N_{gal}	D1	D2	D3	D4
SDSS (all)	516368	54942	173320	208210	66884
SDSS (spirals)	234837	32963	86239	85749	23123
SDSS (ellipticals)	127446	7837	36718	57965	22026

Notes: N_{gal} – the number of galaxies in a sample; D1 to D4 – the number of galaxies in a given density environment (D1 is the least dense and D4 is the most dense environment). The sum of D1 to D4 is less than N_{gal} due to the edges of the survey, where densities are undetermined.

5.2 Luminosity functions in different environments

In this sections, we present the luminosity functions for different morphological types of galaxies (spirals and ellipticals) in different global environments. The calculation of environmental densities is described in Sect. 2.5, and the numbers of galaxies in each sample are given in Table 5.1.

Figure 5.2 shows the LFs in different environments: D1 to D4, where D1 is the least dense (void) environment and D4 is the most dense (supercluster) environment. In each panel the attenuation-corrected LFs are shown. The most notable trend is that while moving from lower global densities toward higher ones, elliptical galaxies start to dominate the bright end of the LF. In the least dense environments, ellipticals and spirals are equally abundant at the bright end of the LF (spirals even slightly dominate at the bright end in the void environment); in the densest environments, the brightest galaxies are mostly ellipticals. At the faint end of the LF, while moving from low density regions to high density regions, the difference between ellipticals and spirals decreases; in denser environments, the fraction of elliptical galaxies increases. This trend is also seen in Table 5.1, where the numbers of galaxies in each sample are given.

A noticeable feature in the LF of ellipticals in the densest environments is a local minimum near $M_r - 5\log h \approx -18$ mag. A seemingly similar feature is present for spirals at $M_r - 5\log h \approx -19$ mag. However, these minima are of different origin: in the case of spirals, the small dip becomes visible because of an interplay with the bump at $M_r - 5\log h \approx -19.8$ mag, probably caused by a selection effect. The number of galaxies in the most dense environment is relatively small in the SDSS sample and the presence or absence of a rich supercluster (the most dense environment) at a given distance interval may leave a notable feature in the LFs because of the apparent luminosity limits of the survey. The bump at $M_r - 5\log h \approx -19.8$ mag is caused by

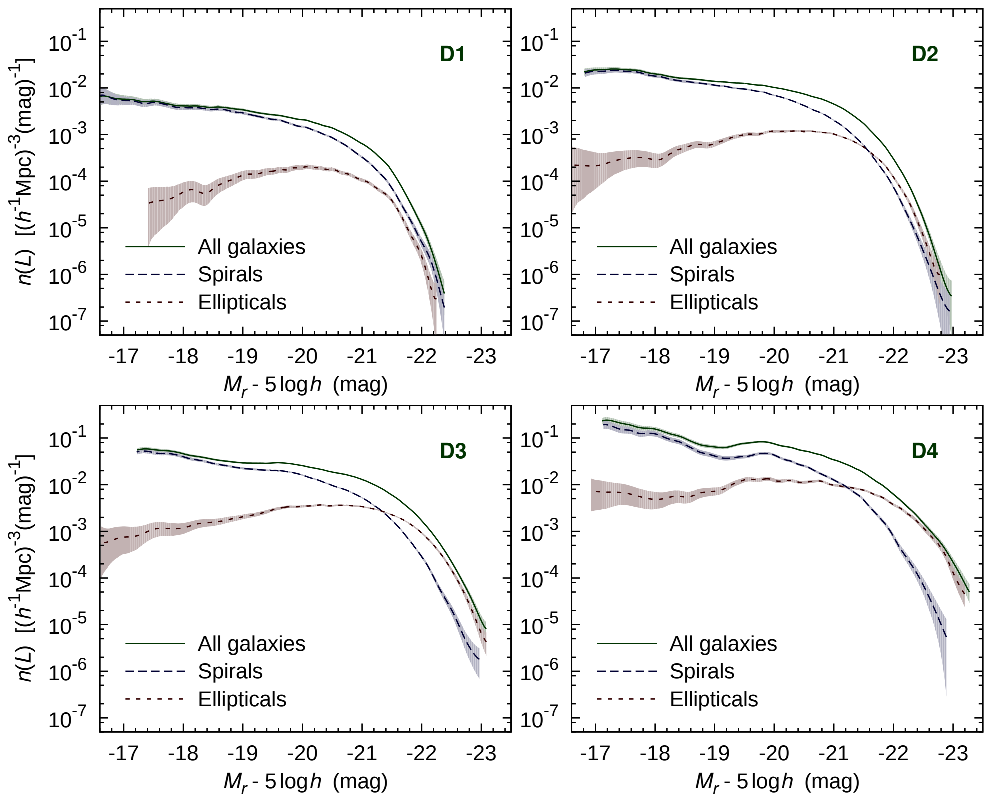

Figure 5.2: Attenuation-corrected luminosity functions for different types of galaxies in different environments: *the upper-left panel* shows the LFs for least dense environment (D1) and *the bottom-right panel* shows the LFs for most dense environment (D4). Green solid lines show the luminosity functions for all galaxies; blue dashed lines show the luminosity functions for spiral galaxies; red dotted lines show the luminosity functions for elliptical galaxies. The filled areas show the 95% confidence regions. The luminosity functions have been normalised to the volume of each sample.

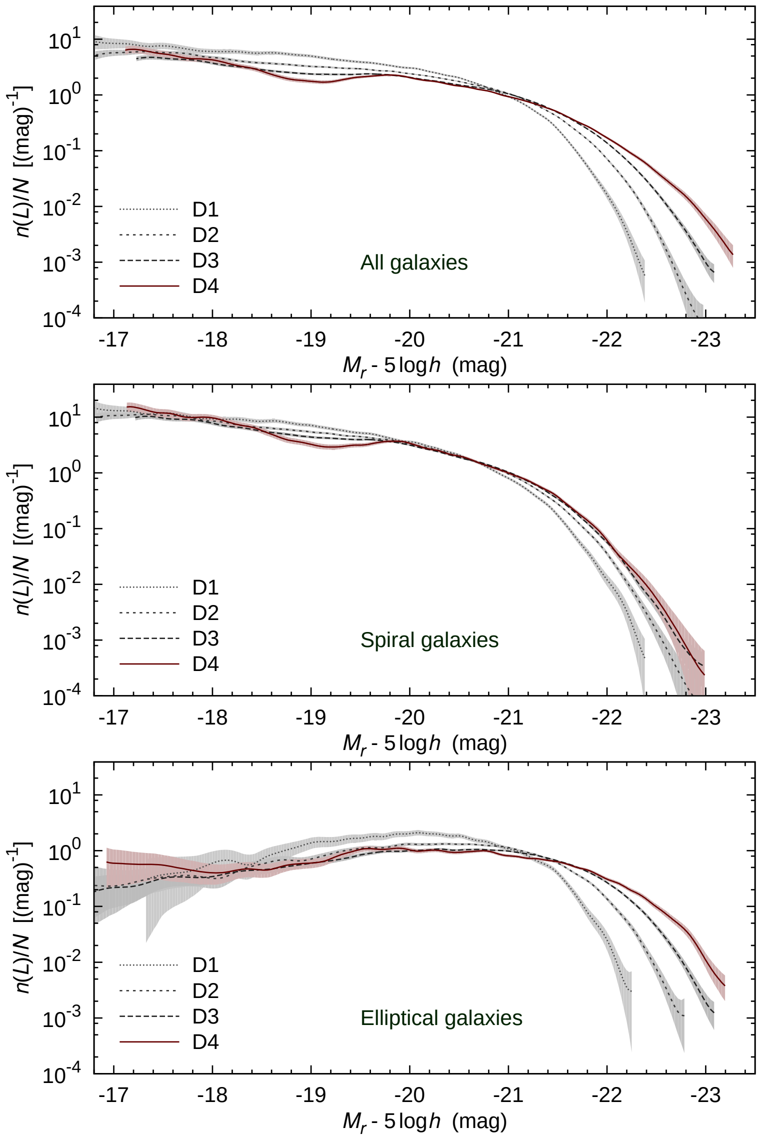

Figure 5.3: Attenuation-corrected luminosity functions for different types of galaxies in different environments. Dotted lines stand for the least dense (D1, void) environments; red solid lines stand for the most dense (D4, supercluster) environments. The filled areas show the 95% confidence regions of the luminosity functions.

the Sloan Great Wall, which is the richest galaxy system in the nearby Universe (e.g. Gott et al. 2005; Luparello et al. 2011). At $M_r - 5\log h \approx -19$ mag, the distance interval between 150 and 200 h^{-1}Mpc determines most of the LF, and as seen from right panel of Fig. 2.5, no rich superclusters are found in this region. However, the decrease of the LF from -20 to -19 mag is not caused only by selection effects. The decrease of the LF in this region in the supercluster environment was also noticed in the 2dFGRS sample in Chapter 4, and therefore we expect that the decrease is actually present.

In Fig. 5.3 the LFs for spiral galaxies, for elliptical galaxies, and for all galaxies together are shown for different environments. For elliptical galaxies, the bright end of the LF moves toward higher luminosities when moving toward higher environmental densities. This means that bright elliptical galaxies are residing mostly in high density environments, e.g., in the cores of galaxy clusters, which are more prominent in superclusters than in voids.

Interestingly, the LF for spiral galaxies is almost independent of environment. The faint end of the LF for the most dense environment is slightly different, but the number of galaxies in this environment is also small and the difference may be caused purely by selection effects in the SDSS, as mentioned above. Likewise, the difference may be real, and the supercluster environment may be different from other environments in this respect. The bright end of the LF for the least dense environment is also slightly different from that for other environments, because generally, very bright galaxies are absent from low density environments (Tempel et al. 2009).

Comparing the LFs of spiral galaxies and elliptical galaxies, the LFs for spirals slightly increase at the faint end for all environments (except for the D4 environment, where in the region from -20 to -19, a decrease can be seen), while the LFs of ellipticals have a maximum at about $M_r - 5\log h \approx -20$ and decrease toward lower luminosities. The LF for all galaxies is a combination of the spiral LF and the elliptical LF: it is mostly determined by ellipticals at the bright end and by spirals at the faint end, except for the void environment, where at the bright end, the spirals and ellipticals are equally important.

Figure 5.4 shows the LFs for red and blue ellipticals and spirals separately in different global environments. For spiral galaxies, the limit to separate the galaxies into red and blue populations is $M_u - M_r = 2.0$; for ellipticals, the limit is $M_u - M_r = 2.7$. In general, the faint end of the LF is mostly built up by bluer galaxies and the bright end includes mostly redder galaxies; this behaviour is the same for spirals and ellipticals.

In Fig. 5.4 we also see that the increase of the number of bright ellipticals in dense environments is mostly caused by red ellipticals. As mentioned above, the LF of spirals is independent of the global environmental density (see Fig. 5.3). However,

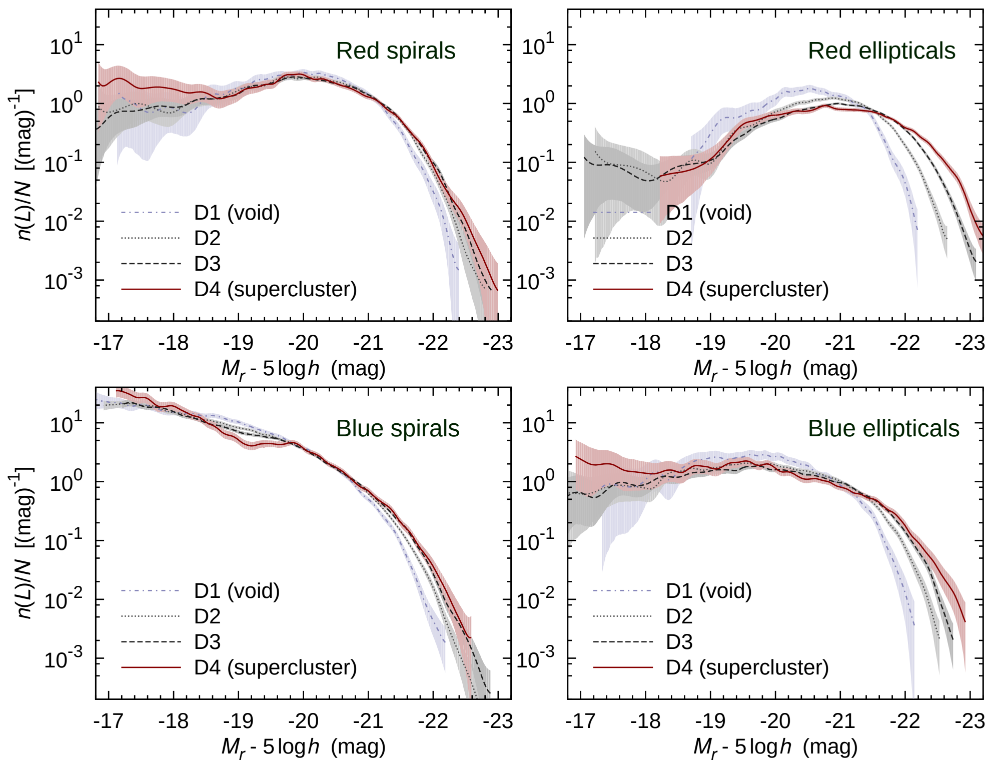

Figure 5.4: Attenuation-corrected luminosity functions for red (*upper panels*) and blue (*lower panels*) populations; for spirals (*left panels*) and ellipticals (*right panels*), in different global environments. D1 is the least dense environment (voids); D4 is the most dense environment (superclusters). The filled areas show the 95% confidence regions of the luminosity functions.

small changes with environment are seen. Figure 5.4 shows that this change is much smaller for the red and blue spirals separately and is increased by the interplay of the differences in the LF shapes of these subpopulations. Once again, these differences concern only the densest environments and are thus subject for general characteristics for supercluster environments, which by nature are significantly different than other environments, as showed previously.

5.3 Luminosity functions for the SDSS galaxies in groups

In this section we calculate the luminosity functions for the SDSS galaxies in groups. We do this in the same manner as we did it for 2dFGRS sample. The purpose of this is to have a comparison between the 2dFGRS and SDSS samples. Similarly to the 2dFGRS sample, we divided the SDSS galaxies into four groups: the first-ranked (group brightest) galaxies, the second-ranked (second brightest) galaxies, satellite galaxies, and isolated galaxies. Once again, the satellite population includes all galaxies in groups except the first- and second-ranked galaxies. Isolated galaxies are all galaxies that do not belong to any group in our group catalogue by Tago et al. (2010).

Figure 5.5 shows the LFs for different types of galaxies in various environments. This Figure can be directly compared with Fig. 4.6 for the 2dFGRS sample. As we see, the general picture is the same for the 2dFGRS and SDSS samples. The biggest difference is for the supercluster environment, where for the SDSS sample, the LF extends to much fainter luminosities. For the 2dFGRS sample, the LF decreases at the faint end for the D4 environment. For the SDSS sample, the decrease is also noticeable in the range -20 to -19 mag, but toward lower luminosities the LFs start to increase. In the 2dFGRS sample, the volume is much smaller, and in the nearby region there are no superclusters. This is the reason, why for the 2dFGRS sample, the LFs do not extend to lower luminosities. For the SDSS sample, the volume is much bigger and there are some superclusters also in the nearby region, as seen in the right panel of Fig. 2.5. Previously we argued that for the SDSS sample, this decrease (minimum at $M_r - 5\log h \approx -18$) can be also a selection effect. Probably, to a small extent it is caused by selection effects, but not entirely. In Fig. 5.3 we see that this feature occurs only for spiral galaxies, and not for ellipticals: if this were caused by selection effects, then it should be visible also for elliptical galaxies. Consequently, the decrease is probably a true observational result.

In summary, the 2dFGRS and SDSS samples give in general the same results. One exception is the supercluster environment, where the much larger SDSS sample extends to much lower luminosities and therefore gives more information for the faint end of the LF for the supercluster environment.

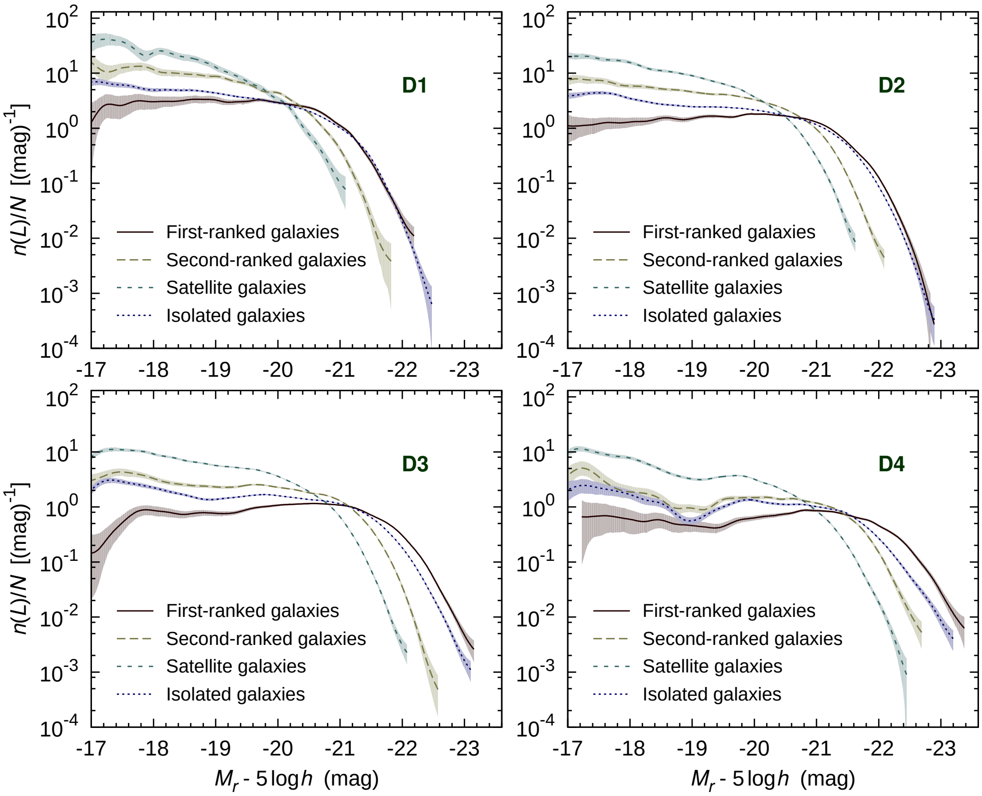

Figure 5.5: Attenuation-corrected luminosity functions in different environments and for different galaxy populations for the SDSS sample. Solid lines stand for the first-ranked galaxies; dashed lines – for the second-ranked galaxies; short-dashed lines – for satellite galaxies; dotted lines – for isolated galaxies. The filled areas show the 95% confidence regions.

CHAPTER 6
DISENTANGLING GALAXY EVOLUTION

6.1 Evolution of galaxies and groups in various environments

Our analysis of the luminosity functions of galaxies of different morphology (spirals and ellipticals) in different global environments (from voids to superclusters) shows that the global environment has played an important role in galaxy evolution. Additionally, the galaxy rank and position (the brightest cluster galaxy, a satellite) in groups/clusters are another important factors for understanding the formation and evolution of galaxies. In this section we use our results to deduce possible evolution histories of different types of galaxies in various global environments.

6.1.1 Evolution of spiral galaxies

One of the interesting results of this study is that the LF of spiral galaxies is almost independent of the global environment (see Fig. 5.3), particularly at the bright end of the LF, when looking at the red and blue spirals separately (see the left panels of Fig. 5.4). However, one has to keep in mind that only the normalised distributions are similar; the actual number densities of spiral galaxies are different. In average, the mean number density of galaxies in superclusters is about 50 times larger than in voids.

The similarity of the LFs of spirals in different global environments suggests that the evolution of spiral galaxies is slightly different for different types (colours) of spirals, but for a fixed type (colour) spiral galaxy, the evolution is independent of the global environmental density. Thus the formation history of spiral galaxies in various global environments has to be similar. This result seems to be contradicting with the general galaxy formation scenario in the ΛCDM cosmology: galaxy luminosity should be determined by the mass of the parent dark matter halo, the distribution of which depends on the environment. Besides, according to Delgado-Serrano et al. (2010), approximately half of the spirals were already in place 6 Gyr ago and another half formed in mergers of irregular galaxies. This result needs a few comments. Firstly, the spirals that were in place 6 Gyr ago, go through secular evolution in which a galaxy gradually accretes gas from the intergalactic medium, hence they have continuous star formation in the galaxy disc and they look like normal spiral galaxies today. Secondly, Delgado-Serrano et al. (2010) showed that the fraction of early-type galaxies does not change significantly during the last 6 Gyr, contrary to that of the spiral galaxies, where the fraction increases about 2.3 times. The increase of the

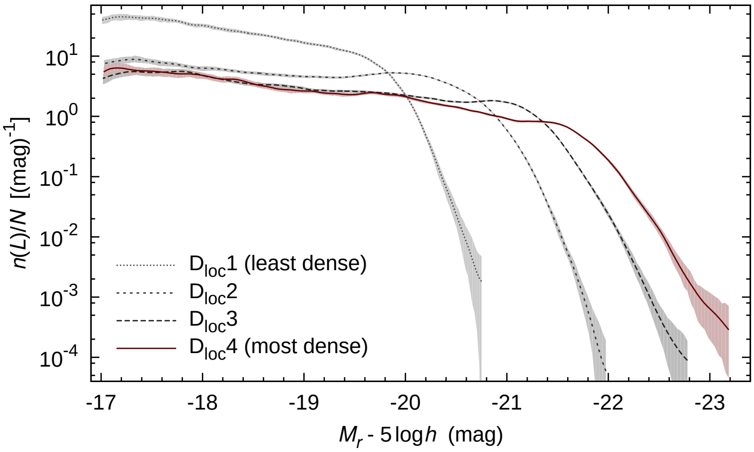

Figure 6.1: The luminosity functions of spiral galaxies in different local (group) environments. The filled areas show the 95% confidence regions.

number of spiral galaxies is accompanied by the decrease of the number of peculiar galaxies, suggesting that peculiar (irregular) galaxies transform through some mechanism to spiral galaxies; one simple mechanism to think about is the gradual merging of peculiar galaxies. Consequently, the Delgado-Serrano et al. (2010) results suggest that minor mergers and quiescent star formation are the dominant factors that determine the formation of spiral galaxies. A possible interpretation of our results may lie in the fragility of spiral galaxies: they form and survive only in specific conditions (e.g., the preservation of the gas, the absence of major mergers) which are typical of low density regions, but to a certain extent can be present also in high density regions; some haloes may remain intact and host a spiral galaxy regardless of the global environment, while most of the potential hosts of spiral galaxies end up hosting ellipticals as demonstrated by the semi-analytical models (Benson & Devereux 2010). Which processes guarantee that the mass distribution of the potential hosts (haloes) of spiral galaxies is similar in the low- and high-density regions (e.g., in voids and superclusters) is still a mystery and deserves a special study.

To quantify the role of the global environment, we show in Fig. 6.1 the LFs of spiral galaxies for different local environmental densities. For local densities, the smoothing scale was $1\,h^{-1}$Mpc, while for the global environment it was $8\,h^{-1}$Mpc. The local densities refer to the group/cluster environment, while the global densities refer to the large-scale environment: e.g., to the superclusters-void environment. In Fig. 6.1 we see that in different local environments the LFs are clearly different. This means that while the global environment determines the number density of spirals, the local (group) environment determines their properties, mostly via the halo-density relation: bigger mass haloes tend to reside in regions of higher local density (see, e.g., Einasto et al. 2005b) and they host larger and more luminous galaxies (van den Bosch et al. 2007).

6.1.2 Evolution of elliptical galaxies

We found that the global environment is not the dominant factor in the evolution of spiral galaxies. On the contrary, for elliptical galaxies, the global environment plays an important role: brighter elliptical galaxies are located mostly in denser environments. In the case of ellipticals, the global environment is more important for the red galaxies than for the blue ones.

The derived LF of elliptical galaxies can be reconciled with the hierarchical galaxy formation through mergers. The denser the environment, the brighter galaxies there should reside because of the increased merger rate. The difference between the LFs of elliptical galaxies in different environments is more notable for red galaxies, in accordance with their supposed merger origin. This interpretation agrees well also with the picture of hierarchical formation of galaxies: for blue galaxies, the evolution is more quiescent and major mergers are not so important; for red ellipticals, merging is the dominant factor of galaxy evolution. Since blue ellipticals are most likely S0-s or late type ellipticals, they have still some gas available for star formation and thereof the evolution of blue ellipticals is closer to the evolution of spiral galaxies – the global environment is less important.

6.1.3 Evolution of galaxies in groups

The study of the LF of galaxies in groups in Chapters 4 and 5 shows that the highest global density regions (superclusters) are significantly different from other regions: here the first-ranked galaxies have larger luminosities than the first-ranked galaxies in other regions and the fainter the galaxies, the less are their numbers. In the void regions, the brightest galaxies are absent. Let us compare the LFs of the first-ranked and satellite galaxies: at the bright end of the LF, the first-ranked galaxies dominate, and at the faint end of the LF, satellite galaxies dominate. This trend is similar in all environments, being more pronounced at the faint end of the LF for higher density environments. See Sect. 4.1 for more detailed results.

The properties of the LFs of various types (the first-ranked, second-ranked, satellites, and isolated) of galaxies in different environments can be interpreted by differences in the evolution of galaxies and groups. In supercluster cores rich groups have formed through many mergers, thus the second-ranked galaxies have been the brightest galaxies of poorer groups before they have been absorbed into a larger group. In a lower-density environment the merger rate is lower and groups of galaxies have been collected only from nearby regions through minor mergers and a continuous infall of matter to galaxies, as firstly suggested by White & Rees (1978). This picture is also supported by N-body simulations, which show that haloes in high-density environments have a higher fraction of their mass assembled in a major merger (Gottlöber et al. 2001; Maulbetsch et al. 2007; Fakhouri & Ma 2009); whereby in the high-density environments, the merger rate is higher in earlier times, contrary to the low-density environments, where the merger rate is higher at the present time.

Moreover, the different properties of the LFs in various environments can arise from gas accretion into galaxies and subsequent star formation. As shown by hydrodynamical simulations by Kereš et al. (2005), gas infall into galaxies (haloes) is very different in various environments. There are two dominant modes of gas accretion: the "cold mode" of gas accretion (often directed along filamentary channels, allowing galaxies efficiently draw gas from large distances) dominates for low-mass galaxies, while the conventional "hot mode" dominates the growth of high-mass systems. The galaxy/halo mass dependence on environment leads to the environment dependence of these two modes of accretion, mostly because higher-mass galaxies are more common in dense environments. Consequently, the cold accretion is dominating at high redshifts and in low-density environments today, while the hot mode is dominating in high-density environments at low redshifts.

Cooray & Milosavljević (2005b) demonstrated that the LF of galaxies can be calculated in the halo model using two premises: firstly, the luminosities of central galaxies in groups/clusters have a lognormal distribution, L^* being the mean luminosity of the central galaxies in massive haloes; and secondly, the luminosities of satellite galaxies are distributed as a power law. These assumptions mean that the bright end of the LF is determined by the first-ranked galaxies, and the faint end by the conditional LF of luminosity differences of satellite galaxies from the luminosity of the brightest galaxy. We found also that the differences between the first-ranked (central) galaxies in groups/clusters and satellite galaxies are very apparent (see Figs. 4.6 and 5.5). These differences can originate in the different merging histories of galaxies: major mergers in group environments are dominated by mergers involving the central halo (the first-ranked galaxy) (Hester & Tasitsiomi 2010), which leads to larger differences between the central and satellite haloes (galaxies). The same trend has been observed for the SDSS galaxies, where McIntosh et al. (2008) found that mergers are common in the centres of groups rather than between satellites.

In general, all studies (see, e.g., Croton et al. 2005; Hoyle et al. 2005) show that as we move from high density regions to low density regions (voids), galaxies become fainter. Interestingly, our study shows that in high-density environments (supercluster regions), the LFs show a decrease at the faint end. This result is new, although the decrease of the LF at low luminosities was noticed in the NGC901/902 supercluster by Wolf et al. (2005) for dust-free old galaxies. We suppose that in the cores of rich superclusters the faintest galaxies have been swallowed up by the brightest galaxies/groups, since in high density environments merger events are much more common. The reason why this has not been found in other studies, is probably a different definition of the high density environment. The cores of rich superclusters are specific regions that contain clusters and groups of galaxies, a few isolated galaxies, and may contain X-ray clusters of galaxies. The morphology of supercluster cores differs from the morphology of supercluster outskirts (Einasto et al. 2008). Thus supercluster cores are not just an environment that contains groups of galaxies, and the LFs of galaxies in supercluster cores are not the same as the LFs of galaxy clusters (see, for example, Hansen et al. 2009). Thus here the definition of the environment is crucial.

6.2 Comparison with other studies

6.2.1 The choice of an analytical luminosity function

In most studies about the LFs, the popular and simple Schechter (1976) function is used for analytical representation of the LF (e.g. Zabludoff & Mulchaey 2000; De Propris et al. 2003; Croton et al. 2005; Hoyle et al. 2005; Li et al. 2006; Zandivarez et al. 2006; Robotham et al. 2010). However, the Schechter function is not always a good choice to fit the LF. This difficulty was noticed already by Biviano et al. (1995) and Bromley et al. (1998). Using the much larger SDSS data Blanton et al. (2005b) showed that the Schechter function does not fit the LF of extremely low luminosity galaxies. For a Shapley Supercluster region Mercurio et al. (2006) conclude that the bright end of the Schechter function is not sufficient to fit the data. Yang et al. (2008) also use different analytical expressions of LFs for different populations: a log-normal distribution for the first-ranked galaxies, and a modified Schechter function for satellite galaxies. The difficulty of the use of the standard Schechter function for satellite galaxies lies in the fact that the slope of the LF at high luminosities is much steeper than in the standard case where the slope is fixed by the exponential law. In our studies (Tempel et al. 2009, 2011a), in addition to the Schechter function, we have also used the double-power-law form for analytical fits. The double-power-law LF overcomes both difficulties and can be used for the brightest as well as for satellite galaxies. This difference is crucial in cases where only very bright galaxies are visible, at the far end of flux-limited samples. Here small differences in the accepted analytical LF can lead to large differences in the expected total luminosities of groups. To determine these luminosities is one of our primary goals (we need them to calculate the luminosity-density field).

6.2.2 Galaxy morphology and colours in different environments

Influence of the global environment on the LF has been previously studied by Hoyle et al. (2005) using the SDSS data and by Croton et al. (2005) using the 2dFGRS data. These works have shown that galaxies in the void environment are primarily of late type. In our results, this effect becomes especially pronounced after applying the absorption corrections: Figure 5.2 shows that in the void regions, spiral galaxies dominate over ellipticals at all luminosities.

The LFs derived by Hoyle et al. (2005) for a considerably smaller sample of galaxies are quite similar for different environments, except for the highest density environment, where the faint-end slope is shallower. Croton et al. (2005) found that the faint end of the LF depends weakly on environment. In general, our analysis confirms this result, except for the highest density environment, where an excess of faint galaxies compared to other environments is found (noticeable for red spirals and for blue ellipticals in Fig. 5.4). This excess has been detected also by Xia et al. (2006). In deep surveys of the Hubble Space Telescope, an excess of faint red galaxies has been found in the field environment: Salimbeni et al. (2008) have seen such trend in the GOODS dataset and Drory et al. (2009) in the COSMOS field. Thus the excess of faint red galaxies appears in all environments, most strongly in dense cluster regions.

Phleps et al. (2007) studied the global environment beyond the redshift 2. Using three different fields with different global environments, they showed that for blue galaxies, the environment plays a smaller role than for red galaxies. Their results are in agreement with our findings for the relatively nearby region.

Many previous works were concentrated only on the local environment. For example, Yang et al. (2009) studied the LF for the central and satellite galaxies in groups, using the SDSS data. They found that in general, red galaxies are the central galaxies and blue galaxies are satellite galaxies; they found that for very low masses, the number of red central galaxies increases. They speculate that these galaxies are located close to large haloes so that their star formation is truncated by the large-scale environment. Our results also show that the faint end of the LF increases when moving toward very high density (see Fig. 5.3). When splitting our galaxies into the red and blue samples (see Fig. 5.4), the increase of the LF at the faint end is noticeable for every subsample, indicating a universal trend. In our case, the increase is also noticeable for blue galaxies. However, a direct comparison with the results of Yang et al. (2009) is difficult, because the environmental densities have been estimated differently.

Zandivarez et al. (2006) show that the local environment (galaxy group mass) is an important factor in galaxy evolution. They show that the faint-end slope is practically constant for the blue cloud galaxies, while for the red sequence galaxies, the faint end is steeper for more massive systems. Their results can be interpreted in

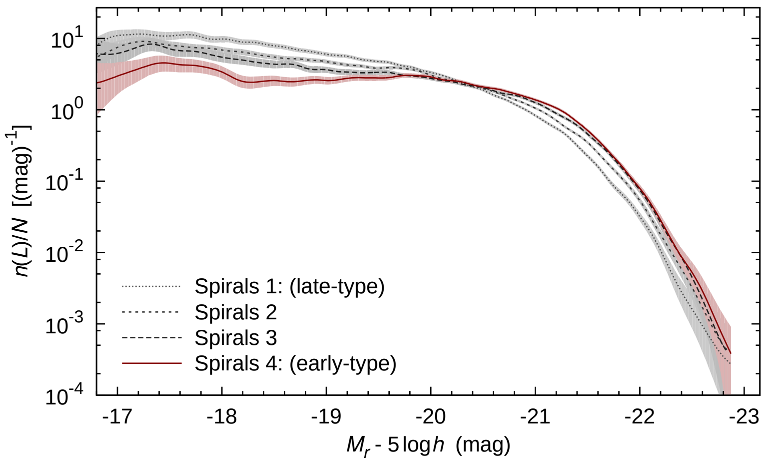

Figure 6.2: The attenuation-corrected luminosity function for spiral galaxies of various Hubble types. The Hubble type indicator is the value of $frac_{\mathrm{deV}}$: low value – late-type; high value – early-type. The filled areas show the 95% confidence regions of the luminosity function.

terms of galaxy mergers as the main driving force behind galaxy evolution in groups. Using local environmental densities, we get similar results: for ellipticals (that are dominantly red), the faint-end slope is changing with density, and for spirals (that are dominantly blue), the faint-end slope is practically constant.

Using the halo occupation model Mo et al. (2004) and Tinker & Conroy (2009) argue that the dependence of the LF on the large-scale environment is determined by differences in the masses of dark matter haloes. Semi-analytic models also predict that void galaxies should be fainter than galaxies in dense regions (Benson et al. 2003a; Tinker & Conroy 2009).

In general, the characteristic magnitudes for ellipticals are brighter than for spirals and the faint-end slopes are steeper for spirals. Devereux et al. (2009) used the K-band luminosity to derive the LF for different Hubble types; classification was performed visually. The average shapes of the LFs of ellipticals and spirals are generally in agreement with our results. In addition, they found that the faint-end slope is steeper for late-type spirals than for early-type (S0) spirals and that the characteristic luminosity is larger for early-type galaxies. In Fig. 6.2 we use the value $frac_{\mathrm{deV}}$ to separate spiral galaxies into the early and late types. This figure shows a similar trend as pointed out by Devereux et al. (2009), but in our case, the differences are smaller.

6.2.3 Groups of galaxies in different environments

Yang et al. (2008) and Hansen et al. (2009) found that the luminosities of the first-ranked galaxies of rich groups have a relatively small dispersion (see fig. 5 of Hansen et al. (2009) and fig. 2 of Yang et al. (2008)). In these studies only rich groups were considered. In our study also poorer groups were investigated, and we found that they have a lower low-luminosity limit in dense environments than rich groups do. Cooray & Milosavljević (2005a) and Yang et al. (2008) showed that the median luminosity of first-ranked galaxies depends strongly on the mass of the halo (group). To compare their results with ours we plot in the lower panel of Fig. 6.3 the luminosities of the first-ranked galaxies as a function of the estimated group total luminosity. The median luminosity of the first-ranked galaxies is shown by a red line. Our results are very close to those by Yang et al., see their fig. 6. Yang et al. use as an argument the estimated group (halo) mass that is closely related to the estimated total luminosity. Our study shows also that the median luminosity and the width of the luminosity distribution of the first-ranked galaxies depend on the density of the environment.

One of the important results of the present study is the conclusion about the nature of isolated galaxies in a flux-limited sample: most isolated galaxies are actually the first-ranked galaxies, where the fainter members of groups lie outside the visibility window. A similar result was obtained by Yang et al. (2008) using the halo occupation model. The arguments used in our study and by Yang et al. are very different, so both studies complement each other.

Yang et al. (2008) also studied the gap between the first-ranked and second-ranked galaxies. Their results show that the width of the gap lies in the range $\log(L_1/L_2) = 0.0 - 0.6$. For our groups, the width of the gap is even larger; see the upper panel of Fig. 6.3. This Figure shows that the gap has the highest values for medium rich groups of a total expected luminosity about $L_{\rm group} = 2 \times 10^{10}\ h^{-2} L_{\odot}$, i.e., for groups of the type of the Local Group.

Hoyle et al. (2005) studied the SDSS void galaxies. Their faint-end slope of the LF is comparable to our results ($\alpha = -1.0 - -1.3$). They also conclude that the faint-end slope is not strongly dependent on the environment, at least up to group densities. This is in agreement with our results, where the faint-end slope is almost the same for all populations, except for the first-ranked galaxies. However, in our samples there are still small changes when moving from voids to superclusters: the faint-end slope is steeper for void galaxies, and becomes flatter when moving toward higher densities. Our faint-end slope α for the galaxy LF is in the range $-1.0 - -1.3$ (except for the first-ranked galaxy), in good agreement with observations and models (see e.g. Baldry et al. 2005; Xia et al. 2006; Khochfar et al. 2007; Liu et al. 2008).

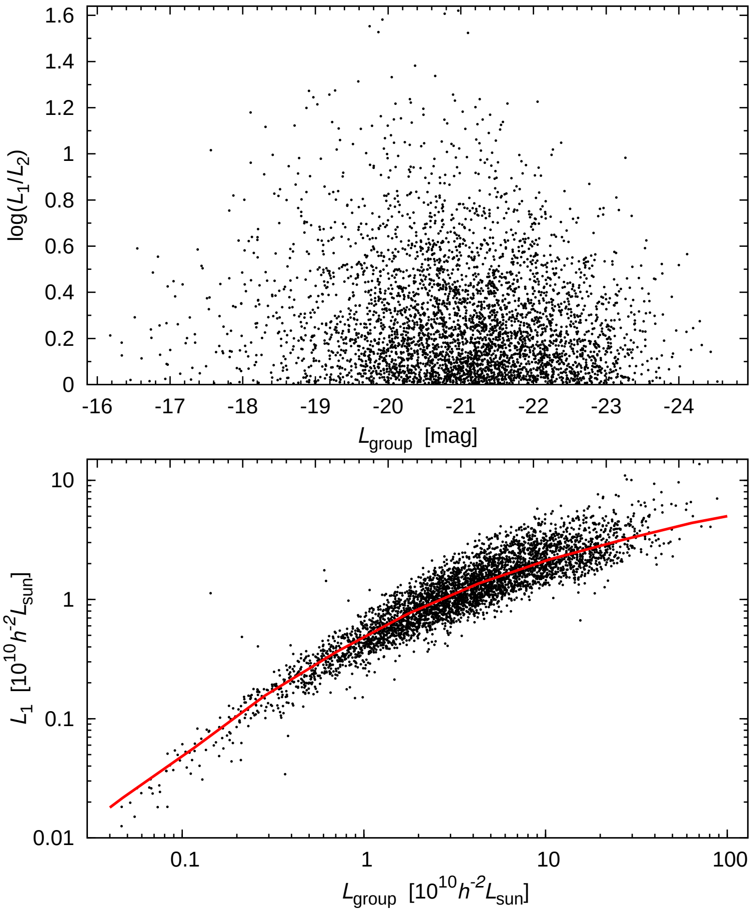

Figure 6.3: *Upper panel*: the luminosity gap between the first-ranked and second-ranked galaxies in groups, $\log L_1 - \log L_2$, as a function of the luminosity of the first-ranked galaxy. *Lower panel*: the luminosity of the first-ranked galaxy as a function of the total estimated luminosity of the group. The red line shows the median luminosity.

CHAPTER 7
THE MAIN RESULTS OF THE THESIS

In the present Thesis the Two-degree Field Galaxy Redshift Survey (2dFGRS) and the Sloan Digital Sky Survey (SDSS) were used to study the luminosity function of galaxies for different samples in various global environments. To study the luminosity function for the galaxies in groups, we used the group catalogues by Tago et al. (2006) and Tago et al. (2010), which for 2dFGRS sample include 178563 galaxies and 25215 groups; and for the SDSS sample include 516368 galaxies and 74511 groups. The global luminosity density field was used to define the large-scale environments with different global densities from voids to supercluster cores.

We used the 2dFGRS sample to derive the luminosity function of group galaxies: for the brightest (first-ranked), second-ranked, satellite, and isolated galaxies. We also studied the nature of isolated galaxies, and demonstrated that isolated galaxies are not truly isolated at all. The last result is in accordance with observations of nearby galaxies, which indicate that practically all galaxies are located in systems of galaxies of various size and richness.

We used the SDSS data to construct the luminosity functions separately for galaxies of different morphology (spiral and elliptical) and of different colours. For the SDSS sample, we took special care to correct the galaxy luminosities for the intrinsic attenuation, since for spiral galaxies the attenuation can affect significantly the galaxy luminosity.

The principal results of the present study are the following:

1. The luminosity function of elliptical galaxies depends strongly on the environment, and the environment is more important for red elliptical galaxies than for blue elliptical galaxies. This suggests that global environmental density is an important driving force (via merging history) of elliptical galaxy formation.

2. The evolution of spiral galaxies (the luminosity function of spiral galaxies) is almost independent of the global environment, especially for blue and red spirals separately, showing that spiral galaxy formation has to be similar regardless of the surrounding global density.

3. The luminosity function of the second-ranked galaxies in high-density regions is similar to the luminosity function of the first-ranked galaxies in lower-density regions. This suggests that the second-ranked galaxies in high-density regions have been the first-ranked galaxies before they have been swallowed by a larger group.

4. Almost all bright isolated galaxies can be identified with the first-ranked galaxies where the remaining galaxies lie outside the observational window used to select the galaxies for the survey. Truly isolated galaxies are rare; they are faint and are located mainly in voids.

5. The highest global density regions (supercluster cores) are significantly different from other regions. Here the first-ranked galaxies have larger luminosities than the first-ranked galaxies in other regions. The fraction of elliptical galaxies is greater than in other environments and there are relatively less faint spiral galaxies than in the low-density counterparts.

6. The brightest galaxies are absent from the void regions. After correcting for the intrinsic absorption, spiral galaxies dominate the luminosity function of void regions at every luminosity. In higher-density environments, the faint end of the luminosity function is determined by spiral galaxies and the bright end by elliptical galaxies. For all environments, the faint end includes mostly blue galaxies and the bright end mostly red galaxies.

7. Detailed studies of luminosity functions require galaxy luminosities to be corrected for the intrinsic absorption by dust. Dust absorption affects mostly the bright end of the luminosity function. For the full luminosity function, including all galaxies, the characteristic luminosity increases after attenuation correction. The faint-end slope of the luminosity function is practically independent of dust attenuation.

A comparison of these results with predictions of numerical simulations and/or semi-analytical models would provide stringent constraints on the driving factors of the formation and evolution of galaxies in dark matter haloes. These results show clearly, that beside the local/group environment, also the global (supercluster-void) environment plays an important role in the formation and evolution of galaxies. Finally, to understand the complex processes that lead to the formation of present-day galaxies, we can not ignore the location in the large-scale environment, where the galaxy resides. Hopefully, accounting for the role of global environment can help to solve some of the unsolved problems in a general picture of galaxy formation and evolution.

ACKNOWLEDGEMENTS

I am deeply grateful to my supervisors Enn Saar and Peeter Tenjes for their patient supervision and teaching. They both have helped me to overcome many obstacles on the bumpy road of becoming an astrophysicist. I am also very thankful for their advice on improving my manuscript.

I feel specially indebted to my senior colleague at the Tartu Observatory, Jaan Einasto, for the fruitful discussions and conversations, which helped to start the study that finally formed the present thesis.

My sincere gratitude goes to my colleagues at the Tartu Observatory Antti Tamm, Lauri Juhan Liivamägi, Maret Einasto, Mirt Gramann, Erik Tago, and Taavi Tuvikene for the fruitful collaboration and their contribution to the studies.

I am also thankful to my colleague Jaan Pelt who offered several time a personal assistance and advice for specific mathematical and statistical problems.

I would like to thank Volker Müller for his support and hospitality during my stays at the Astrophysikalisches Institut Potsdam. This visits provided vital support to my research and allowed to finalise my thesis.

Carrying out this study has become possible due to the existence of the SDSS and 2dFGRS surveys and I express my gratitude to all the people involved.

I gratefully acknowledge the financial support by the Estonian Science Foundation and the Estonian Ministry of Education.

References

Abazajian, K. N., Adelman-McCarthy, J. K., Agüeros, M. A., et al. 2009, *The seventh data release of the Sloan Digital Sky Survey*, ApJS, 182, 543

Abell, G. O. 1977, *The luminosity function and structure of the Coma cluster*, ApJ, 213, 327

Adami, C., Durret, F., Mazure, A., et al. 2007, *Spatial variations of the optical galaxy luminosity functions and red sequences in the Coma cluster: clues to its assembly history*, A&A, 462, 411

Adelman-McCarthy, J. K., Agüeros, M. A., Allam, S. S., et al. 2008, *The sixth data release of the Sloan Digital Sky Survey*, ApJS, 175, 297

Andersen, D. & Bershady, M. A. 2002, *The intrinsic ellipticity of spiral disks*, in Astronomical Society of the Pacific Conference Series, Vol. 275, Disks of galaxies: kinematics, dynamics and peturbations, ed. E. Athanassoula, A. Bosma, & R. Mujica, 39

Baldry, I. K., Glazebrook, K., Budavári, T., et al. 2005, *The Sloan Digital Sky Survey u-band galaxy survey: luminosity functions and evolution*, MNRAS, 358, 441

Ball, N. M., Loveday, J., & Brunner, R. J. 2008, *Galaxy colour, morphology and environment in the Sloan Digital Sky Survey*, MNRAS, 383, 907

Balogh, M. L., Navarro, J. F., & Morris, S. L. 2000, *The origin of star formation gradients in rich galaxy clusters*, ApJ, 540, 113

Bamford, S. P., Rojas, A. L., Nichol, R. C., et al. 2008, *Revealing components of the galaxy population through non-parametric techniques*, MNRAS, 391, 607

Banerji, M., Lahav, O., Lintott, C. J., et al. 2010, *Galaxy Zoo: reproducing galaxy morphologies via machine learning*, MNRAS, 406, 342

Barnes, J. E. & Hernquist, L. E. 1991, *Fueling starburst galaxies with gas-rich mergers*, ApJ, 370, L65

Baugh, C. M. 2006, *A primer on hierarchical galaxy formation: the semi-analytical approach*, Reports on Progress in Physics, 69, 3101

Bell, E. F., McIntosh, D. H., Katz, N., & Weinberg, M. D. 2003, *The optical and near-infrared properties of galaxies. I. Luminosity and stellar mass functions*, ApJS, 149, 289

Benson, A. J. & Devereux, N. 2010, *The origin of the Hubble sequence in* Λ*CDM cosmology*, MNRAS, 402, 2321

Benson, A. J., Bower, R. G., Frenk, C. S., et al. 2003a, *What shapes the luminosity* *function of galaxies?*, ApJ, 599, 38

Benson, A. J., Frenk, C. S., Baugh, C. M., Cole, S., & Lacey, C. G. 2003b, *The effects of photoionization on galaxy formation – III. Environmental dependence in the luminosity function*, MNRAS, 343, 679

Berlind, A. A., Frieman, J., Weinberg, D. H., et al. 2006, *Percolation galaxy groups and clusters in the SDSS redshift survey: identification, catalogs, and the multiplicity function*, ApJS, 167, 1

Bernardi, M., Sheth, R. K., Nichol, R. C., Schneider, D. P., & Brinkmann, J. 2005, *Colors, magnitudes, and velocity dispersions in early-type galaxies: implications for galaxy ages and metallicities*, AJ, 129, 61

Binney, J. 1985, *Testing for triaxiality with kinematic data*, MNRAS, 212, 767

Birnboim, Y. & Dekel, A. 2003, *Virial shocks in galactic haloes?*, MNRAS, 345, 349

Biviano, A., Durret, F., Gerbal, D., et al. 1995, *On the galaxy luminosity function in the central regions of the Coma cluster*, A&A, 297, 610

Blanton, M. R. & Roweis, S. 2007, *K-corrections and filter transformations in the ultraviolet, optical, and near-infrared*, AJ, 133, 734

Blanton, M. R., Brinkmann, J., Csabai, I., et al. 2003a, *Estimating fixed-frame galaxy magnitudes in the Sloan Digital Sky Survey*, AJ, 125, 2348

Blanton, M. R., Hogg, D. W., Bahcall, N. A., et al. 2003b, *The galaxy luminosity function and luminosity density at redshift* $z = 0.1$, ApJ, 592, 819

Blanton, M. R., Eisenstein, D., Hogg, D. W., Schlegel, D. J., & Brinkmann, J. 2005a, *Relationship between environment and the broadband optical properties of galaxies in the Sloan Digital Sky Survey*, ApJ, 629, 143

Blanton, M. R., Lupton, R. H., Schlegel, D. J., et al. 2005b, *The properties and luminosity function of extremely low luminosity galaxies*, ApJ, 631, 208

Bond, J. R., Kofman, L., & Pogosyan, D. 1996, *How filaments of galaxies are woven into the cosmic web*, Nature, 380, 603

Bromley, B. C., Press, W. H., Lin, H., & Kirshner, R. P. 1998, *Spectral classification and luminosity function of galaxies in the Las Campanas Redshift Survey*, ApJ, 505, 25

Butcher, H. & Oemler, Jr., A. 1978, *The evolution of galaxies in clusters. II – The galaxy content of nearby clusters*, ApJ, 226, 559

Byrd, G. & Valtonen, M. 1990, *Tidal generation of active spirals and S0 galaxies by rich clusters*, ApJ, 350, 89

Chernin, A., Einasto, I., & Saar, E. 1976, *The role of diffuse matter in galactic coronas*, Ap&SS, 39, 53

Christensen, C. G. 1975, *Luminosity function of nearby galaxies*, AJ, 80, 282

Christlein, D. 2000, *The dependence of the galaxy luminosity function on environment*, ApJ, 545, 145

Cole, S., Percival, W. J., Peacock, J. A., et al. 2005, *The 2dF Galaxy Redshift Survey: power-spectrum analysis of the final data set and cosmological implications*, MNRAS, 362, 505

Colless, M. 2004, *Luminosity functions from the 2dF Galaxy Redshift Survey*, Publications of the Astronomical Society of Australia, 21, 352

Colless, M., Dalton, G., Maddox, S., et al. 2001, *The 2dF Galaxy Redshift Survey: spectra and redshifts*, MNRAS, 328, 1039

Colless, M., Peterson, B. A., Jackson, C., et al. 2003, *The 2dF Galaxy Redshift Survey: final data release*, arXiv:astro-ph/0306581

Cooray, A. 2006, *Halo model at its best: constraints on conditional luminosity functions from measured galaxy statistics*, MNRAS, 365, 842

Cooray, A. & Cen, R. 2005, *The rise of dwarfs and the fall of giants: galaxy formation feedback signatures in the halo satellite luminosity function*, ApJ, 633, L69

Cooray, A. & Milosavljević, M. 2005a, *Dissipationless merging and the assembly of central galaxies*, ApJ, 627, L85

Cooray, A. & Milosavljević, M. 2005b, *What is L_*? Anatomy of the galaxy luminosity function*, ApJ, 627, L89

Costa-Duarte, M. V., Sodré, Jr., L., & Durret, F. 2010, *Morphological properties of superclusters of galaxies*, MNRAS, 1822

Cross, N., Driver, S. P., Couch, W., et al. 2001, *The 2dF Galaxy Redshift Survey: the number and luminosity density of galaxies*, MNRAS, 324, 825

Croton, D. J., Farrar, G. R., Norberg, P., et al. 2005, *The 2dF Galaxy Redshift Survey: luminosity functions by density environment and galaxy type*, MNRAS, 356, 1155

Cuesta-Bolao, M. J. & Serna, A. 2003, *Environmental and morphological dependence of the luminosity function of galaxies*, A&A, 405, 917

Davison, A. C. & Hinkley, D. V. 1997, Bootstrap methods and their application (Cambridge University Press)

de Lapparent, V., Geller, M. J., & Huchra, J. P. 1986, *A slice of the universe*, ApJ, 302, L1

de Lapparent, V., Galaz, G., Bardelli, S., & Arnouts, S. 2003, *The ESO-Sculptor Survey: luminosity functions of galaxies per spectral type at redshifts 0.1–0.5*, A&A, 404, 831

De Propris, R., Colless, M., Driver, S. P., et al. 2003, *The 2dF Galaxy Redshift Sur-*

vey: the luminosity function of cluster galaxies, MNRAS, 342, 725

Delgado-Serrano, R., Hammer, F., Yang, Y. B., et al. 2010, *How was the Hubble sequence 6 Gyr ago?*, A&A, 509, A78

Devereux, N., Willner, S. P., Ashby, M. L. N., Willmer, C. N. A., & Hriljac, P. 2009, *Nearby galaxies in the 2 μm All Sky Survey. I. K-band luminosity functions*, ApJ, 702, 955

Dressler, A. 1980, *Galaxy morphology in rich clusters – Implications for the formation and evolution of galaxies*, ApJ, 236, 351

Driver, S. P., Allen, P. D., Graham, A. W., et al. 2006, *The Millennium Galaxy Catalogue: morphological classification and bimodality in the colour-concentration plane*, MNRAS, 368, 414

Driver, S. P., Allen, P. D., Liske, J., & Graham, A. W. 2007a, *The Millennium Galaxy Catalogue: the luminosity functions of bulges and disks and their implied stellar mass densities*, ApJ, 657, L85

Driver, S. P., Popescu, C. C., Tuffs, R. J., et al. 2007b, *The Millennium Galaxy Catalogue: the B-band attenuation of bulge and disc light and the implied cosmic dust and stellar mass densities*, MNRAS, 379, 1022

Drory, N. & Fisher, D. B. 2007, *A connection between bulge properties and the bimodality of galaxies*, ApJ, 664, 640

Drory, N., Bundy, K., Leauthaud, A., et al. 2009, *The bimodal galaxy stellar mass function in the COSMOS Survey to $z \approx 1$: a steep faint end and a new galaxy dichotomy*, ApJ, 707, 1595

Efstathiou, G., Ellis, R. S., & Peterson, B. A. 1988, *Analysis of a complete galaxy redshift survey. II – The field-galaxy luminosity function*, MNRAS, 232, 431

Einasto, J. 1965, *On the construction of a composite model for the Galaxy and on the determination of the system of galactic parameters*, Tartu Astr. Obs. Teated, 17

Einasto, J., Saar, E., Kaasik, A., & Chernin, A. D. 1974, *Missing mass around galaxies – morphological evidence*, Nature, 252, 111

Einasto, J., Joeveer, M., & Saar, E. 1980, *Superclusters and galaxy formation*, Nature, 283, 47

Einasto, J., Hütsi, G., Einasto, M., et al. 2003a, *Clusters and superclusters in the Sloan Digital Sky Survey*, A&A, 405, 425

Einasto, J., Tago, E., Einasto, M., et al. 2005a, *Toward understanding environmental effects in SDSS clusters*, A&A, 439, 45

Einasto, M. 1991, *Structure and formation of superclusters. XII – Morphological and luminosity segregation of normal and dwarf galaxies*, MNRAS, 250, 802

Einasto, M. & Einasto, J. 1987, *Structure and formation of superclusters. VI – Morphology-density-luminosity relation of isolated and grouped galaxies*, MNRAS, 226, 543

Einasto, M., Einasto, J., Müller, V., Heinämäki, P., & Tucker, D. L. 2003b, *Environmental enhancement of loose groups around rich clusters of galaxies*, A&A, 401, 851

Einasto, M., Jaaniste, J., Einasto, J., et al. 2003c, *Las Campanas Loose Groups in the supercluster-void network*, A&A, 405, 821

Einasto, M., Suhhonenko, I., Heinämäki, P., Einasto, J., & Saar, E. 2005b, *Environmental enhancement of DM haloes*, A&A, 436, 17

Einasto, M., Einasto, J., Tago, E., et al. 2007, *Superclusters of galaxies in the 2dF redshift survey. III. The properties of galaxies in superclusters*, A&A, 464, 815

Einasto, M., Saar, E., Martínez, V. J., et al. 2008, *Toward understanding rich superclusters*, ApJ, 685, 83

Einasto, M., Tago, E., Saar, E., et al. 2010, *The Sloan Great Wall. Rich clusters*, A&A, 522, A92

Eke, V. R., Frenk, C. S., Baugh, C. M., et al. 2004, *Galaxy groups in the Two-degree Field Galaxy Redshift Survey: the luminous content of the groups*, MNRAS, 355, 769

Fakhouri, O. & Ma, C.-P. 2009, *Environmental dependence of dark matter halo growth – I. Halo merger rates*, MNRAS, 394, 1825

Fasano, G., Poggianti, B. M., Couch, W. J., et al. 2000, *The Evolution of the galactic morphological types in clusters*, ApJ, 542, 673

Fiorio, C. V. 2004, *Confidence intervals for kernel density estimation*, The Stata Journal, 4, 168-179

Folkes, S., Ronen, S., Price, I., et al. 1999, *The 2dF Galaxy Redshift Survey: spectral types and luminosity functions*, MNRAS, 308, 459

Gavazzi, G., Fumagalli, M., Cucciati, O., & Boselli, A. 2010, *A snapshot on galaxy evolution occurring in the Great Wall: the role of nurture at $z = 0$*, A&A, 517, A73

Gómez, P. L., Nichol, R. C., Miller, C. J., et al. 2003, *Galaxy star formation as a function of environment in the early data release of the Sloan Digital Sky Survey*, ApJ, 584, 210

González, R. E., Padilla, N. D., Galaz, G., & Infante, L. 2005, *The galaxy luminosity function around groups*, MNRAS, 363, 1008

Goto, T., Yamauchi, C., Fujita, Y., et al. 2003, *The morphology-density relation in* *the Sloan Digital Sky Survey*, MNRAS, 346, 601

Gott, III, J. R., Jurić, M., Schlegel, D., et al. 2005, *A Map of the Universe*, ApJ, 624, 463

Gottlöber, S., Klypin, A., & Kravtsov, A. V. 2001, *Merging history as a function of halo environment*, ApJ, 546, 223

Gunn, J. E. & Gott, III, J. R. 1972, *On the infall of matter into clusters of galaxies and some effects on their evolution*, ApJ, 176, 1

Hamilton, A. J. S. 1988, *Evidence for biasing in the CfA survey*, ApJ, 331, L59

Hansen, S. M., Sheldon, E. S., Wechsler, R. H., & Koester, B. P. 2009, *The galaxy content of SDSS clusters and groups*, ApJ, 699, 1333

Hester, J. A. & Tasitsiomi, A. 2010, *Dark matter halo mergers: dependence on environment*, ApJ, 715, 342

Hoyle, F., Rojas, R. R., Vogeley, M. S., & Brinkmann, J. 2005, *The luminosity function of void galaxies in the Sloan Digital Sky Survey*, ApJ, 620, 618

Hubble, E. 1936, *The luminosity function of nebulae. II. The luminosity function as indicated by residuals in velocity-magnitude relations*, ApJ, 84, 270

Hubble, E. & Humason, M. L. 1931, *The velocity-distance relation among extra-Galactic nebulae*, ApJ, 74, 43

Huchra, J. P. & Geller, M. J. 1982, *Groups of galaxies. I – Nearby groups*, ApJ, 257, 423

Huertas-Company, M., Foex, G., Soucail, G., & Pelló, R. 2009, *The role of environment in the morphological transformation of galaxies in 9 rich intermediate redshift clusters*, A&A, 505, 83

Huertas-Company, M., Aguerri, J. A. L., Bernardi, M., Mei, S., & Sánchez Almeida, J. 2011, *Revisiting the Hubble sequence in the SDSS DR7 spectroscopic sample: a publicly available Bayesian automated classification*, A&A, 525, A157

Kauffmann, G., White, S. D. M., Heckman, T. M., et al. 2004, *The environmental dependence of the relations between stellar mass, structure, star formation and nuclear activity in galaxies*, MNRAS, 353, 713

Kereš, D., Katz, N., Weinberg, D. H., & Davé, R. 2005, *How do galaxies get their gas?*, MNRAS, 363, 2

Khochfar, S., Silk, J., Windhorst, R. A., & Ryan, Jr., R. E. 2007, *The evolving faint end of the luminosity function*, ApJ, 668, L115

Kiang, T. 1961, *The galaxian luminosity function*, MNRAS, 122, 263

Kiang, T. 1976, *Interstellar absorption and the luminosity function of galaxies*, MNRAS, 174, 425

Kirshner, R. P., Oemler, Jr., A., & Schechter, P. L. 1979, *A study of field galaxies. II - The luminosity function and space distribution of galaxies*, AJ, 84, 951

Kochanek, C. S., Pahre, M. A., Falco, E. E., et al. 2001, *The K-band galaxy luminosity function*, ApJ, 560, 566

Komatsu, E., Smith, K. M., Dunkley, J., et al. 2011, *Seven-year Wilkinson Microwave Anisotropy Probe (WMAP) observations: cosmological interpretation*, ApJS, 192, 18

Larson, R. B., Tinsley, B. M., & Caldwell, C. N. 1980, *The evolution of disk galaxies and the origin of S0 galaxies*, ApJ, 237, 692

Lewis, I., Balogh, M., De Propris, R., et al. 2002, *The 2dF Galaxy Redshift Survey: the environmental dependence of galaxy star formation rates near clusters*, MNRAS, 334, 673

Li, C., Kauffmann, G., Jing, Y. P., et al. 2006, *The dependence of clustering on galaxy properties*, MNRAS, 368, 21

Liivamägi, L. J., Tempel, E., & Saar, E. 2010, *SDSS DR7 superclusters. The catalogues*, A&A, submitted, arXiv:1012.1989

Lin, H., Kirshner, R. P., Shectman, S. A., et al. 1996, *The luminosity function of galaxies in the Las Campanas Redshift Survey*, ApJ, 464, 60

Lin, Y., Mohr, J. J., Gonzalez, A. H., & Stanford, S. A. 2006, *Evolution of the K-band galaxy cluster luminosity function and scaling relations*, ApJ, 650, L99

Lintott, C. J., Schawinski, K., Slosar, A., et al. 2008, *Galaxy Zoo: morphologies derived from visual inspection of galaxies from the Sloan Digital Sky Survey*, MNRAS, 389, 1179

Liu, C. T., Capak, P., Mobasher, B., et al. 2008, *The faint-end slopes of galaxy luminosity functions in the COSMOS field*, ApJ, 672, 198

Loveday, J., Peterson, B. A., Efstathiou, G., & Maddox, S. J. 1992, *The Stromlo-APM Redshift Survey. I – The luminosity function and space density of galaxies*, ApJ, 390, 338

Luparello, H. E., Lares, M., Lambas, D. G., & Padilla, N. D. 2011, *Future virialized structures: an analysis of superstructures in SDSS-DR7*, MNRAS, submitted, arXiv:1101.1961

Madgwick, D. S., Lahav, O., Baldry, I. K., et al. 2002, *The 2dF Galaxy Redshift Survey: galaxy luminosity functions per spectral type*, MNRAS, 333, 133

Martínez, V. J. & Saar, E. 2002, Statistics of the galaxy distribution (Chapman & Hall)

Marzke, R. O., Geller, M. J., Huchra, J. P., & Corwin, Jr., H. G. 1994, *The luminosity* *function for different morphological types in the CfA Redshift Survey*, AJ, 108, 437

Marzke, R. O., da Costa, L. N., Pellegrini, P. S., Willmer, C. N. A., & Geller, M. J. 1998, *The galaxy luminosity function at $z < 0.05$: dependence on morphology*, ApJ, 503, 617

Maulbetsch, C., Avila-Reese, V., Colín, P., et al. 2007, *The dependence of the mass assembly history of cold dark matter halos on environment*, ApJ, 654, 53

McIntosh, D. H., Guo, Y., Hertzberg, J., et al. 2008, *Ongoing assembly of massive galaxies by major merging in large groups and clusters from the SDSS*, MNRAS, 388, 1537

Mercurio, A., Merluzzi, P., Haines, C. P., et al. 2006, *Shapley Optical Survey – I. Luminosity functions in the supercluster environment*, MNRAS, 368, 109

Mihos, J. C. & Hernquist, L. 1996, *Gasdynamics and starbursts in major mergers*, ApJ, 464, 641

Mo, H. J. & White, S. D. M. 1996, *An analytic model for the spatial clustering of dark matter haloes*, MNRAS, 282, 347

Mo, H. J., Yang, X., van den Bosch, F. C., & Jing, Y. P. 2004, *The dependence of the galaxy luminosity function on large-scale environment*, MNRAS, 349, 205

Montero-Dorta, A. D. & Prada, F. 2009, *The SDSS DR6 luminosity functions of galaxies*, MNRAS, 399, 1106

Moore, B., Katz, N., Lake, G., Dressler, A., & Oemler, A. 1996, *Galaxy harassment and the evolution of clusters of galaxies*, Nature, 379, 613

Mottmann, J. & Abell, G. O. 1977, *The luminosity function of galaxies in cluster A2670*, ApJ, 218, 53

Muñoz-Mateos, J. C., Gil de Paz, A., Boissier, S., et al. 2009, *Radial Distribution of stars, gas, and dust in SINGS galaxies. II. Derived dust properties*, ApJ, 701, 1965

Nakamura, O., Fukugita, M., Yasuda, N., et al. 2003, *The luminosity function of morphologically classified galaxies in the Sloan Digital Sky Survey*, AJ, 125, 1682

Norberg, P., Baugh, C. M., Hawkins, E., et al. 2002a, *The 2dF Galaxy Redshift Survey: the dependence of galaxy clustering on luminosity and spectral type*, MNRAS, 332, 827

Norberg, P., Cole, S., Baugh, C. M., et al. 2002b, *The 2dF Galaxy Redshift Survey: the b_J-band galaxy luminosity function and survey selection function*, MNRAS, 336, 907

Oemler, Jr., A. 1974, *The systematic properties of clusters of galaxies. Photometry of 15 clusters*, ApJ, 194, 1

Park, C. & Hwang, H. S. 2009, *Interactions of galaxies in the galaxy cluster environ-*

ment, ApJ, 699, 1595

Park, C. & Choi, Y. 2009, *Combined effects of galaxy interactions and large-scale environment on galaxy properties*, ApJ, 691, 1828

Park, C., Choi, Y., Vogeley, M. S., Gott, III, J. R., & Blanton, M. R. 2007, *Environmental dependence of properties of galaxies in the Sloan Digital Sky Survey*, ApJ, 658, 898

Pasquali, A., Leroy, A., Rix, H., et al. 2008, *The large binocular telescope panoramic view of the recent star formation activity in IC 2574*, ApJ, 687, 1004

Petrosian, V. 1976, *Surface brightness and evolution of galaxies*, ApJ, 210, L53

Phleps, S., Wolf, C., Peacock, J. A., Meisenheimer, K., & van Kampen, E. 2007, *COMBO-17 measurements of the effect of environment on the type-dependent galaxy luminosity function*, A&A, 468, 113

Pierini, D., Gordon, K. D., Witt, A. N., & Madsen, G. J. 2004, *Dust attenuation in late-type galaxies. I. Effects on bulge and disk components*, ApJ, 617, 1022

Postman, M. & Geller, M. J. 1984, *The morphology-density relation – The group connection*, ApJ, 281, 95

Press, W. H. & Davis, M. 1982, *How to identify and weigh virialized clusters of galaxies in a complete redshift catalog*, ApJ, 259, 449

Robotham, A., Phillipps, S., & de Propris, R. 2010, *The variation of the galaxy luminosity function with group properties*, MNRAS, 403, 1812

Rocha, M., Jonsson, P., Primack, J. R., & Cox, T. J. 2008, *Dust attenuation in hydrodynamic simulations of spiral galaxies*, MNRAS, 383, 1281

Ryden, B. S. 2004, *The ellipticity of the disks of spiral galaxies*, ApJ, 601, 214

Saar, E. 2009, *Multiscale methods*, in Lecture Notes in Physics, Berlin Springer Verlag, Vol. 665, ed. V. J. Martinez, E. Saar, E. M. Gonzales, & M. J. Pons-Borderia , 523

Salimbeni, S., Giallongo, E., Menci, N., et al. 2008, *The red and blue galaxy populations in the GOODS field: evidence for an excess of red dwarfs*, A&A, 477, 763

Sandage, A. 1976, *The absolute magnitude of first-ranked cluster galaxies as a function of cluster richness*, ApJ, 205, 6

Schawinski, K., Virani, S., Simmons, B., et al. 2009, *Do moderate-luminosity active galactic nuclei suppress star formation?*, ApJ, 692, L19

Schechter, P. 1976, *An analytic expression for the luminosity function for galaxies*, ApJ, 203, 297

Sérsic, J. L. 1968, Atlas de galaxias Australes (Cordoba, Argentina: Observatorio

Astronomico, 1968)

Shao, Z., Xiao, Q., Shen, S., et al. 2007, *Inclination-dependent luminosity function of spiral galaxies in the Sloan Digital Sky Survey: implications for dust extinction*, ApJ, 659, 1159

Sheth, R. K. & Tormen, G. 2002, *An excursion set model of hierarchical clustering: ellipsoidal collapse and the moving barrier*, MNRAS, 329, 61

Sheth, R. K., Jimenez, R., Panter, B., & Heavens, A. F. 2006, *Environment and the cosmic evolution of star formation*, ApJ, 650, L25

Silverman, B. W. 1997, Density estimation for statistics and data analysis (Chapman & Hall)

Silverman, B. W. & Young, G. A. 1987, *The bootstrap: to smooth or not to smooth?*, Biometrika, 74, 469

Spitzer, Jr., L. & Baade, W. 1951, *Stellar populations and collisions of galaxies*, ApJ, 113, 413

Stoughton, C., Lupton, R. H., Bernardi, M., et al. 2002, *Sloan Digital Sky Survey: early data release*, AJ, 123, 485

Strauss, M. A., Weinberg, D. H., Lupton, R. H., et al. 2002, *Spectroscopic target selection in the Sloan Digital Sky Survey: the main galaxy sample*, AJ, 124, 1810

Tago, E., Einasto, J., Saar, E., et al. 2006, *Clusters and groups of galaxies in the 2dF galaxy redshift survey: a new catalogue*, Astronomische Nachrichten, 327, 365

Tago, E., Einasto, J., Saar, E., et al. 2008, *Groups of galaxies in the SDSS Data Release 5. A group-finder and a catalogue*, A&A, 479, 927

Tago, E., Saar, E., Tempel, E., et al. 2010, *Groups of galaxies in the SDSS Data Release 7 . Flux- and volume-limited samples*, A&A, 514, A102

Tamm, A. & Tenjes, P. 2005, *Structure of visible and dark matter components in spiral galaxies at redshifts* $z = 0.5-0.9$, A&A, 433, 31

Tempel, E., Einasto, J., Einasto, M., Saar, E., & Tago, E. 2009, *Anatomy of luminosity functions: the 2dFGRS example*, A&A, 495, 37

Tempel, E., Tamm, A., & Tenjes, P. 2010, *Dust-corrected surface photometry of M 31 from Spitzer far-infrared observations*, A&A, 509, A91

Tempel, E., Saar, E., Liivamägi, L. J., et al. 2011a, *Galaxy morphology, luminosity, and environment in the SDSS DR7*, A&A, 529, A53

Tempel, E., Tuvikene, T., Tamm, A., & Tenjes, P. 2011b, *SDSS surface photometry of M 31 with absorption corrections*, A&A, 526, A155

Tenjes, P., Haud, U., & Einasto, J. 1994, *Galactic models with massive coronae IV. The Andromeda galaxy, M 31*, A&A, 286, 753

Tinker, J. L. & Conroy, C. 2009, *The void phenomenon explained*, ApJ, 691, 633

Toomre, A. & Toomre, J. 1972, *Galactic bridges and tails*, ApJ, 178, 623

Tovmassian, H. M. & Plionis, M. 2009, *The relation between morphology and dynamics of poor groups of galaxies*, ApJ, 696, 1441

Tuffs, R. J., Popescu, C. C., Völk, H. J., Kylafis, N. D., & Dopita, M. A. 2004, *Modelling the spectral energy distribution of galaxies. III. Attenuation of stellar light in spiral galaxies*, A&A, 419, 821

Tully, R. B. 1988, *The galaxy luminosity function and environmental dependencies*, AJ, 96, 73

Turner, E. L. & Gott, III, J. R. 1976, *Groups of galaxies. I. A catalog*, ApJS, 32, 409

Vale, A. & Ostriker, J. P. 2008, *A non-parametric model for linking galaxy luminosity with halo/subhalo mass: are brightest cluster galaxies special?*, MNRAS, 383, 355

van den Bosch, F. C., Yang, X., & Mo, H. J. 2003, *Linking early- and late-type galaxies to their dark matter haloes*, MNRAS, 340, 771

van den Bosch, F. C., Yang, X., Mo, H. J., et al. 2007, *Towards a concordant model of halo occupation statistics*, MNRAS, 376, 841

van den Bosch, F. C., Aquino, D., Yang, X., et al. 2008a, *The importance of satellite quenching for the build-up of the red sequence of present-day galaxies*, MNRAS, 387, 79

van den Bosch, F. C., Pasquali, A., Yang, X., et al. 2008b, *Satellite ecology: the dearth of environment dependence*, arXiv:0805.0002

van den Bosch, R. C. E. & van de Ven, G. 2009, *Recovering the intrinsic shape of early-type galaxies*, MNRAS, 398, 1117

Wand, M. P. & Jones, M. C. 1995, Kernel Smoothing (Chapman & Hall)

Wang, L., Cooray, A., & Oliver, S. 2010, *A halo model of local IRAS galaxies selected at 60 micron using conditional luminosity functions*, MNRAS, submitted, arXiv:1010.5484

Weinmann, S. M., van den Bosch, F. C., Yang, X., & Mo, H. J. 2006a, *Properties of galaxy groups in the Sloan Digital Sky Survey – I. The dependence of colour, star formation and morphology on halo mass*, MNRAS, 366, 2

Weinmann, S. M., van den Bosch, F. C., Yang, X., et al. 2006b, *Properties of galaxy groups in the Sloan Digital Sky Survey – II. Active galactic nucleus feedback and star formation truncation*, MNRAS, 372, 1161

White, S. D. M. & Rees, M. J. 1978, *Core condensation in heavy halos – A two-stage theory for galaxy formation and clustering*, MNRAS, 183, 341

Whitmore, B. C. & Gilmore, D. M. 1991, *On the interpretation of the morphology-density relation for galaxies in clusters*, ApJ, 367, 64

Wild, V., Kauffmann, G., Heckman, T., et al. 2007, *Bursty stellar populations and obscured active galactic nuclei in galaxy bulges*, MNRAS, 381, 543

Wolf, C., Gray, M. E., & Meisenheimer, K. 2005, *Red-sequence galaxies with young stars and dust: the cluster Abell 901/902 seen with COMBO-17*, A&A, 443, 435

Wolf, C., Gray, M. E., Aragón-Salamanca, A., Lane, K. P., & Meisenheimer, K. 2007, *Morphology-dependent trends of galaxy age with environment in A 901/2 seen with COMBO-17*, MNRAS, 376, L1

Xia, L., Zhou, X., Yang, Y., Ma, J., & Jiang, Z. 2006, *Evolution of the galaxy luminosity function for redshift and density environment at* $0.03 < z < 0.5$, ApJ, 652, 249

Yang, X., Mo, H. J., & van den Bosch, F. C. 2003, *Constraining galaxy formation and cosmology with the conditional luminosity function of galaxies*, MNRAS, 339, 1057

Yang, X., Mo, H. J., Jing, Y. P., van den Bosch, F. C., & Chu, Y. 2004, *Populating dark matter haloes with galaxies: comparing the 2dFGRS with mock galaxy redshift surveys*, MNRAS, 350, 1153

Yang, X., Mo, H. J., & van den Bosch, F. C. 2008, *Galaxy groups in the SDSS DR4. II. Halo occupation statistics*, ApJ, 676, 248

Yang, X., Mo, H. J., & van den Bosch, F. C. 2009, *Galaxy groups in the SDSS DR4. III. The luminosity and stellar mass functions*, ApJ, 695, 900

Zabludoff, A. I. & Mulchaey, J. S. 2000, *The properties of poor groups of galaxies. III. The galaxy luminosity function*, ApJ, 539, 136

Zandivarez, A., Martínez, H. J., & Merchán, M. E. 2006, *On the luminosity function of galaxies in groups in the Sloan Digital Sky Survey*, ApJ, 650, 137

Zehavi, I., Zheng, Z., Weinberg, D. H., et al. 2005, *The luminosity and color dependence of the galaxy correlation function*, ApJ, 630, 1

Zeldovich, I. B., Einasto, J., & Shandarin, S. F. 1982, *Giant voids in the universe*, Nature, 300, 407

SUMMARY IN ESTONIAN

Galaktikate evolutsiooni mõistmine nende heledusfunktsiooni abil

Galaktikad, mis koosnevad kuni sadadest miljarditest tähtedest, gaasist ja tolmust, on ühed tähelepanuväärsemad süsteemid Universumis. Juba visuaalsete vaatluste põhjal on näha, et neid on väga mitmesuguseid: spiraalseid, elliptilisi ning lisaks ka korrapäratu kujuga. Selline mitmekesisus tekitab küsimuse, kuidas galaktikad on tekkinud ning millised füüsikalised protsessid on galaktikate evolutsioonis olulised? Kuna galaktikate tekkimine ja evolutsioon hõlmab paljusid erinevaid füüsikalisi protsesse ning on seetõttu üsna komplitseeritud, siis on galaktikate tekkimine tänapäeva kosmoloogias üks aktuaalsemaid teemasid. Galaktikate evolutsioni parem mõistmine on ka antud uurimuse üks eesmärke.

Praeguse üldtunnustatud arusaama järgi tekivad galaktikad tumeaine halodes, kuhu koondub gaas ning kus peale gaasi piisavat jahtumist algab täheteke. Galaktikate tekkimine ja evolutsioon toimub hierarhilise arenguna: kõigepealt tekivad väiksemad süsteemid ning nende järk-järgulisel liitumisel tekivad üha suuremad süsteemid. Sellise hierarhilise kuhjumise kestel toimub väga palju galaktikate omavahelisi põrkeid ning ühinemisi, mis kõik mõjutavad galaktikate arengut.

Tänapäeva kosmoloogias on küllaltki hästi teada põhilised füüsikalised protsessid, mis mõjutavad galaktikate arengut. Peamiste protsessidena võib välja tuua galaktikate põrgetel toimuvad gravitatsioonilised häiritused, tekkivad lööklained, gaasi ümberpaiknemine, tiheduse muutused, täheteke ja supernoovade plahvatused, aktiivsete galaktikatuumade mõju ning galaktikate liikumine läbi galaktikate vahelise keskkonna. Hoolimata sellest, et me teame olulisemaid galaktikate arengut mõjutavaid protsesse, on galaktikate tekkimine tervikuna tunduvalt halvemini teada. Peamiseks põhjuseks on asjaolu, et me ei tea piisava täpsusega, milliste füüsikaliste tingimuste juures ja milliste keskkonna parameetrite puhul on eelpool nimetatud füüsikalised protsessid olulised. Kasutades pool-analüütilisi mudeleid, on praeguseks siiski küllaltki palju uuritud erinevaid protsesse sõltuvana kujunevate galaktikate lokaalsest ümbrusest. Lokaalse ümbrusena vaadeldakse peamiselt galaktika gruppe ja parvi.

Vaatluslikust kosmoloogiast on teada, et galaktika grupid ja parved ei paikne Universumis juhuslikult, vaid moodustavad suuremastaabilise kärgstruktuuri – superparvede ja tühikute võrgustiku. Kuidas galaktikate areng sõltub suuremastaabilisest struktuurist ning kas tühikutes ja superparvedes tekivad galaktikad sarnaselt või erinevalt, on küllaltki vähe uuritud. Et uurida suuremastaabilise sturktuuri mõju, on vaja kasutada suuri galaktikate valimeid. Kasutades viimastel aastatel valminud suuri galaktikate taevaülevaateid on tekkinud võimalus antud probleemi uurida vaatluslikult. Ühtedeks olulistemaks taevaülevaadeteks on 2dFGRS ja SDSS, mis kokku katavad ära umbkaudu veerand taevast ning mis sisaldavad enam kui pool miljonit galaktikat.

Käesoleva töö peamiseks eesmärgiks on uurida, kuidas galaktikate evolutsioon sõltub Universumi suuremastaabilisest struktuurist ning kuivõrd erinevad on galaktikate evolutsiooni põhiprotsessid galaktikaparvede tsentraalsete, satelliitgalaktikate ja isoleeritud galaktikate jaoks. Uurimiseks kasutame praeguse hetke suurimaid galaktikate ülevaateid 2dFGRS ja SDSS. Universumi suuremastaabilise struktuuri kirjeldamiseks kasutame heledus-tiheduse välja, mis pärast vaatluslikke ja selektsiooni parandeid võimaldab küllalt usaldusvääruselt eristada Universumis eri tihedusega piirkondi: tühikuid, filamente ja superparvi. Galaktika gruppide uurimiseks kasutame galaktika gruppide ja parvede kataloogi, mis võimaldab eristada grupi tsentraalseid ja satelliitgalaktikaid ning isoleeritud galaktikaid.

Galaktikate evolutsiooni jälgimiseks kasutame galaktikate heledusfunktsiooni, mis on üks fundamentaalsemaid meetodeid vaatluslikus kosmoloogias. Me võrdleme galaktikate heledusfunktsiooni taevaülevaadete erinevatel alamvalimitel ning teeme sellest järeldusi galaktikate evolutsiooni määravate protsesside kohta. Galaktikad jagame alamvalimiteks nende morfoloogia (spiraalsed, elliptilised) ning värvuse (punased, sinised) alusel. Samuti uurime heledusfunktsiooni eraldi galaktikagruppide tsentraalsete, satelliit ja isoleeritud galaktikate jaoks. Kõiki eelpool nimetatud valimeid vaatleme sõltuvana suuremastaabilisest struktuurist ehk globaalsest tihedusest.

Galaktikate heledusfunktsiooni arvutamine eeldab, et me teame galaktikate tegelikke heledusi. Vaadeldud galaktikate heledused sõltuvad paraku sellest, kas ja kui palju on galaktikates tolmu. Galaktikasisene tolm neelab galaktika tähtede valgust ning seega näeme vaadeldud galaktikat nõrgemana. Kuna tolmu on märkimisväärses koguses eelkõige spiraalgalaktikatel, siis spiraalgalaktikate vaadeldud heledus on neeldumisest kõige rohkem mõjutatud. Antud töös korrigeerime spiraalgalaktikate heledusi, et taastada galaktikate tegelik heledus. Neeldumise korrektuuri arvutamiseks kasutasime üksiku galaktika detailset modelleerimist. Selline ühe galaktika detailne modelleerimine võimaldas kindlaks teha, et neeldumine galaktikas sõltub nii galaktika sisemisest struktuurist kui ka kaldenurgast, mille all galaktika meile paistab. Galaktikates, kus domineerib mõhn, on neeldumine suurem kui galaktikates, kus domineerib ketas. Galaktika kaldenurgast sõltuvuse analüüs näitas, et neeldumine on suurim peaaegu serviti paistvate galaktikate korral. Arvutuste tulemusena selgus, et tolmu korrektsioon mõjutab spiraalgalaktikate heledusi kuni kaks korda.

Uurides galaktikate heledusfunksiooni grupi galaktikatele ning isoleeritud galaktikatele, järeldasime, et näivalt isoleeritud galaktikad ei pruugi olla täielikult isoleeritud. Enamus näivalt isoleerituid galaktikaid on pigem grupi tsentraalsed (heledaimad) galaktikad. Visuaalselt isoleeritud galaktikate olemasolu galaktikate valimis on tingitud suures osas vaatluslikust selektsioonist: galaktikate ülevaadetes vaadeldakse ainult teatud heledusest heledamaid galaktikaid. Sellise vaatlusliku selektsiooniga registreeritakse paljudes gruppides ainult heledaim galaktika ning grupi ülejäänud galaktikad jäävad vaatlemata. Analüüs grupi heledamate ja heleduselt järgmiste galaktikate kohta näitas, et heledusfunktsioon grupi heledamatele galaktiatele alatihedusega piirkondades langeb kokku heledusfunktsiooniga grupi heleduselt teistele galaktikatele ületihedusega piirkondades. See tulemus viitab, et suure tihedusega piirkondades olevad grupi heleduselt teised galaktikad on oma varasemas arengus tõenäoliselt olnud grupi tsentraalsed (heledaimad) galaktikad, enne kui see grupp on ühinenud mõne suurema grupiga. Saadud tulemus on kooskõlas hierarhilise kuhjumise teooriaga.

Uurides galaktikate heledusfunktsiooni sõltuvana suuremastaabilisest struktuurist, järeldasime, et elliptiliste galaktikate evolutsioon sõltub tugevalt ümbritsevast suuremastaabilisest keskkonnast, seevastu spiraalsete galaktikate heledusfunktsioon jääb erineva tihedusega piirkondades muutumatuks. Elliptiliste galaktikate heleduste üldine sõltuvus globaalsest keskkonnast oli oodatav, kuna elliptilised galaktikad tekivad vastavalt praegusele galaktikate tekke paradigmale peamiselt galaktikate ühinemise tulemusel ning tihedamates piirkondades on galaktikate ühinemisi keskmiselt rohkem. Spiraalgalaktikate heledusfunktsiooni sarnasus erinevates piirkondades viitab, et spiraalgalaktikate tekkimine erinevates keskkondades on sarnane. Kuna hierarhilise kuhjumise teooria järgi peaks ka spiraalgalaktikatel olema sõltuvus ümbritsevast globaalsest keskkonnast, siis antud tulemus viitab, et spiraalgalaktikate tekkimiseks on vajalikud spetsiifilised tingimused. Antud tulemuse detailne analüüs nõuab põhjalikumaid uurimusi, mis on jäetud edaspidiseks.

Heledusfunktsiooni analüüs sõltuvana galaktikate morfoloogilisest tüübist osutas, et heledate galaktikate hulgas domineerivad elliptilised galaktikad ning nõrgemate galaktikate hulgas domineerivad spiraalsed galaktikad. Eelpool mainitud trend on ka globaalsest keskkonnast sõltuv: tihedamates piirkondades domineerivad heledamas otsas elliptilised galaktikad jõulisemalt kui hõredamas piirkonnas. Kui vaadelda ainult tühikuid suuremastaabilises struktuuris, siis seal domineerivad kogu heledusvahemikus spiraalgalaktikad. See viitab samuti asjaolule, et elliptilite galaktikate tekkimises on olulised galaktikte omavahelised põrked ja ühinemised, mida hõredates piirkondades esineb keskmisest vähem.

Antud töö keskendus galaktikate evolutsiooni vaatluslikule uurimisele ning töö tulemusi saab edaspidi rakendada vastavates numbrilistes ning pool-analüütilistes mudelites, mis võimaldavad täpsemalt määrata, millised füüsikalised protsessid on olulised erinevates keskkondades. Käesoleva töö tulemused näitasid selgelt, et lisaks lokaalsele (gruppide) keskkonnale on galaktikate evolutsioonis oluline ka globaalne, suuremastaabiline ümbrus. Loodetavasti aitab suuremastaabilise keskkonna mõju arvestamine lahendada mõnesid huvipakkuvaid probleeme galaktikate tekke stsenaariumites.

PUBLICATIONS

CURRICULUM VITAE

Personal data

Name	Elmo Tempel
Date and place of birth	16 June 1980, Paide, Estonia
Citizenship	Estonian
Marital status	married
Current employment	Tartu Observatory (research associate)
Address	Tartu Observatory 61602 Tõravere Tartumaa, Estonia
Phone	(+372) 50 79 048
E-mail	elmo@aai.ee

Education

1987 – 1999	Türi Economic Gymnasium
1999 – 2003	University of Tartu, undergraduate student, BSc 2003 (astrophysics)
2003 – 2005	University of Tartu, graduate student, MSc 2005 (astrophysics)
2005 – 2011	University of Tartu, PhD student

Employment

2005 – 2010	Tartu Observatory, extraordinary research associate
2010 – …	Tartu Observatory, research associate

Professional training

03.09 – 07.09 2007	Summer school "The Finnish graduate school in astronomy and space physics 2007: time series analysis", Elva, Estonia
10.09 – 21.09 2007	Summer school "Novicosmo 2007: fiat lux – formation and evolution of cosmic structures", Novigrad, Cittanova, Croatia
30.06 – 04.07 2008	Summer school "Cosmology: an astrophysical perspective", Heraklion, Crete, Greece
17.11 – 28.11 2008	Winter school "XX Canary Islands winter school of

	astrophysics: Local Group cosmology", Puerto de la Cruz, Tenerife, Spain
28.03 – 02.04 2009	Summer school "EuroVO-AIDA school 2009", Garching, Germany
18.05 – 20.05 2009	Summer school "Scientific writing for young astronomers", Blankenberge, Belgium
01.07 – 03.07 2009	Summer school "International summer school: future cosmic sky surveys and huge databases", Tartu, Estonia
12.06 – 20.06 2010	Summer school "CSC summer school in scientific and high-performance computing", Espoo, Finland

Conference presentations

16.07 – 20.07 2007	Conference "Galaxy growth in a dark Universe", Heidelberg, Germany. *Poster presentation*: "Dark matter distribution and a self-consistent model of the Andromeda galaxy"
03.10 – 05.10 2007	Conference "Tuorla and Tartu Observatories autumn meeting in cosmology and large-scale structure", Tuorla, Finland. *Oral presentation*: "Dark matter distribution and a self-consistent model of the Andromeda galaxy"
01.10 – 04.10 2008	Conference "Tartu – Tuorla annual meeting 2008. Cosmology: from observations to simulations and beyond", Tartu, Estonia. *Oral presentation*: "Anatomy of luminosity functions"

Language skills

Estonian	the first language
English	good
German	basic

Honours and Awards

2005	E. Öpik stipend (Tartu Observatory)
2008	E. Öpik stipend (Tartu Observatory)

Fields of research

Photometrical and dynamical modelling of galaxies.
Galaxy and group evolution in large-scale environment.

Publications

1. **Tempel, E.**, & Tenjes, P. 2006, *Line-of-sight velocity dispersions and a mass-distribution model of the Sa galaxy NGC 4594*, Monthly Notices of the Royal Astronomical Society, 371, 1269–1279.
2. Tamm, A., **Tempel, E.**, & Tenjes, P. 2007, *Visible and dark matter in M 31. I. Properties of stellar components*, arXiv:0707.4375v3 [astro-ph] (11 pages)
3. **Tempel, E.**, Tamm, A., & Tenjes, P. 2007, *Visible and dark matter in M 31. II. A dynamical model and dark matter density distribution*, arXiv:0707.4374v2 [astro-ph] (12 pages)
4. Tago, E., Einasto, J., Saar, E., **Tempel, E.**, Einasto, M., Vennik, J., & Müller, V. 2008, *Groups of galaxies in the SDSS Data Release 5. A group-finder and a catalogue*, Astronomy & Astrophysics, 479, 927–937
5. Nurmi, P., Heinämäki, P., Niemi, S., Saar, E., Tago, E., Einasto, M., **Tempel, E**., Einasto, J., & Martínez, V. J. 2008, *Galaxy groups in ΛCDM simulations and SDSS DR6*, Proceedings of the international conference held at Russian Geographical Society, Problems of practical cosmology, ed. by Y. V. Baryshev, I. N. Taganov, and P. Teerikorpi, Vol. 1, p78–85
6. Heinämäki, P., Nurmi, P., Tago, E., Saar, E., Liivamägi, L. J., **Tempel, E.**, Einasto, M., Einasto, J., Lietzen, H., & Takalo, L. 2008, *Nearby quasars in SDSS*, Proceedings of the international conference held at Russian Geographical Society, Problems of practical cosmology, ed. by Y. V. Baryshev, I. N. Taganov, and P. Teerikorpi, Vol. 1, p123–128
7. **Tempel, E.**, Einasto, J., Einasto, M., Saar, E., Tago, E. 2009, *Anatomy of luminosity functions: the 2dFGRS example*, Astronomy & Astrophysics, 495, 37–51
8. Tamm, A., **Tempel, E.**, & Tenjes, P. 2009, *Luminous and dark matter in the Andromeda galaxy*, Proceedings of the International Astronomical Union, IAU Symposium, Volume 254, The galaxy disk in cosmological context, ed. J. Andersen, J. Bland-Hawthorn, and B. Nordström, p73
9. Lietzen, H., Heinämäki, P., Nurmi, P., Tago, E., Saar, E., Liivamägi, J., **Tempel, E.**, Einasto, M., Einasto, J., Gramann, M., & Takalo, L. O. 2009, *Environments of nearby quasars in Sloan Digital Sky Survey*, Astronomy & Astrophysics, 501, 145–155
10. Martínez, V. J., Arnalte-Mur, P., Saar, E., de la Cruz, P., Pons-Bordería, M. J., Paredes, S., Fernández-Soto, A., & **Tempel, E**. 2009, *Reliability of the detection of the baryon acoustic peak*, Astrophysical Journal Letters, 696, L93–L97
11. **Tempel, E.**, Tamm, A., & Tenjes, P. 2010, *Dust-corrected surface photometry*

of M 31 from Spitzer far-infrared observations, Astronomy & Astrophysics, 509, A91 (13 pages)

12. Tago, E., Saar, E., **Tempel, E.**, Einasto, J., Einasto, M., Nurmi, P., & Heinämägi, P. 2010, *Groups of galaxies in the SDSS Data Release 7. Flux- and volume-limited samples*, Astronomy & Astrophysics, 514, A102 (11 pages)
13. Lietzen, H., Heinämäki, P., Nurmi, P., Liivamägi, L. J., Saar, E., Tago, E., **Tempel, E.**, Einasto, M., Einasto, J., Gramann, M., & Takalo, L. O. 2010, *Large Scale Environments of Nearby Quasars*, AIP Conference Proceedings, Hunting for the dark: the hidden side of galaxy formation, ed. V. P. Debattista and C. C. Popescu, Vol. 1240, p249–250
14. Einasto, M., Tago, E., Saar, E., Nurmi, P., Enkvist, I., Einasto, P., Heinämäki, P., Liivamägi, L. J., **Tempel, E.**, Einasto, J., Martínez, V. J., Vennik, J., & Pihajoki, P. 2010, *The Sloan great wall. Rich clusters*, Astronomy & Astrophysics, 522, A92 (19 pages)
15. **Tempel, E.**, Tuvikene, T., Tamm, A., & Tenjes, P. 2011, *SDSS surface photometry of M 31 with absorption corrections*, Astronomy & Astrophysics, 526, A155 (6 pages)
16. **Tempel, E.**, Saar, E., Liivamägi, L. J., Tamm, A., Einasto, J., Einasto, M., & Müller, V. 2011, *Galaxy morphology, luminosity, and environment in the SDSS DR7*, Astronomy & Astrophysics, 529, A53 (14 pages)
17. Liivamägi, L. J., **Tempel, E.**, & Saar, E. 2011, *SDSS DR7 superclusters. The catalogues*, Astronomy & Astrophysics, submitted, arXiv:1012.1989
18. Einasto, J., Hütsi, G., Saar, E., Suhhonenko, I., Liivamägi, L. J., Einasto, M., Müller, V., Tago, E., Starobinsky A. A., & **Tempel, E.** 2011, *Wavelet analysis of the formation of the cosmic web*, Astronomy & Astrophysics, submitted, arXiv:1012.3550
19. Suhhonenko, I., Einasto, J., Liivamägi, L. J., Saar, E., Einasto, M., Hütsi, G., Müller, V., Starobinsky, A. A., Tago, E., & **Tempel, E.** 2011, *The cosmic web for density perturbations of various scales*, Astronomy & Astrophysics, submitted, arXiv:1101.0123
20. Tamm, A., **Tempel, E.**, & Tenjes, P. 2011, *Luminous and dark matter in the Andromeda galaxy*, Proceedings of the International Astronomical Union, IAU Symposium, Volume 277, Tracing the ancestry of galaxies
21. Einasto, M., Liivamägi, L. J., Tago, E., Saar, E., **Tempel, E.**, Einasto, J., Martínez, V. J., & Heinämäki, P. 2011, *SDSS superclusters. Morphology*, Astronomy & Astrophysics, submitted

ELULOOKIRJELDUS

Isikuandmed

Nimi	Elmo Tempel
Sünniaeg ja -koht	16. juuni 1980, Paide, Eesti
Kodakondsus	eesti
Perekonnaseis	abielus
Praegune töökoht	Tartu Observatoorium (teadur)
Aadress	Tartu Observatoorium 61602 Tõravere Tartumaa, Eesti
Telefon	(+372) 50 79 048
E-post	elmo@aai.ee

Haridustee

1987 – 1999	Türi Majandusgümnaasium
1999 – 2003	Tartu Ülikool, üliõpilane, BSc 2003 (astrofüüsika)
2003 – 2005	Tartu Ülikool, magistrant, MSc 2005 (astrofüüsika)
2005 – 2011	Tartu Ülikool, doktorant

Teenistuskäik

2005 – 2010	Tartu Observatoorium, erakorraline teadur
2010 – . . .	Tartu Observatoorium, teadur

Täiendkoolitus

03.09 – 07.09 2007	Suvekool “The Finnish graduate school in astronomy and space physics 2007: time series analysis”, Elva, Eesti
10.09 – 21.09 2007	Suvekool “Novicosmo 2007: fiat lux – formation and evolution of cosmic structures”, Novigrad, Horvaatia
30.06 – 04.07 2008	Suvekool “Cosmology: an astrophysical perspective”, Heraklion, Kreeta, Kreeka
17.11 – 28.11 2008	Talvekool “XX Canary Islands winter school of astrophysics: Local Group cosmology”, Puerto de la Cruz, Tenerife, Hispaania
28.03 – 02.04 2009	Suvekool “EuroVO-AIDA school 2009”, Garching, Saksamaa

18.05 – 20.05 2009	Suvekool “Scientific writing for young astronomers”, Blankenberge, Belgia
01.07 – 03.07 2009	Suvekool “International summer school: future cosmic sky surveys and huge databases”, Tartu, Eesti
12.06 – 20.06 2010	Suvekool “CSC summer school in scientific and high-performance computing”, Espo, Soome

Konverentside ettekanded

16.07 – 20.07 2007	Konverents “Galaxy growth in a dark Universe”, Heidelberg, Saksamaa. *Posterettekanne*: “Dark matter distribution and a self-consistent model of the Andromeda galaxy”
03.10 – 05.10 2007	Konverents “Tuorla and Tartu Observatories autumn meeting in cosmology and large-scale structure”, Tuorla, Soome. *Suuline ettekanne*: “Dark matter distribution and a self-consistent model of the Andromeda galaxy”
01.10 – 04.10 2008	Konverents “Tartu – Tuorla annual meeting 2008. Cosmology: from observations to simulations and beyond”, Tartu, Eesti. *Suuline ettekanne*: “Anatomy of luminosity functions”

Keelteoskus

eesti keel	emakeel
inglise keel	hea
saksa keel	vähene

Uurimistoetused ja stipendiumid

2005	E. Öpik stipendium (Tartu Observatoorium)
2008	E. Öpik stipendium (Tartu Observatoorium)

Peamised uurimissuunad

Galaktikate fotomeetriline ja dünaamiline modelleerimine.
Galaktikate ja galaktikaparvede evolutsioon Universumis.

DISSERTATIONES ASTRONOMIAE UNIVERSITATIS TARTUENSIS

1. **Tõnu Viik.** Numerical realizations of analytical methods in theory of radiative transfer. Tartu, 1991.
2. **Enn Saar.** Geometry of the large scale structure of the Universe. Tartu, 1991.
3. **Maret Einasto.** Morphological and luminosity segregation of galaxies. Tartu, 1991.
4. **Urmas Haud.** Dark Matter in galaxies. Tartu, 1991.
5. **Eugene A. Ustinov.** Inverse problems of radiative transfer in sounding of planetary atmospheres. Tartu, 1992.
6. **Peeter Tenjes.** Models of regular galaxies. Tartu, 1993.
7. **Ivar Suisalu.** Simulation of the evolution of large scale structure elements with adaptive multigrid method. Tartu, 1995.
8. **Teimuraz Shvelidze.** Automated quantitative spectral classification of stars by means of objective prism spectra: the method and applications. Tartu, 1999.
9. **Jelena Gerškevitš.** Formation and evolution of binary systems with compact objects. Tartu, 2002.
10. **Ivan Suhhonenko**. Large-scale motions in the universe. Tartu, 2003.
11. **Antti Tamm.** Structure of distant disk galaxies. Tartu, 2006.
12. **Vladislav-Veniamin Pustynski.** Modeling the reflection effect in pre-cataclysmic binary systems. Tartu, 2007.
13. **Anna Aret.** Evolutionary separation of mercury isotopes in atmospheres of chemically peculiar stars. Tartu, 2009.
14. **Mari Burmeister.** Characteristics of the hot components of symbiotic stars. Tartu, 2010.